When during galaxy assembly did AGN growth take place?

or: Who came first: The Beauty or the Beast?

Rogier A. Windhorst (ASU)

Collaborators: Seth Cohen, Russell Ryan Jr., Amber Straughn, & Nimish Hathi (ASU)

and Haojing Yan (Carnegie)

Sponsored by NASA & STScI

hubblesite.org/newscenter/archive/2004/28/ *hubblesite.org/newscenter/archive/2006/04/*

Colloquium at the Royal Observatory, Edinburgh, Scotland, Wednesday July 2, 2008

"For God's sake, Edwards. Put the laser pointer away."

The danger of having Quasar-like devices too close to home ...

Outline

- (1) Introduction: (How) did AGN/SMBH-growth go hand-in-hand with the process of Galaxy Assembly?
- (2) Tadpole Galaxies in the HUDF: A measure of Galaxy Assembly?
- (3) A Study of Variable Objects in the HUDF: A measure of AGN Growth?
- (4) Epoch dependent major merger rate to AB$\lesssim$27 and Chandra N(z).
- (5) Ages of radio and X-ray hosting galaxies as a function of epoch.
- (6) Summary and Conclusions: Delta t(X-ray/Radio X— field) $\lesssim$1 Gyr.
- (7) Future studies with the James Webb Space Telescope and HST/WFC3.

Sponsored by NASA

ASU Arizona State University

(1) Introduction: Hierarchical Galaxy Assembly

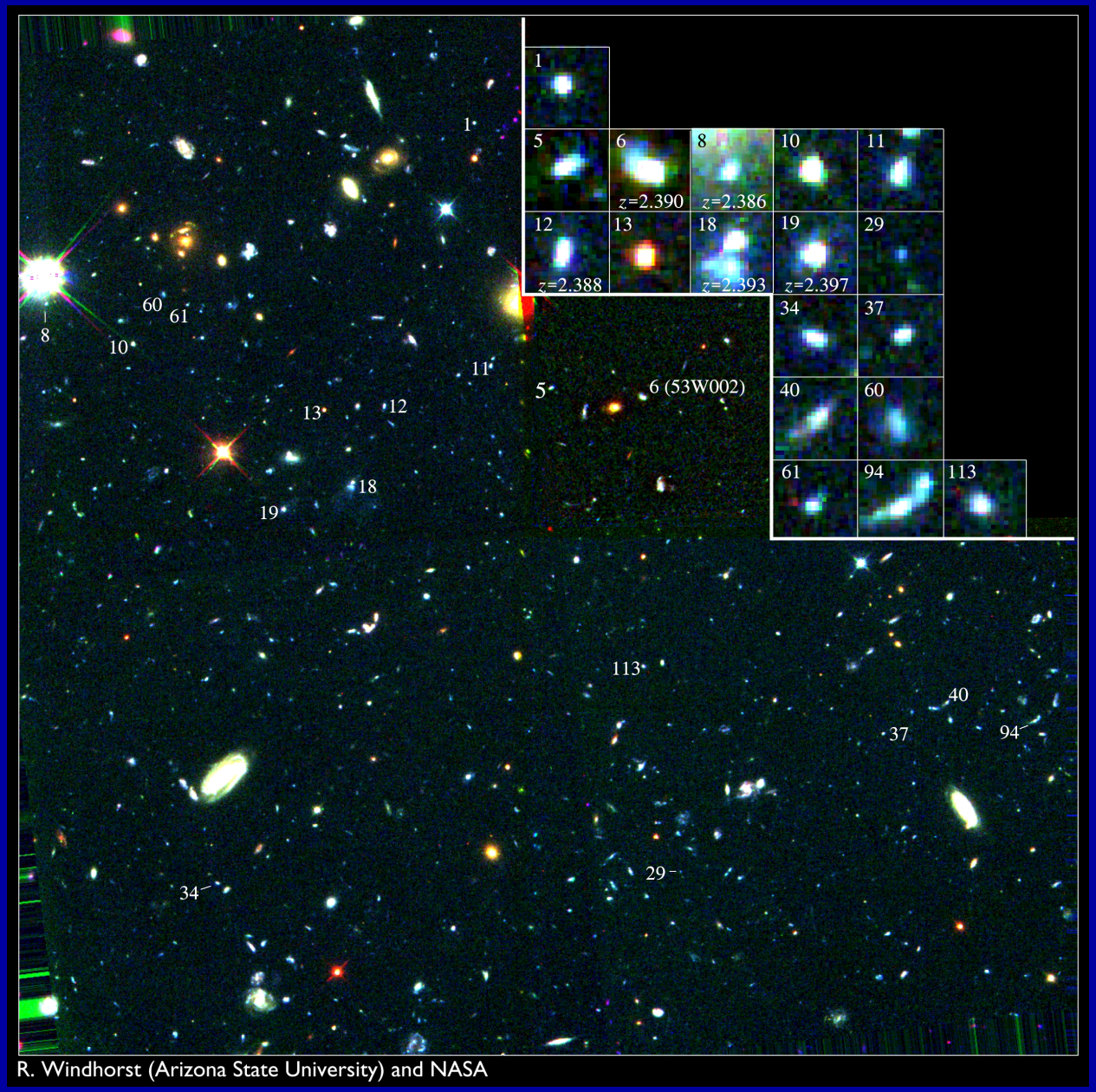

One of the remarkable discoveries of HST was how numerous and small faint galaxies are — the building blocks of the giant galaxies seen today.

THE HUBBLE DEEP FIELD CORE SAMPLE ($I < 26.0$)

(1) Introduction: Hierarchical Galaxy Assembly

• HST constrained how galaxies formed over cosmic time, by measuring their distribution over rest-frame structure and type as a function of redshift.

• Galaxies of all Hubble types formed over a wide range of cosmic time, but with a notable transition around $z \simeq 0.5$–1.0:

(1) Subgalactic units rapidly merge from $z \simeq 7 \longrightarrow 1$ to grow bigger units.

(2) Merger products start to settle as galaxies with giant bulges or large disks around $z \simeq 1$. These evolved mostly passively since then, resulting in the giant galaxies that we see today.

($e.g.$, Driver et al. 1998, ApJL, 496, L93, astro-ph/9802092; Windhorst et al. 2002, ApJS, 143, 113, astro-ph/0204398).

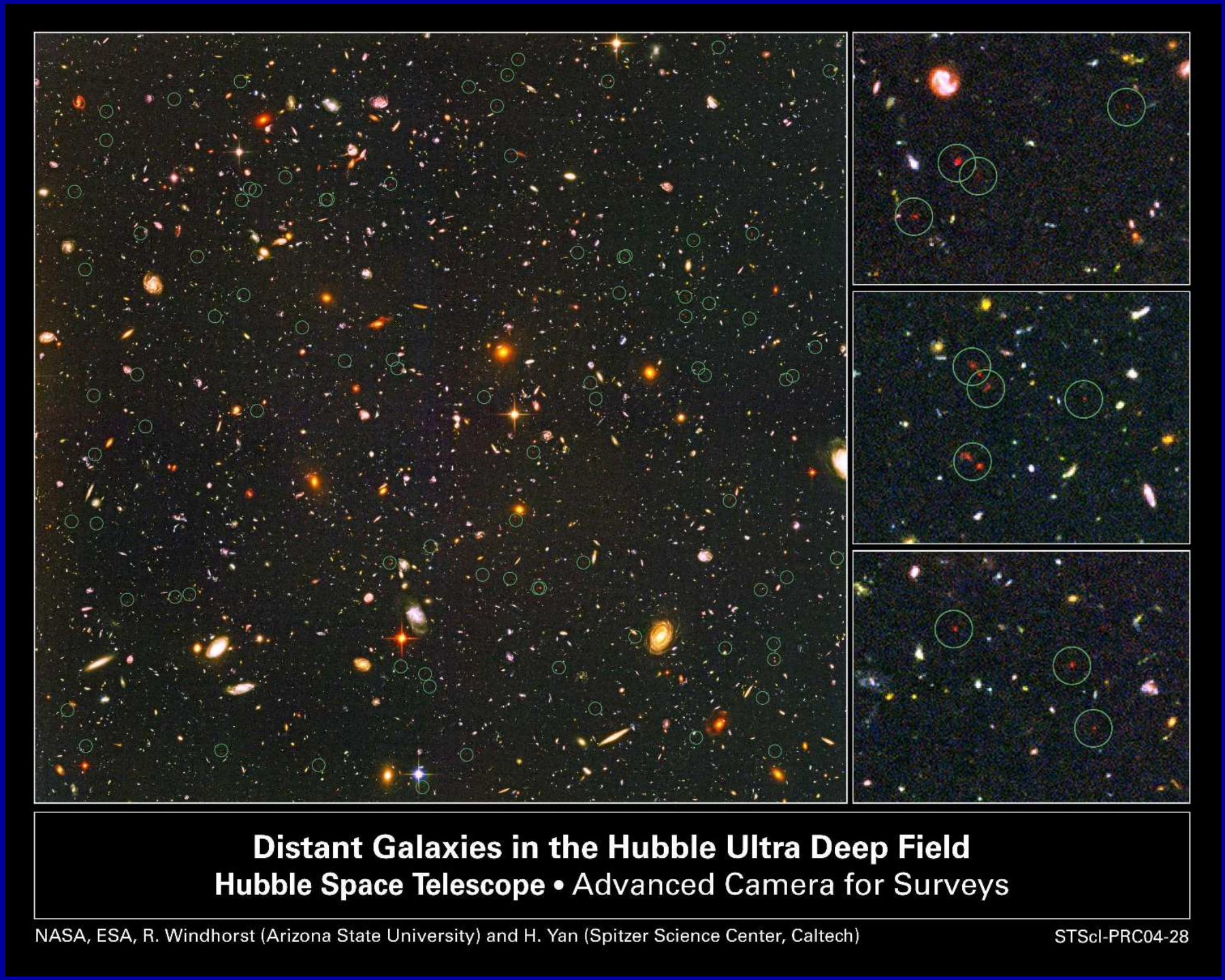

HUDF i-drops: faint galaxies at $z \simeq 6$ (Yan & Windhorst 2004), most spectroscopically confirmed at $z \simeq 6$ to AB$\lesssim$27.0 mag (Malhotra et al. 2005).

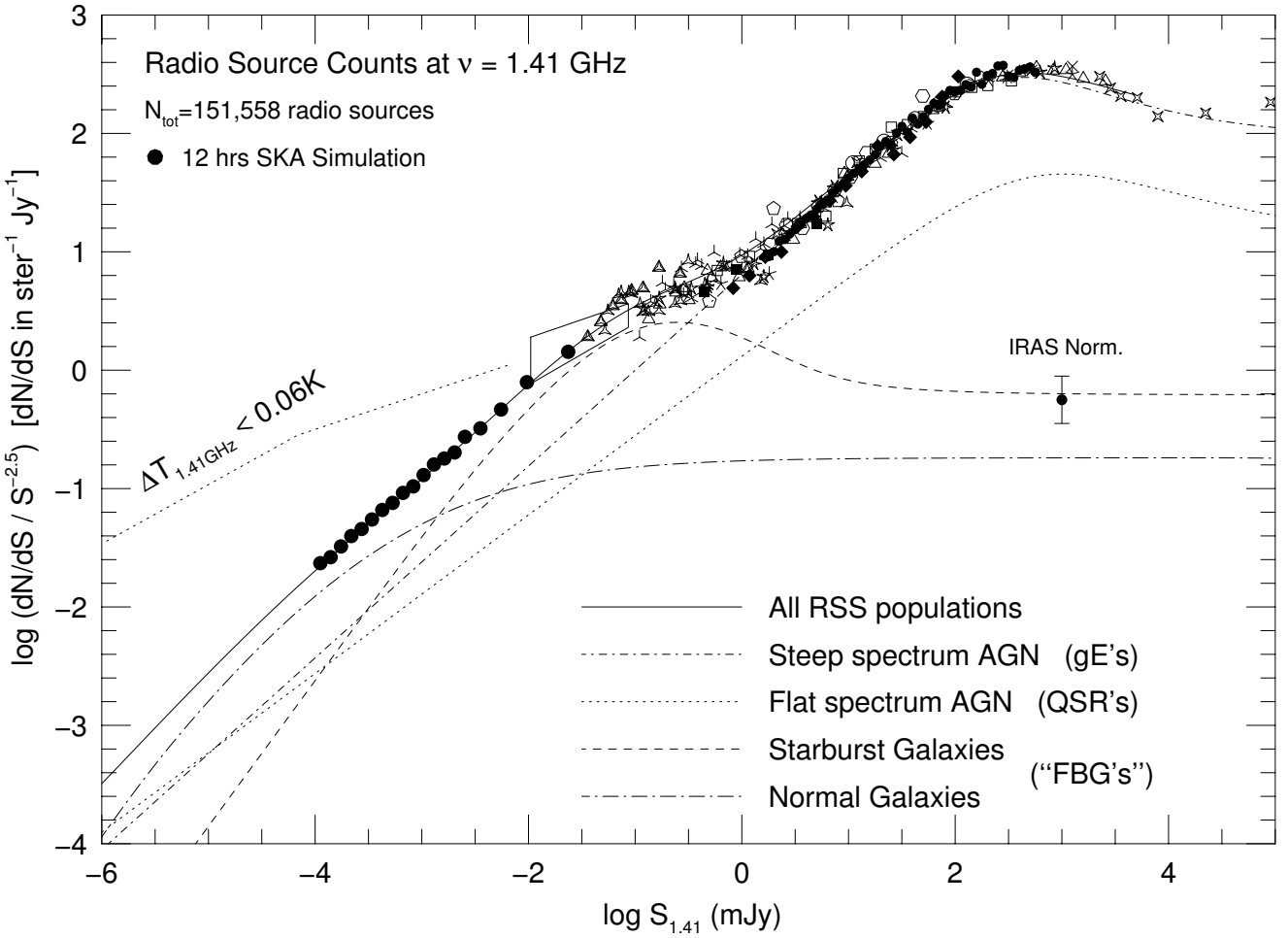

Normalized differential 1.41 GHz radio source counts (Windhorst et al. 1993, 2003; Hopkins et al. 2000) from 100 Jy down to 100 nJy. Filled circles below 10μJy show the 12-hr SKA simulation of Hopkins et al. (2000).

Models: giant ellipticals (dot-dash) and quasars dominate the counts to $\sim$1 mJy, starbursts (dashed) below 1 mJy. Spirals and starbursts (dot-long dash) will dominate the counts below 100 nJy (slope $\gamma \simeq 1.5$–1.8).

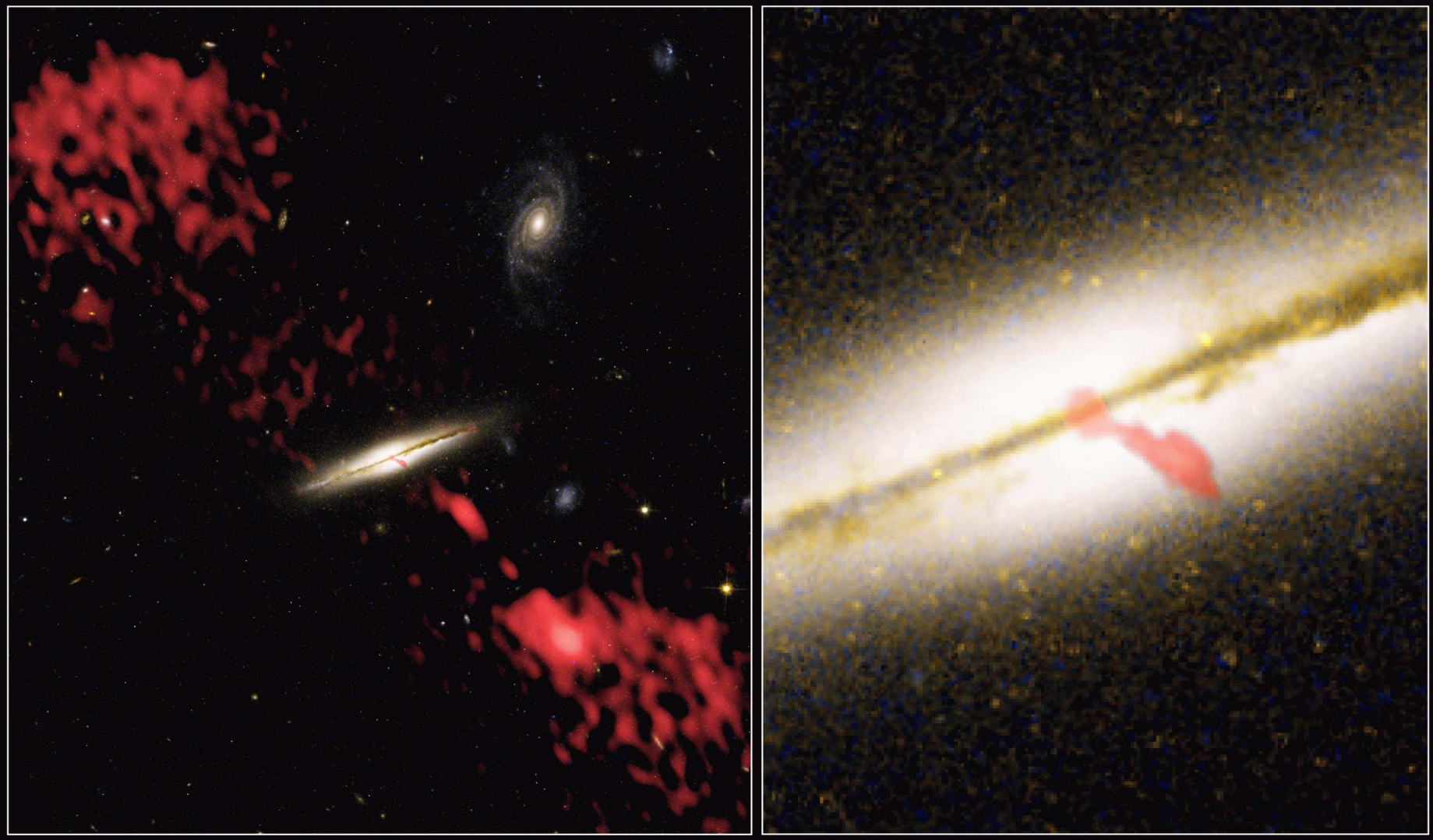

Radio Galaxy 0313-192

Hubble Space Telescope ACS WFC ▪ **Very Large Array**

NASA, NRAO/AUI/NSF and W. Keel (University of Alabama) ▪ STScI-PRC03-04

Question: How long after last (major) merger does AGN activity show?

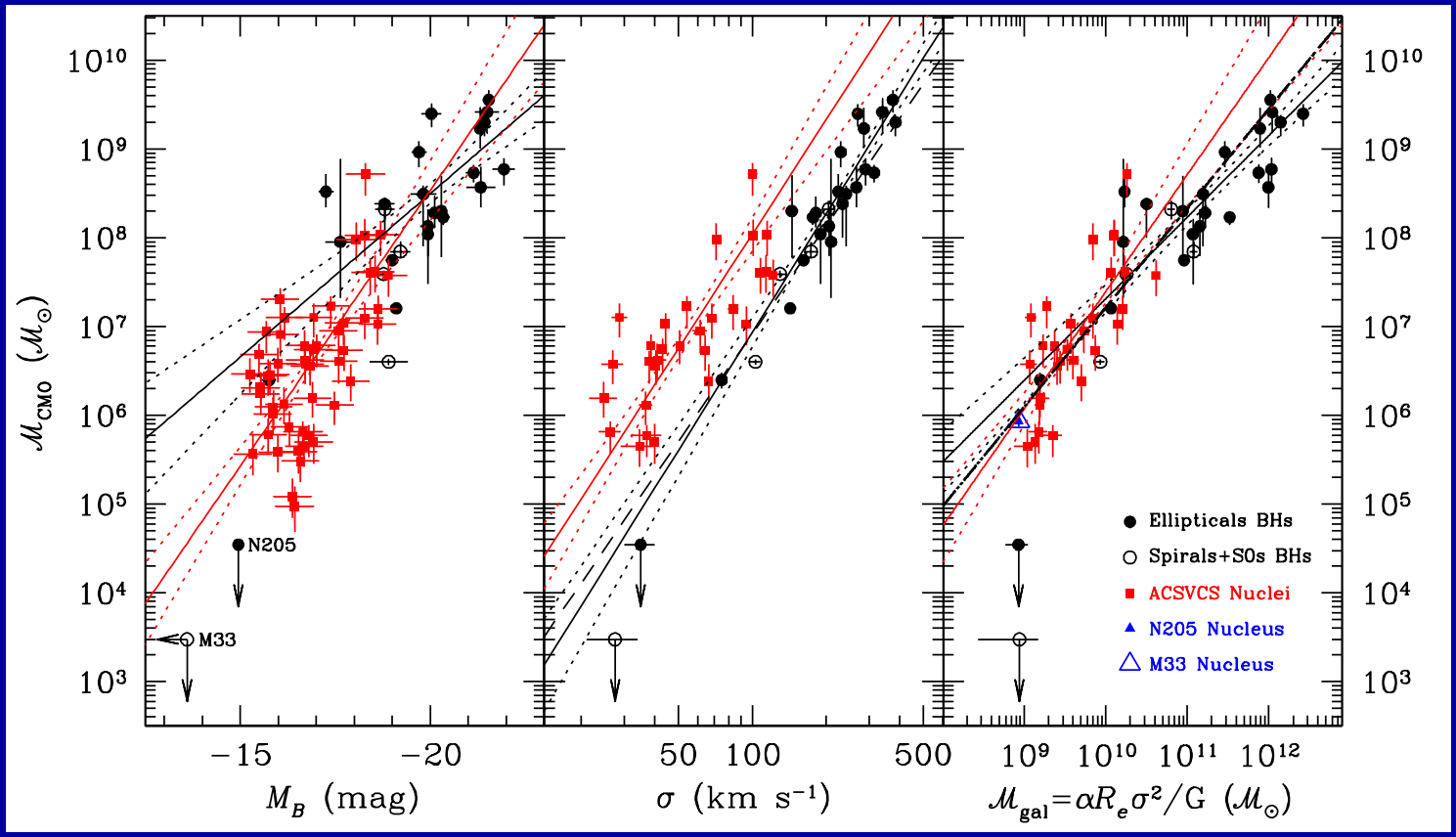

M$_{bulge}\simeq 10^{11}$ $M_\odot$ yields M$_{smbh}\simeq 10^{8.3}$ $M_\odot$ (Ferrarese et al. 2006).

$\Rightarrow$ On average $\sim$0.2% of bulge mass ends up in central SMBH.

QUESTIONS: If all galaxies & SMBHs formed by hierarchical merging:

- (1) How exactly did SMBH growth keep pace with galaxy assembly?
- (2) How do we observe this (since we don't live long enough)?

Growing a $\sim$100 $M_\odot$ Pop III star BH at z$\sim$15 into a 10^9 $M_\odot$ SMBH at z=0 takes 23 equal-mass mergers, or one every $\sim$0.6 Gyr.

(2) A study of Tadpole Galaxies in the HUDF

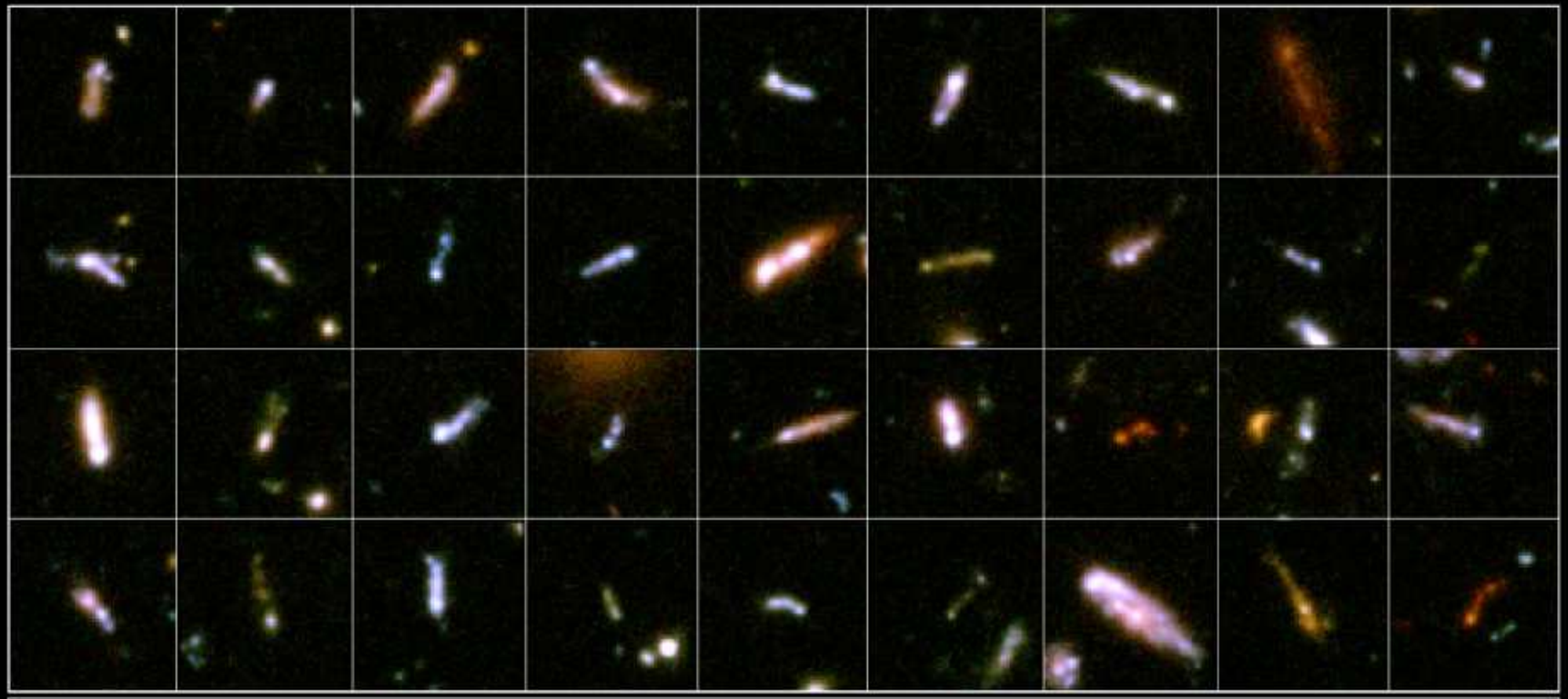

"Tadpole" Galaxies in the Hubble Ultra Deep Field
Hubble Space Telescope ▪ ACS/WFC

NASA, ESA, A. Straughn, S. Cohen and R. Windhorst (Arizona State University), and the HUDF team (STScI) STScI-PRC06-04

Tadpole galaxies in HUDF: www.hubblesite.org/newscenter/archive/2006/04/

Straughn, A. N., et al. 2006, ApJ, 639, 724 (astro-ph/0511423)

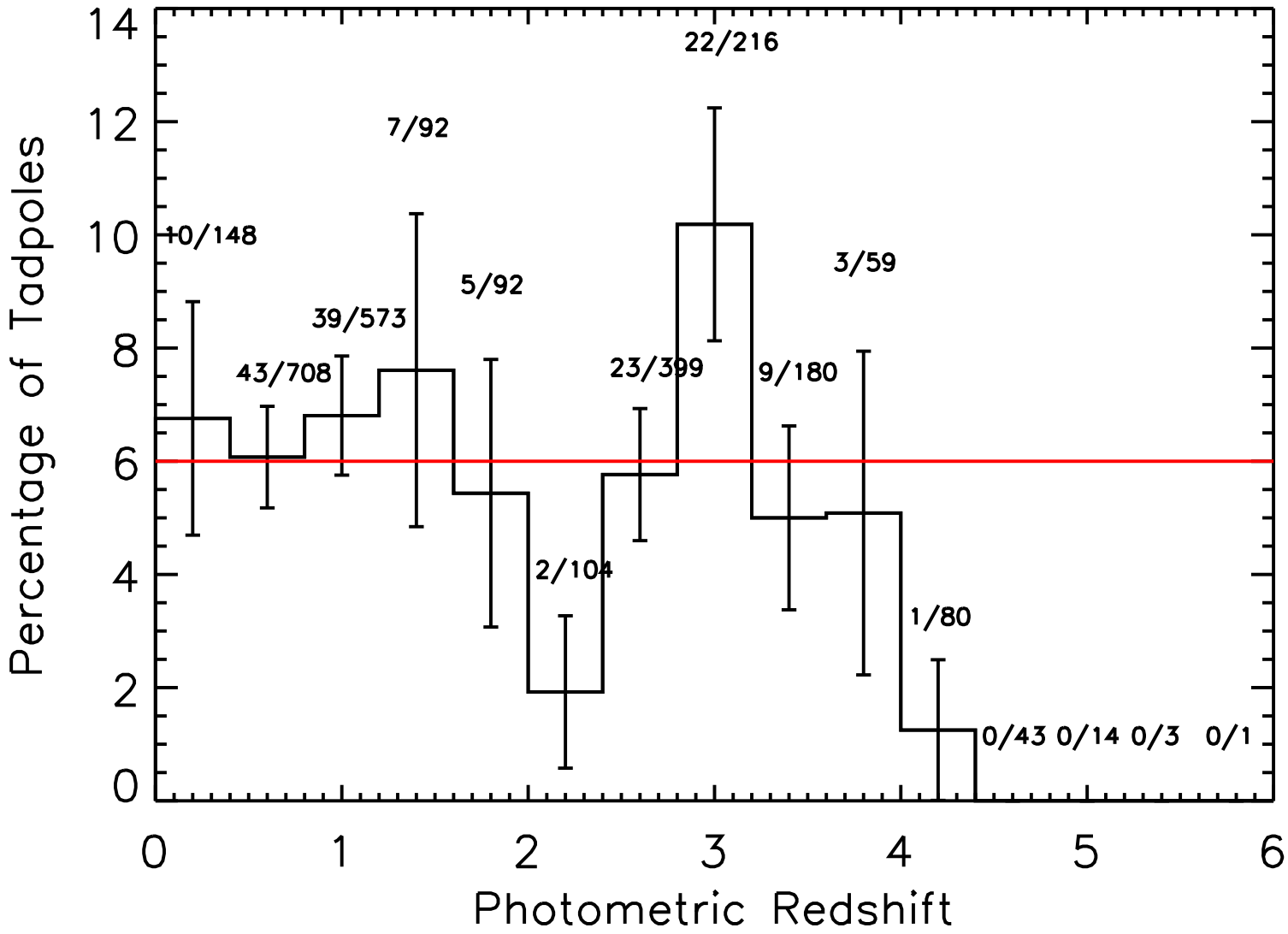

Fractional redshift distribution of tadpoles compared to all HUDF galaxies.

- To first order, shape of tadpole galaxy redshift distribution is the same as that of field galaxies: average $N(z)_{tadpoles} \simeq 6\% \cdot N(z)_{field}$.

(3) A Study of Variable Objects in the HUDF

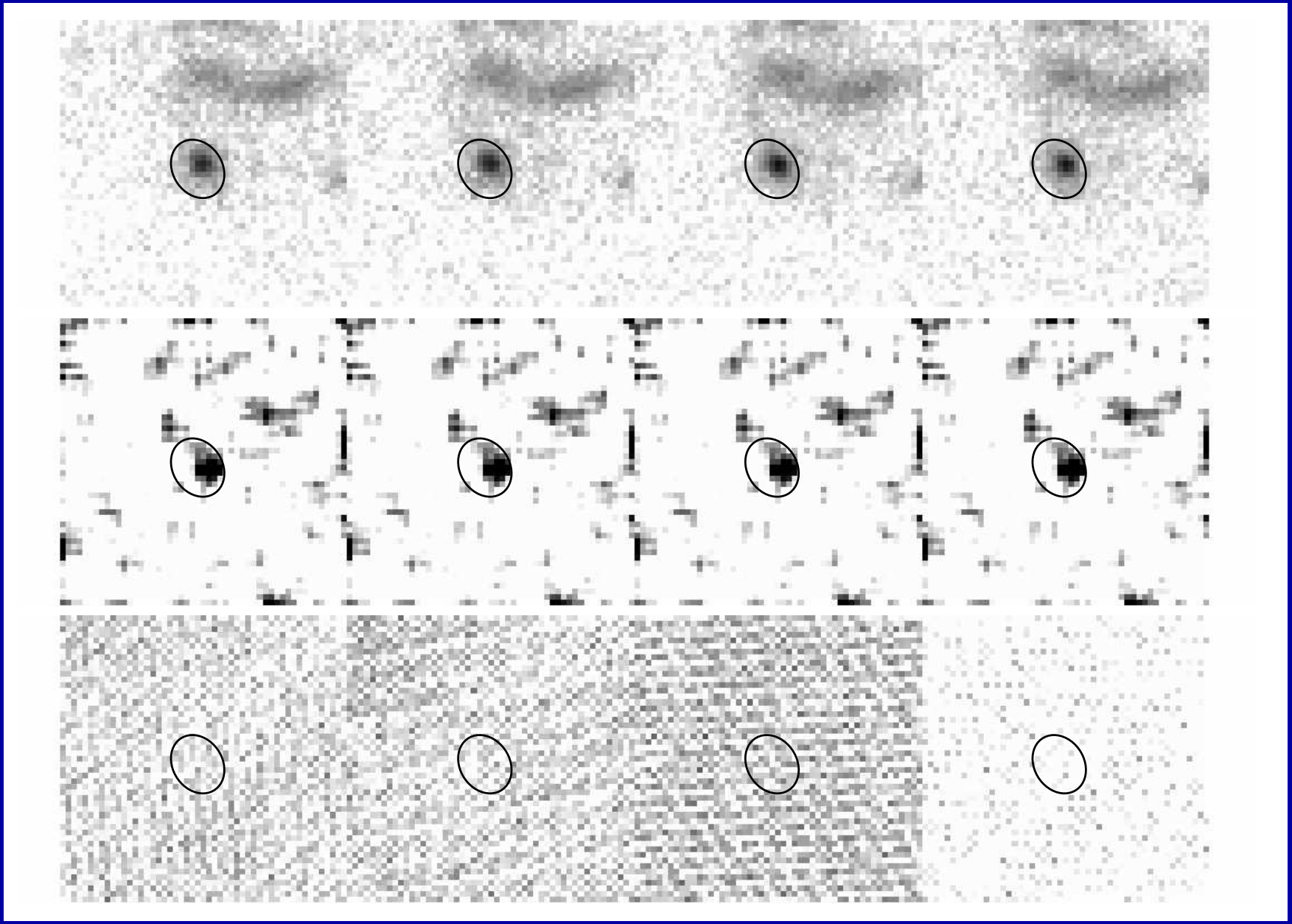

Top: 4 HUDF Epochs; Middle: 1 Variance map; Bottom: 4 Weight-maps.

Cohen, S. H., et al. 2006, ApJ, 639, 731 (astro-ph/0511414)

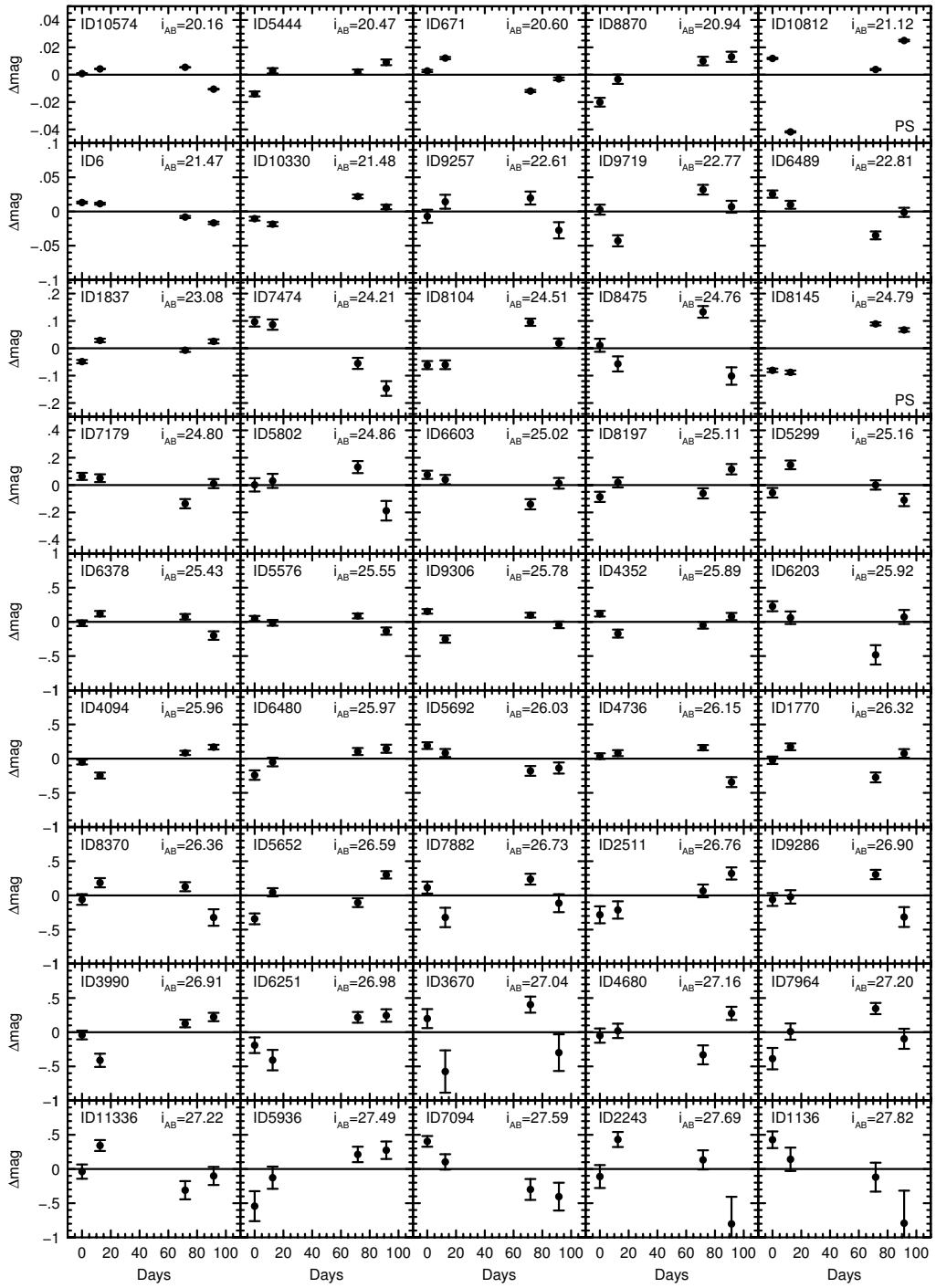

- Light curves: Can detect bright HUDF variables if $|\Delta\text{mag}| \lesssim 1$–$2\%$!

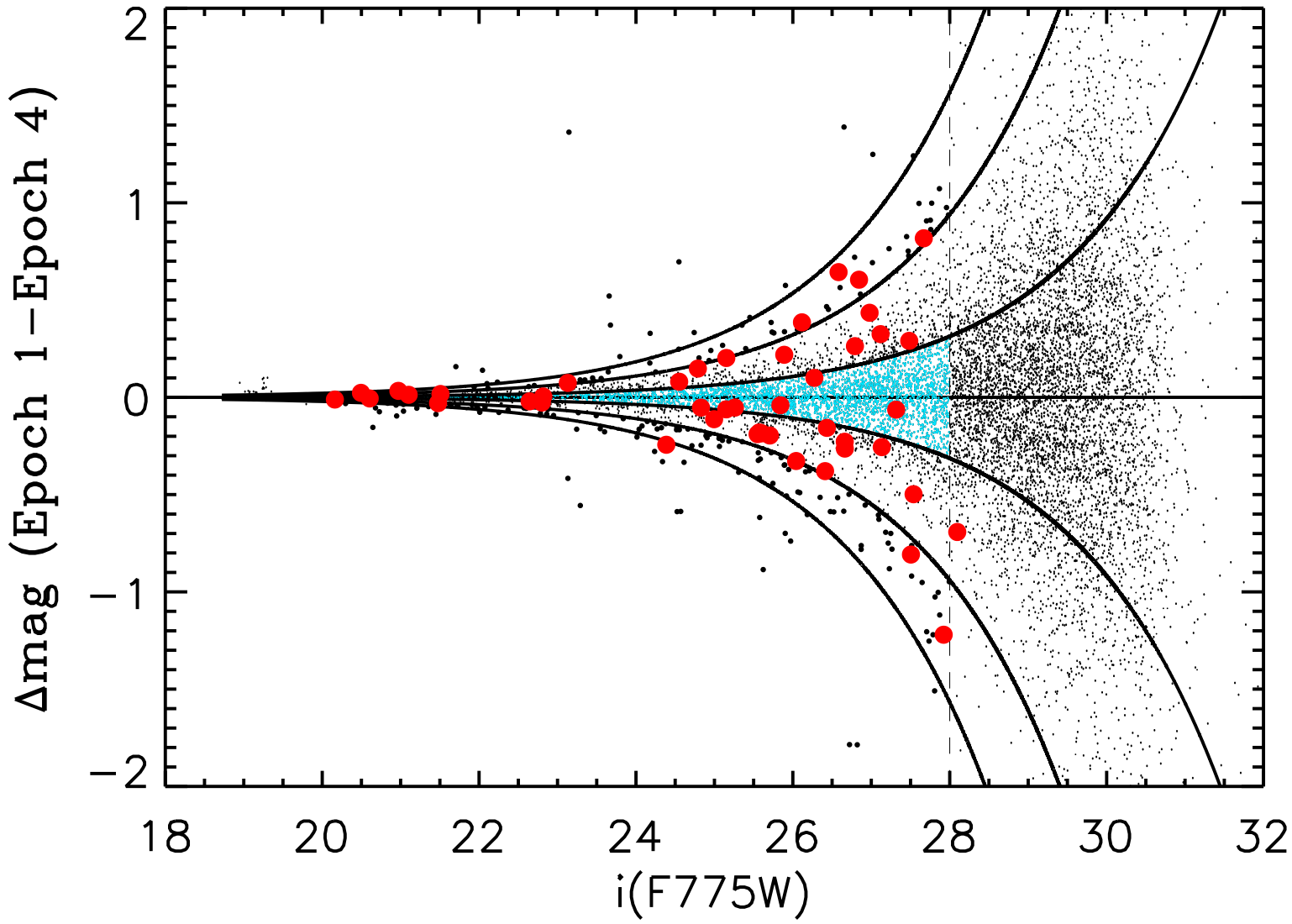

Flux ratio of all objects between two HUDF epochs (Δt$\simeq$few weeks–months) vs. total i-band flux. Lines are at $\pm 1.0\sigma$ (blue), $\pm 3.0\sigma$, $\pm 5.0\sigma$.

- All objects with |Delta mag|$\geq 3.0\sigma$ were inspected for plausible variability. This will yield $\lesssim$13 bogus detections if the noise were purely Gaussian.

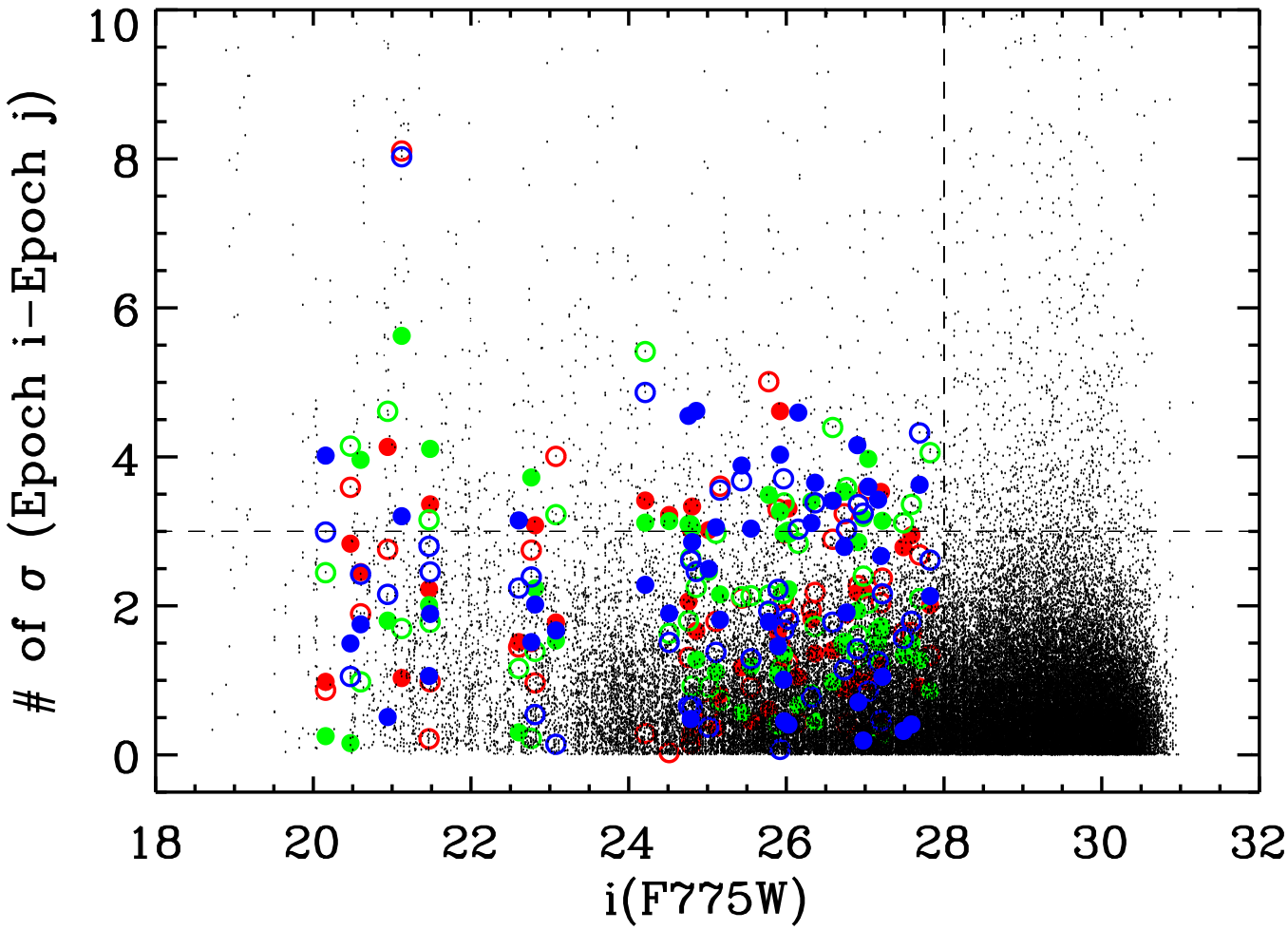

- 3 out of 16 Chandra sources are faint point-like variable objects at $\gtrsim 3.0\sigma$.
- Other 13 Chandra sources are mostly brighter (early-type) galaxies, one is $\gtrsim 3.0\sigma$ variable $\Rightarrow$ Variable point sources are valid AGN candidates.
- We only sample ΔFlux $\gtrsim$10%—30% on timescales of months. The AGN sample is not complete — we miss all non-variable and obscured AGN.

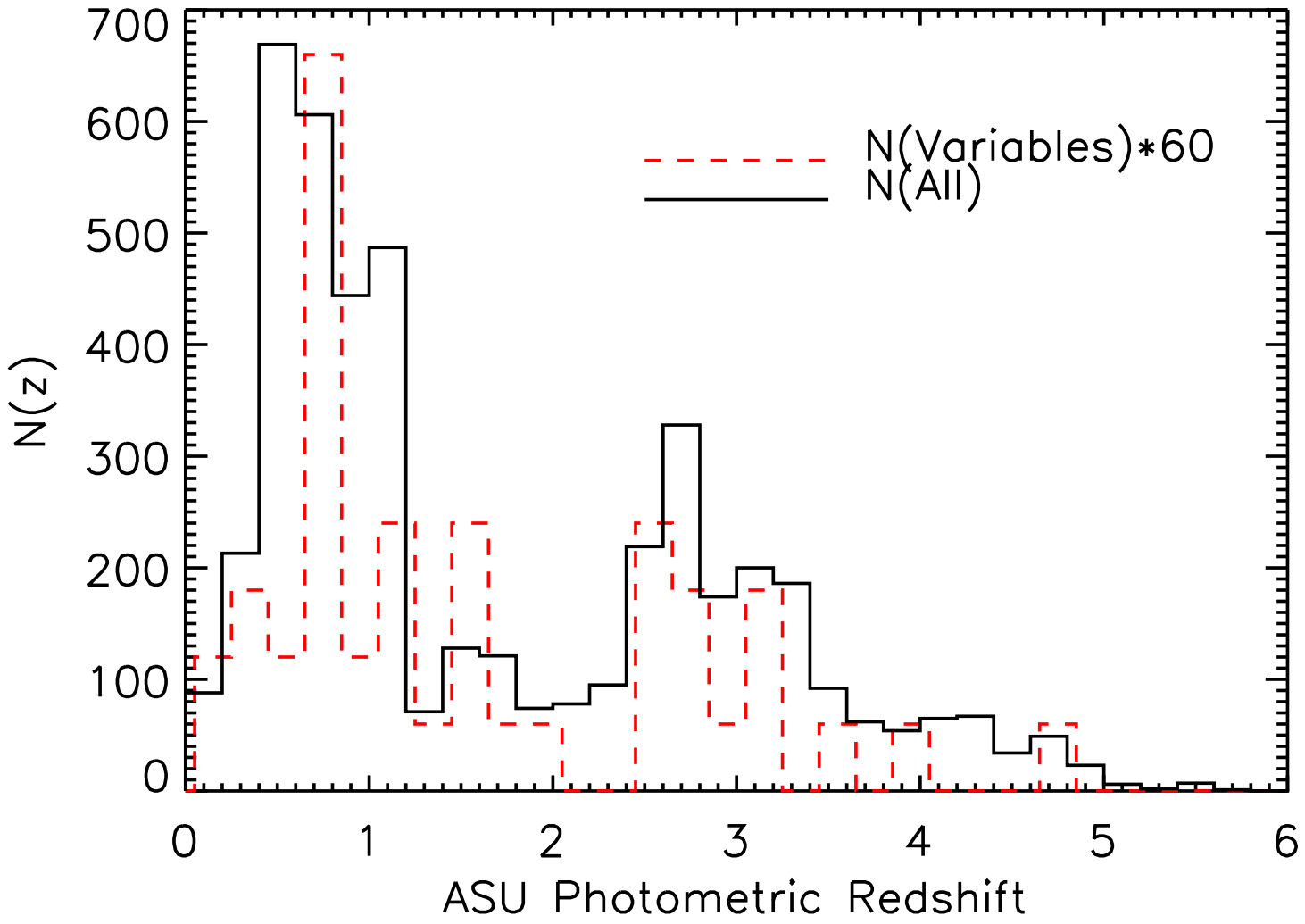

BViz(JH) Photo-z distribution of HUDF field gxys and variable objects:

- Variable objects show a similar N(z) as field galaxies. About 1% of all field galaxies have variable weak AGN at all redshifts.

$\Rightarrow$ If variable objects are representative of all weak AGN, SMBH growth keeps pace with the cosmic SFR (which peaks at $z \simeq 1$–2).

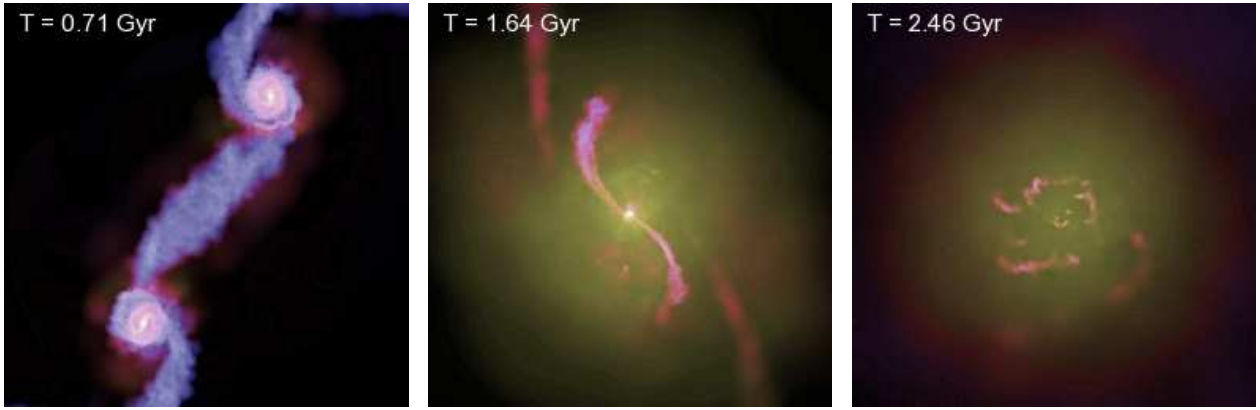

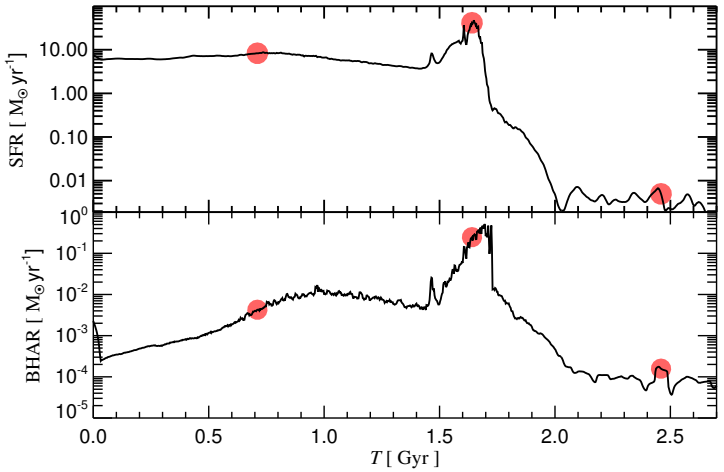

• [LEFT] Simulated merger of two disk galaxies at three different times, including the effects of SMBH growth and AGN feedback by Springel, di Matteo, Hernquist (2005, ApJ, 620, 79). Shown is the gas distribution with color indicating temperature, and brightness indicating gas density.

• [RIGHT] Evolution of the accretion rate onto the SMBH (top) and the SF-rate (bottom). Red dots mark the times of the three images.

• Overlap between Tadpoles and Variables is very small — 1 object!

$\Leftrightarrow$ In hydrodynamical simulations, the object resembles a tadpole galaxy $\sim$0.7 Gyr after the merger starts, the AGN is triggered and expels the dust $\gtrsim$1.6 Gyr after the merger starts, $i.e.$, $\gtrsim$1 Gyr after the tadpole stage.

(4) Epoch dependent major merger rate to AB$\lesssim$27 mag.

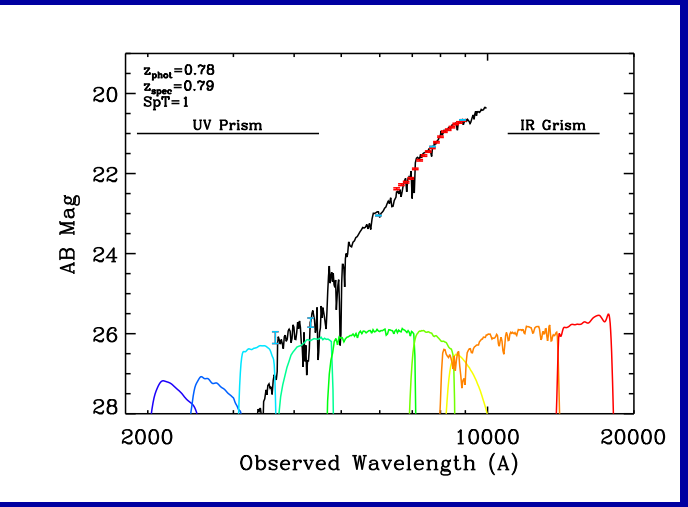

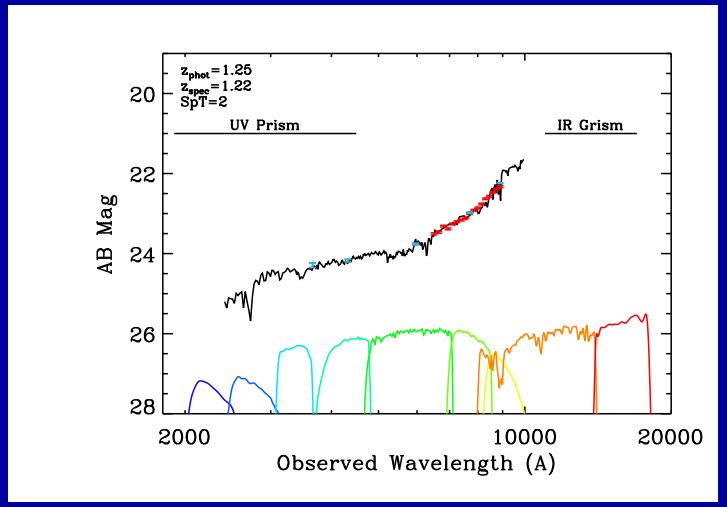

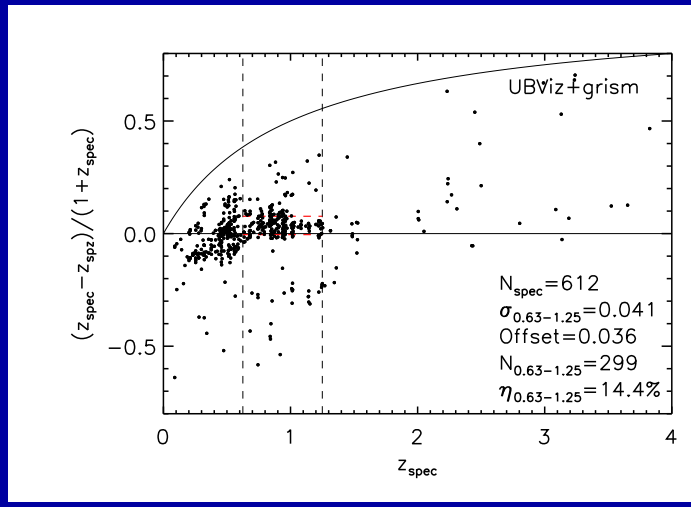

Ryan et al. (2007, ApJ, 668, 83; astro-ph/0703743), Cohen et al. (2008):

- (a) Spectro-photo-z's from HST grism + BViz(JH) considerably more accurate than photo-z's alone, with much smaller catastrophic failure %.
- (b) Redshifts for $\gtrsim$13,000 objects to AB$\gtrsim$27–27.5 mag with $\sigma_z/(1+z)\lesssim 0.04$.
- Expect $\sigma_z/(1+z)\lesssim$0.02–0.03 with new capabilities of WFC3: UV and near-IR broad-band imaging and low-res grism spectra.

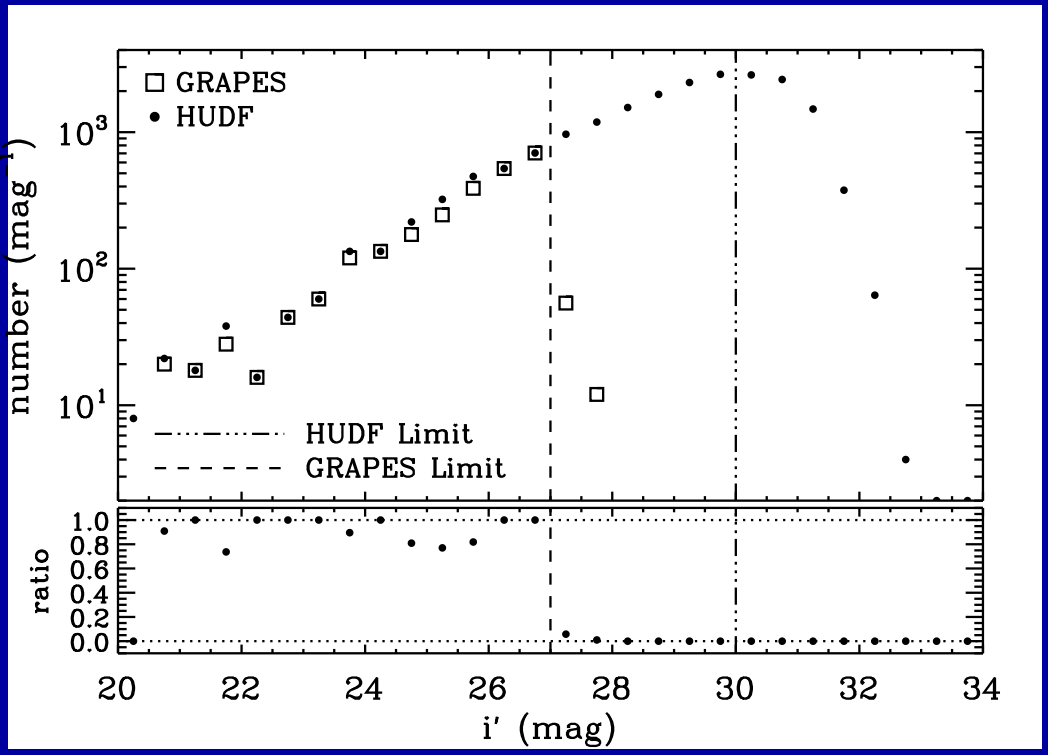

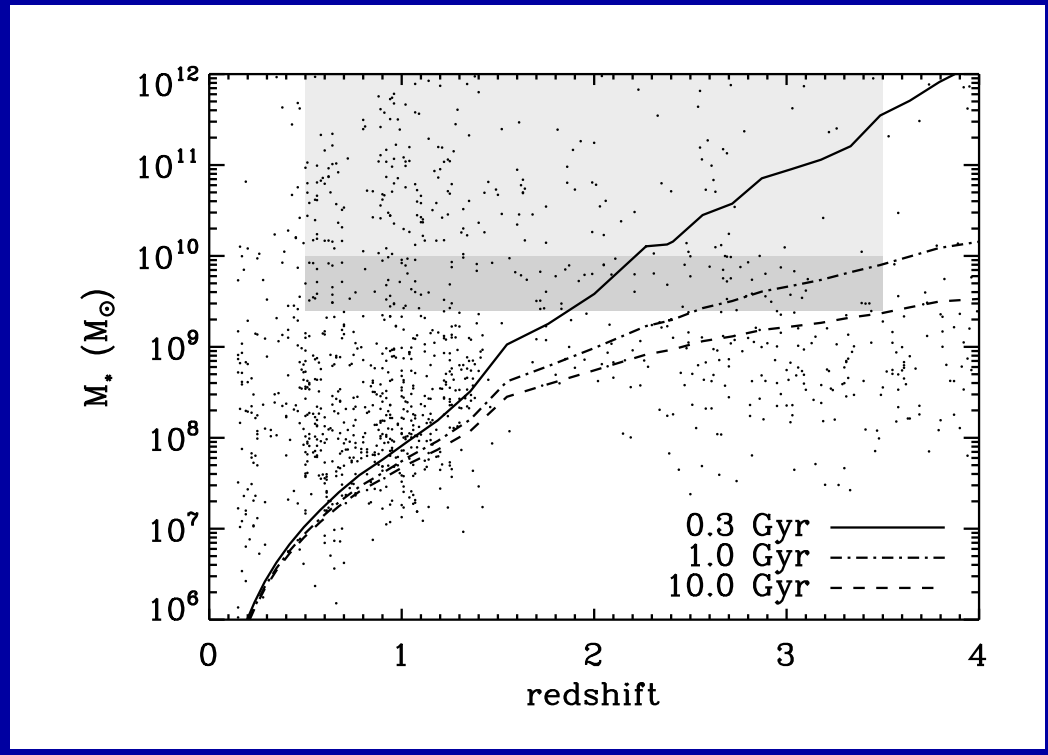

Ryan et al. (2007): HST/ACS grism pair-fraction(z) — sample selection:

- HUDF broad-band point source completeness at $i_{AB} \lesssim$30.0 mag.
- HUDF ACS grism point source completeness at $i_{AB} \lesssim$27.0 mag

Mass completeness limit for z$\lesssim$2 from flux limits/SED fitting:

- M$\gtrsim 10^{10.0}\ M_\odot$ for primary galaxy mass in pair.
- M$\gtrsim 10^{9.4}\ M_\odot$ for secondary galaxy mass in pair (0.25$\leq$M$_2$/M$_1\leq$1).

(4) Epoch dependent major merger rate to AB$\lesssim$27, X-ray n(z)

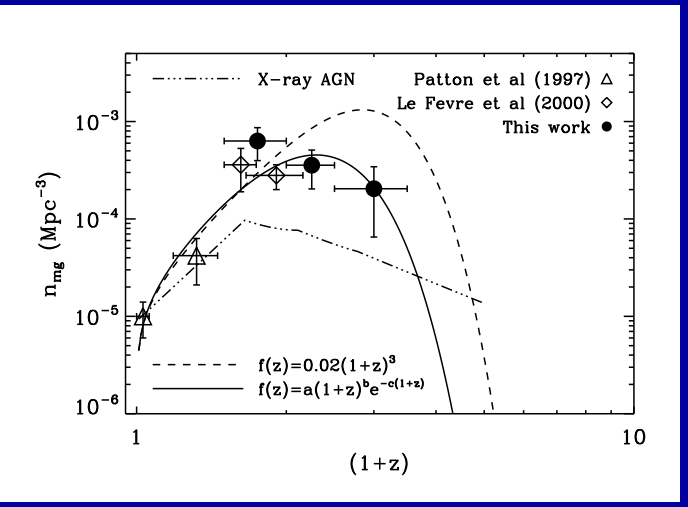

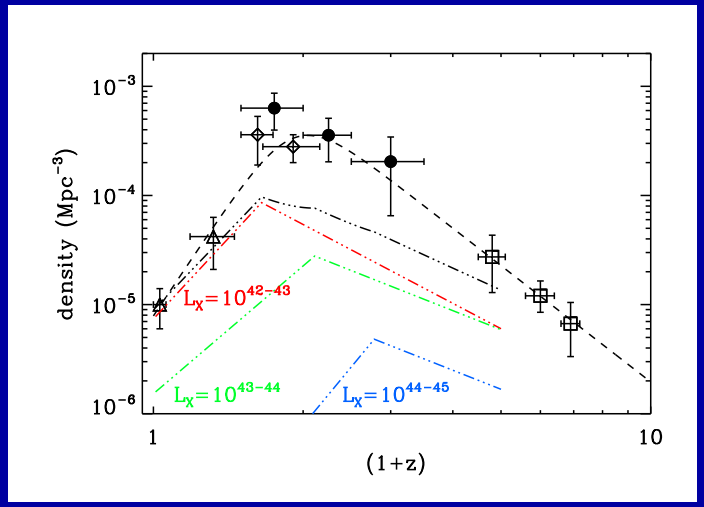

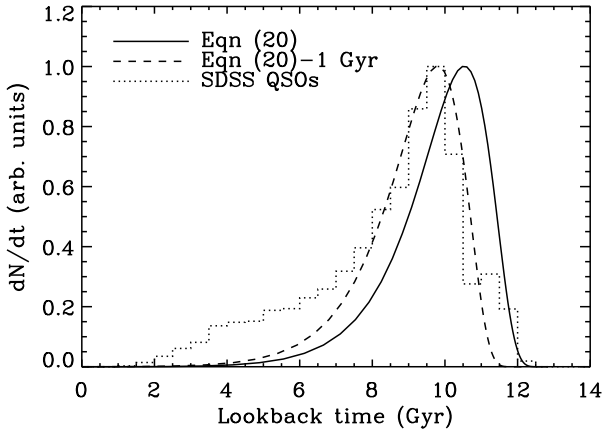

Ryan et al. (2007, 2008): HST/ACS grism epoch-dependent galaxy pairs fraction for AB$\lesssim$27, z$\lesssim$6: spectro-photo-z's for both objects in pair.

Galaxy major ($0.25 \leq M_2/M_1 \leq 1$) merger density compared to Chandra SDSS QSO density vs. epoch: similar curves except for $\sim$1 Gyr offset?

$\Rightarrow$ Qualitatively supports the presented picture: there may be a $\sim$1 Gyr delay between major mergers and visible SMBH feeding — AGN.

• The Beast feeds like fireflies in the night, and well after the Beauty produces its spectacular galaxy merging ...

(5) Ages of radio and X-ray hosting galaxies vs. epoch.

1) DATA: HST GOODS BVizJHK photometry and VLT JHK + redshifts.

2) METHOD: SED fitting for 0.12$\lesssim\lambda_{rest}\lesssim$1.6 μm, using:

- (a) Bruzual-Charlot (2003) stellar population models.
- (b) + AGN power law $S_\nu \propto \nu^\alpha$ bluewards of the IR dust emission.
- VLT redshifts for all objects AB$\lesssim$24–25 (Le Fèvre et al. 2004; Szokoly et al. 2004; Vanzella et al. 2005, 2008; see www.eso.org/science/goods/)

For typical z$\simeq$0.5-1.5, BVizJHK bracket the Balmer+4000Å breaks.

3) SED fitting:

- Use solar metallicity and Salpeter IMF (most objects at z$\lesssim$2).
- E-folding times τ in log spaced n=16 grid from 0.01-100 Gyr.
- n=244 ages $\lesssim$ age of Universe at each redshift in WMAP-cosmology.
- Calzetti et al. dust extinction: A_V = [0, 4.0] in 0.2 mag steps (n=21).
- α=[0, 1.5] in steps of 0.1 (n=16 values).

4) Yields $\sim 10^6$ models for 1549 GOODS galaxies with VLT redshifts.

Find best fit stellar mass and possible AGN UV–optical power-law component via χ^2 minimization.

Method follows Windhorst et al. (1991, 1994, 1998), where HST + ground-based UBgriJHK images showed non-negligible AGN components in mJy radio galaxies.

5) Work in progress on other potential caveats:

- Young stellar populations have power-law UV spectra (Hathi et al. 2008), and may overestimate UV AGN power-law.

- See if incorporating 1–2 Gyr red AGB population makes a difference.

- Fit the BC03 stellar SED only to objects where χ^2 doesn't require both.

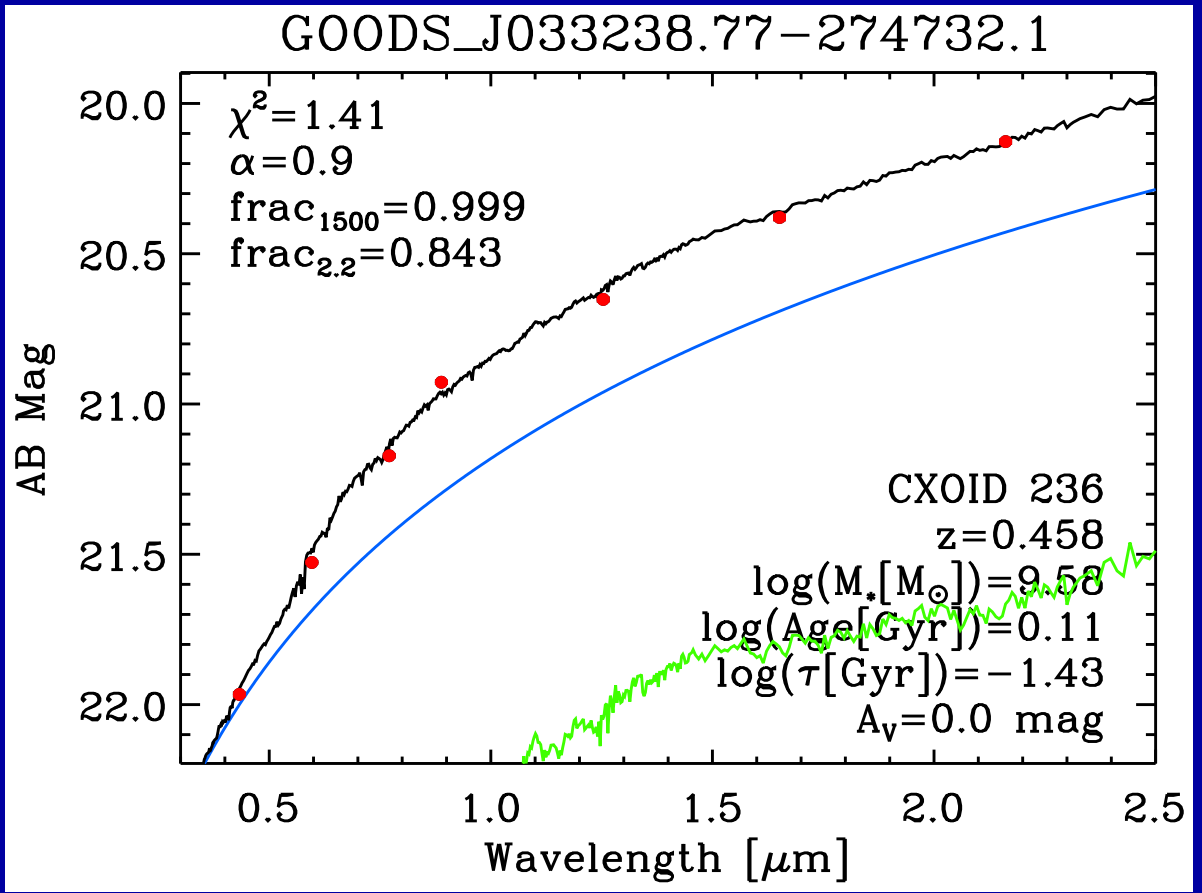

Cohen et al. (2008):

GOODS/VLT BVizJHK images

Best fit Bruzual-Charlot (2003) SED

+ power law AGN.

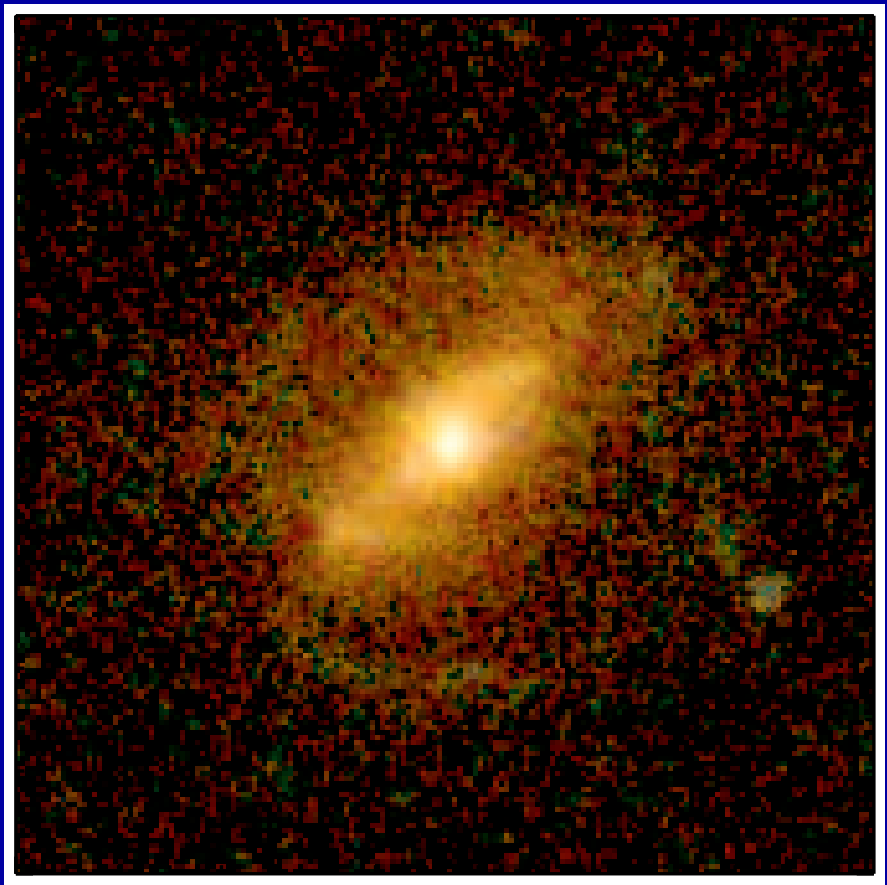

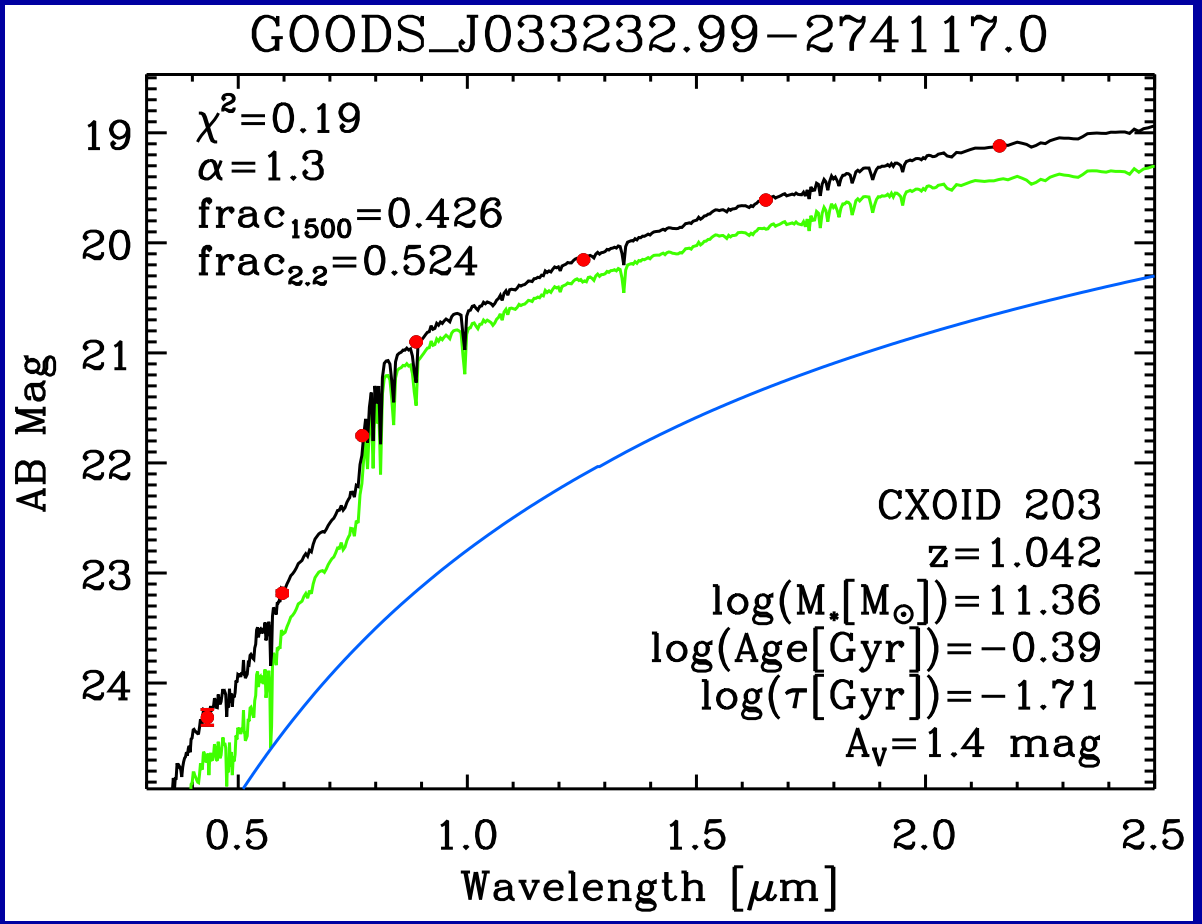

Cohen et al. (2008):

GOODS/VLT BVizJHK images

Best fit Bruzual-Charlot (2003) SED

+ power law AGN.

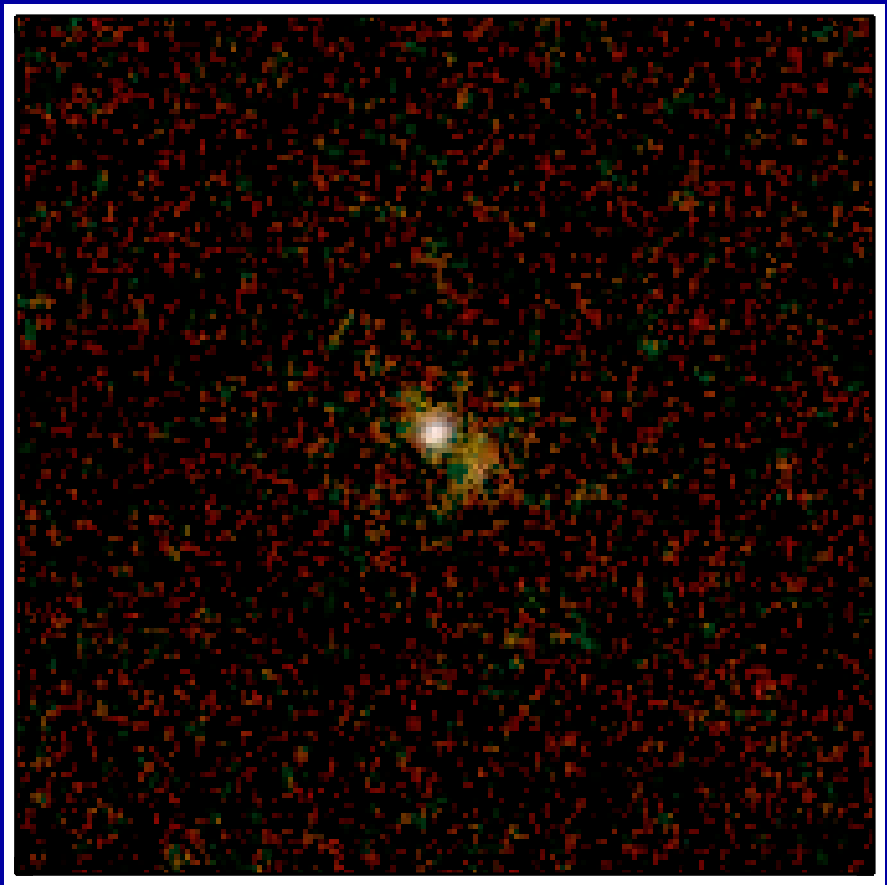

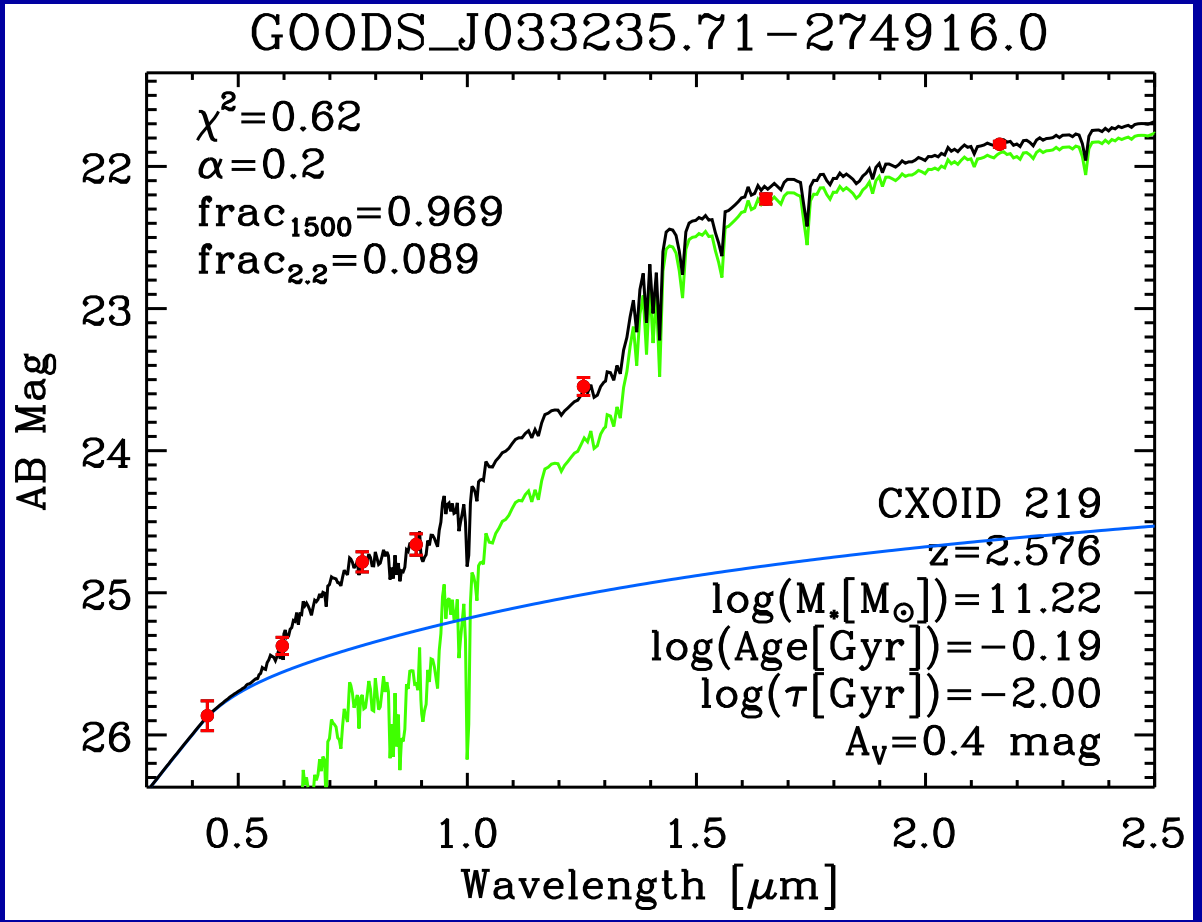

Cohen et al. (2008):

GOODS/VLT BVizJHK images

Best fit Bruzual-Charlot (2003) SED

+ power law AGN.

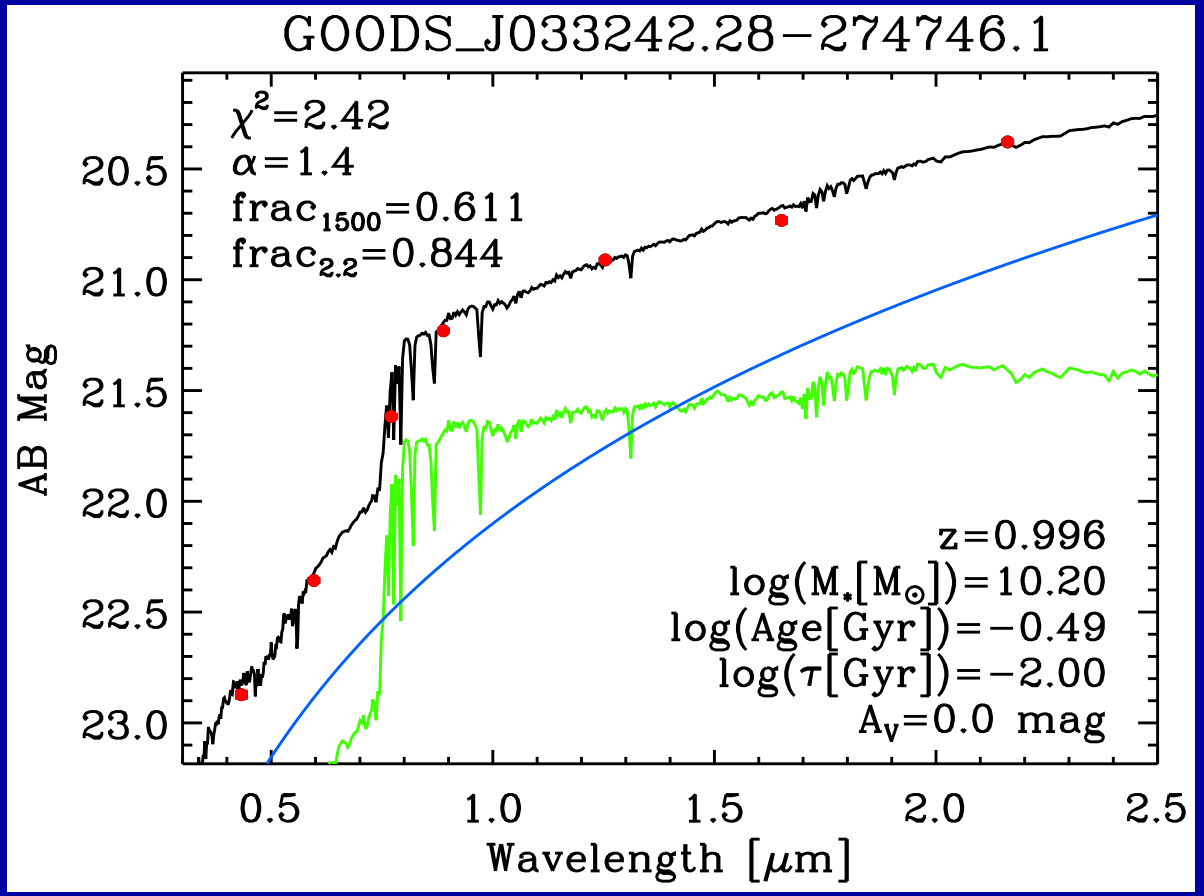

Cohen et al. (2008):

GOODS/VLT BVizJHK images

Best fit Bruzual-Charlot (2003) SED

+ power law AGN.

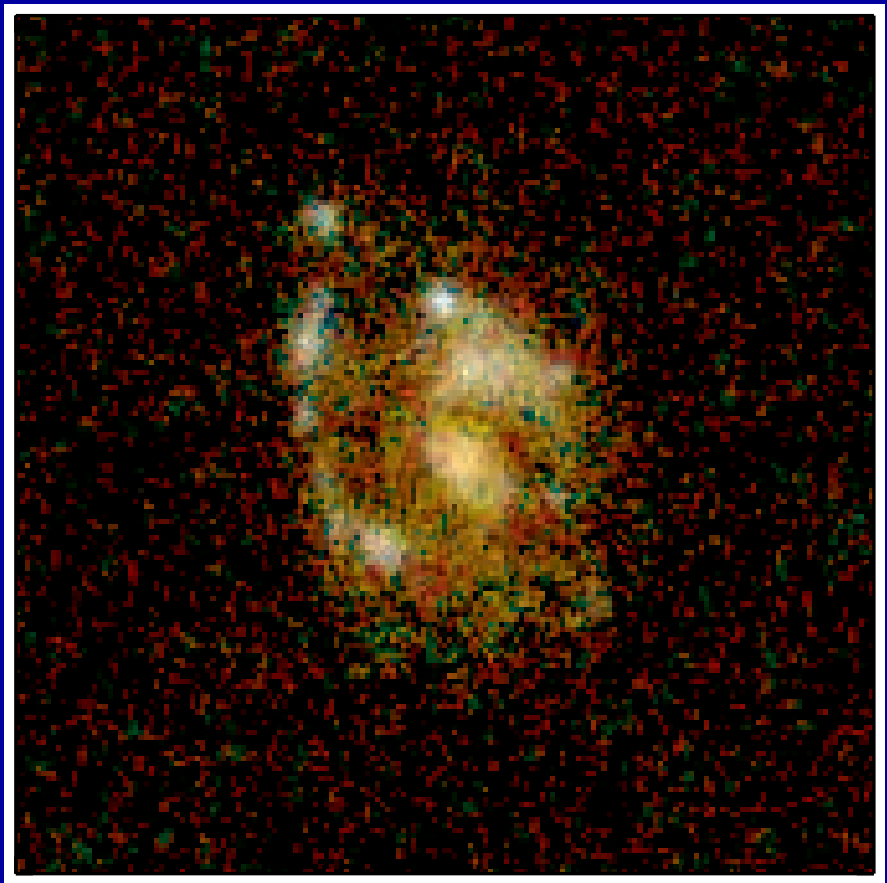

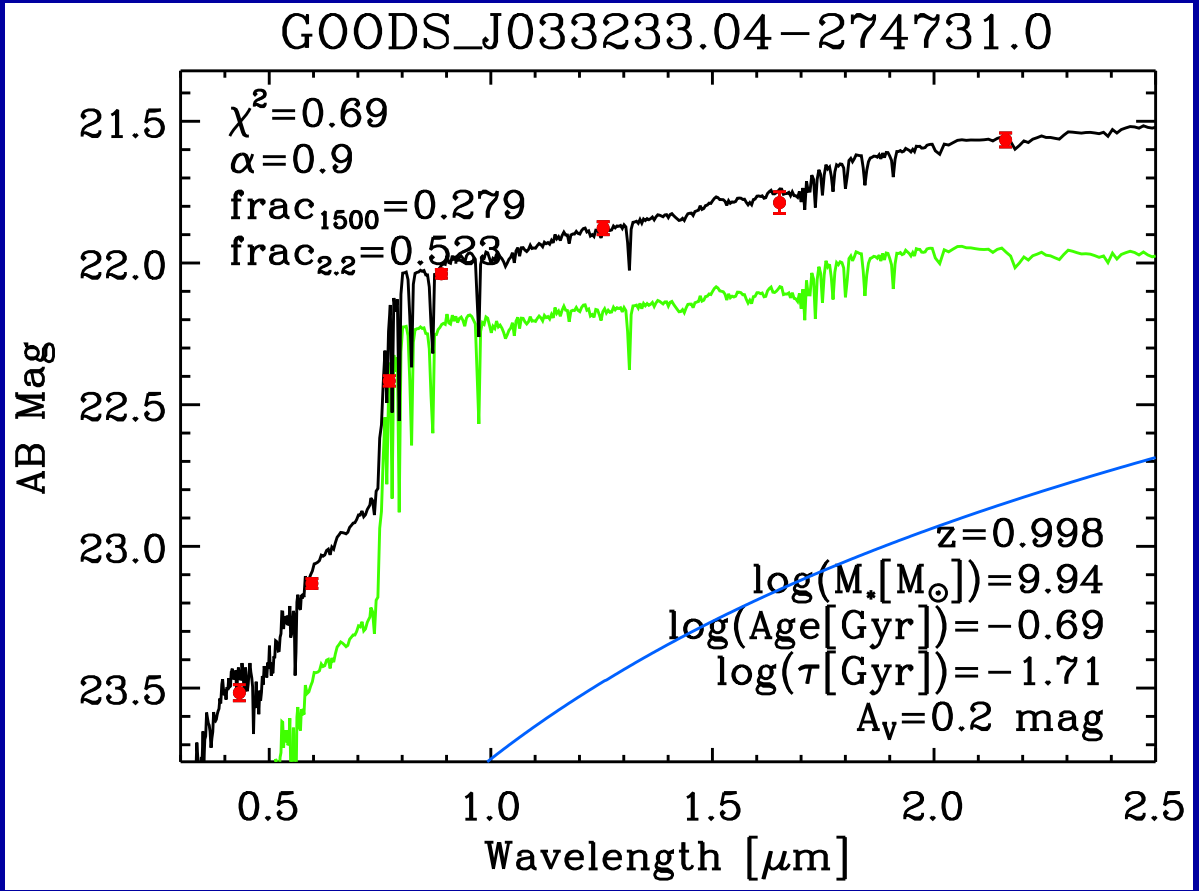

Cohen et al. (2008):

GOODS/VLT BVizJHK images

Best fit Bruzual-Charlot (2003) SED

+ power law AGN.

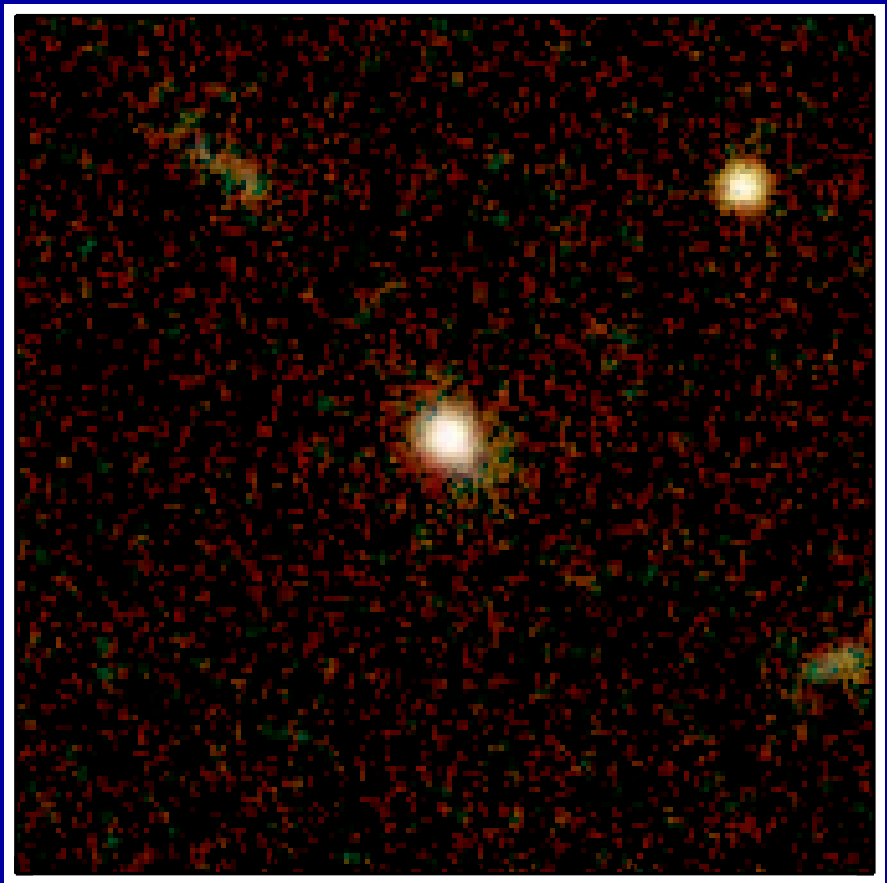

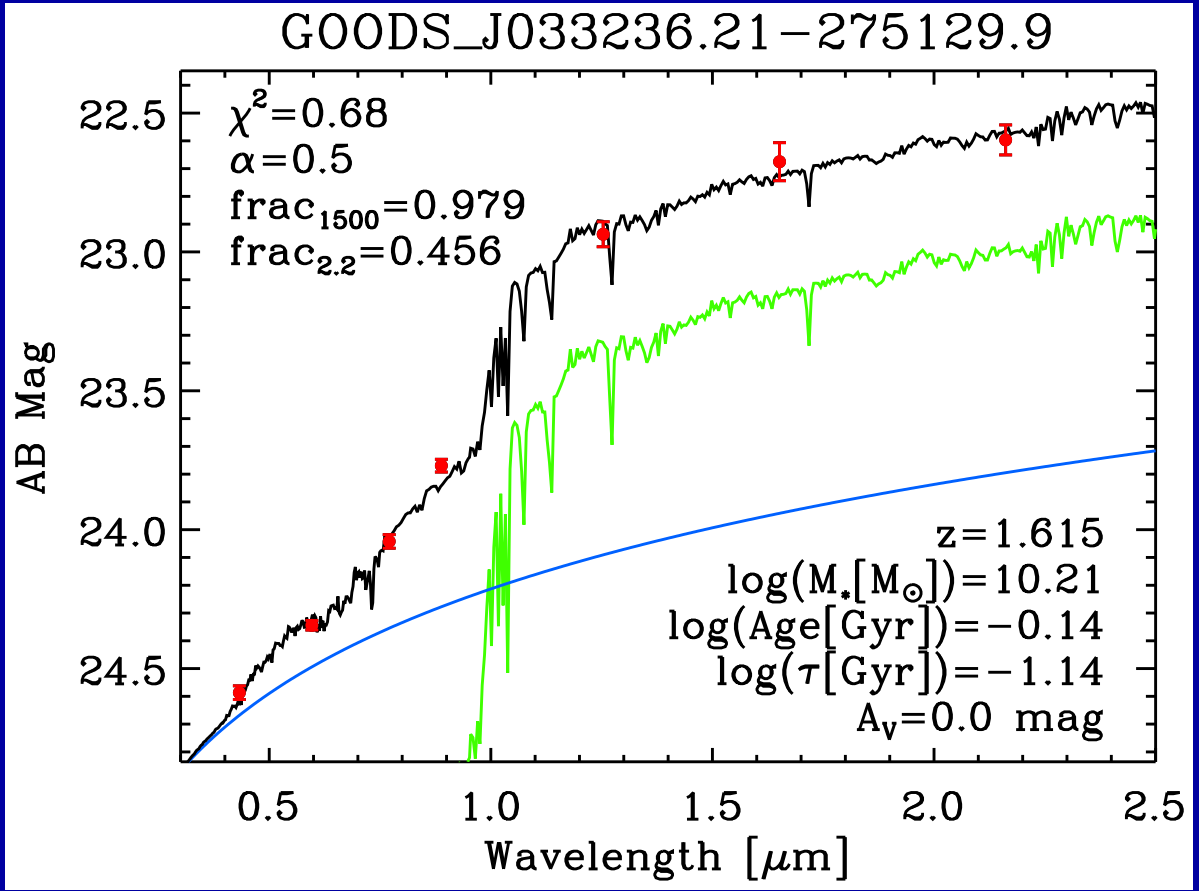

Cohen et al. (2008):

GOODS/VLT BVizJHK images

Best fit Bruzual-Charlot (2003) SED

+ power law AGN.

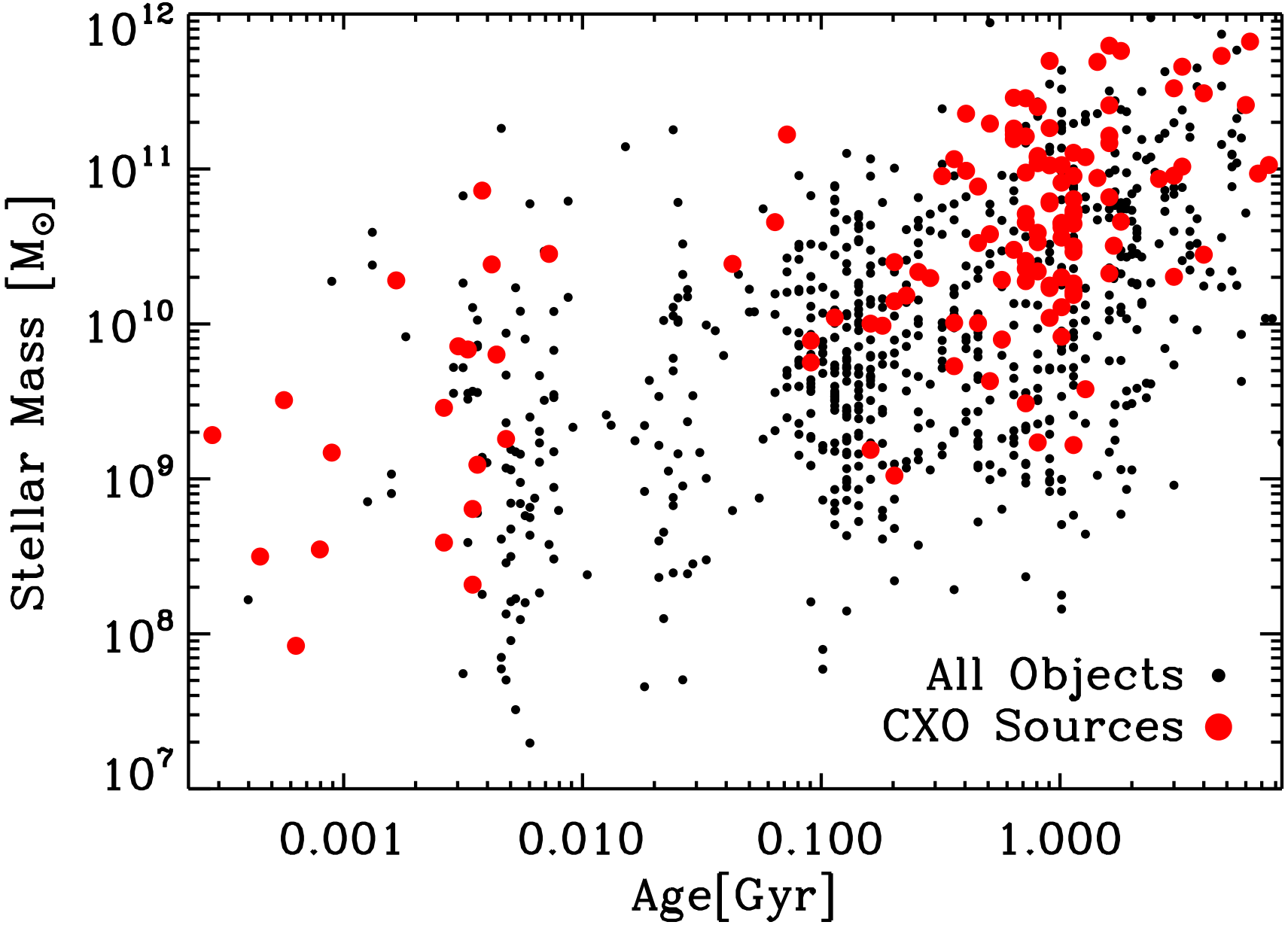

Cohen et al. (2008): Best fit Stellar Mass vs. Age: X-ray and field galaxies.

- X-ray sources reside in galaxies that are a bit older than the general field population, but by no more than $\lesssim$0.5–1 Gyr on average.

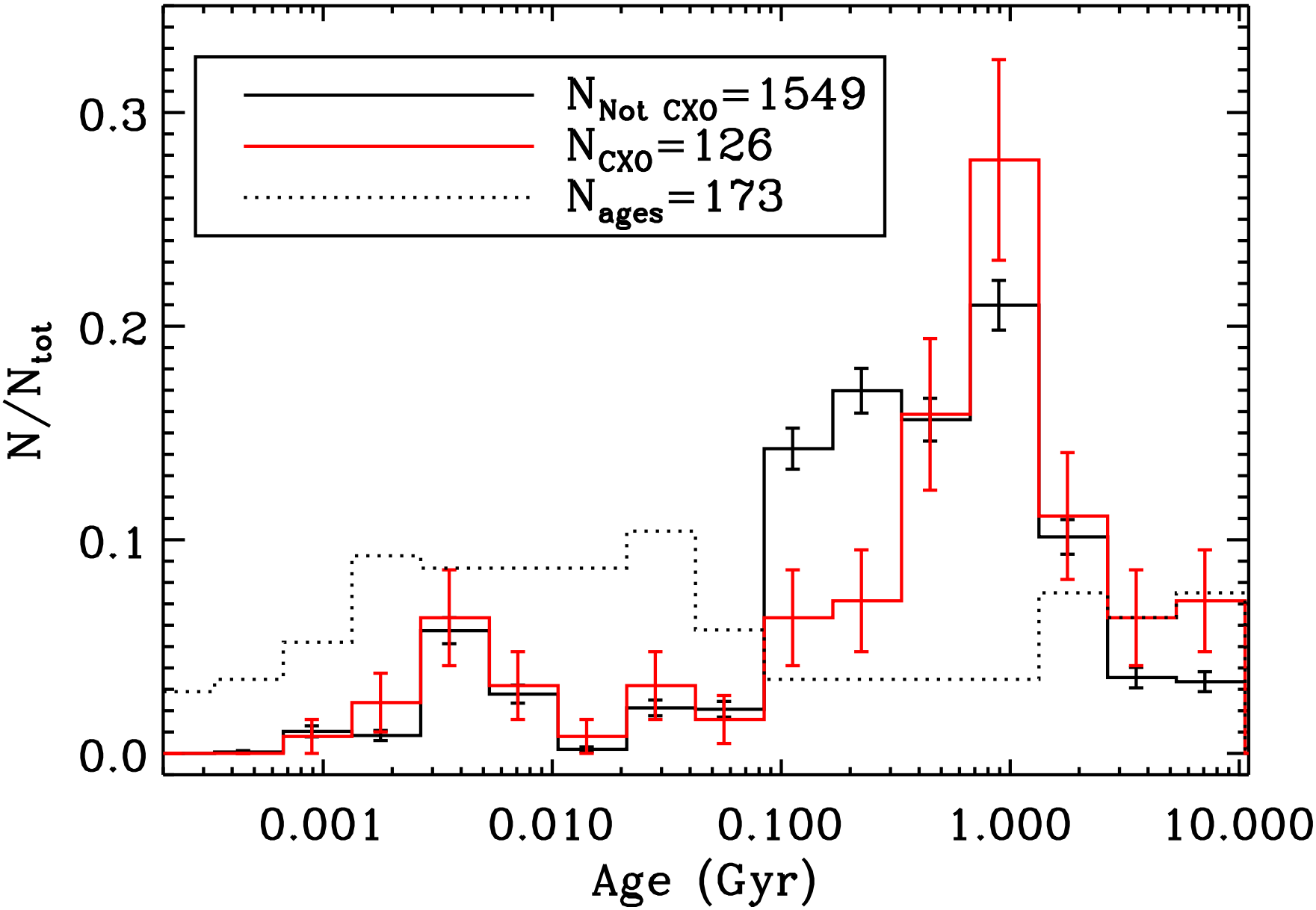

Cohen et al. (2008): Best fit Stellar Mass distribution: X-ray and field.

For t$\gtrsim$0.1 Gyr: Best fit Δt(X-ray—field)$\simeq$0.5–1 Gyr. $\chi^2(\Delta t{=}0){>}{>}1$.

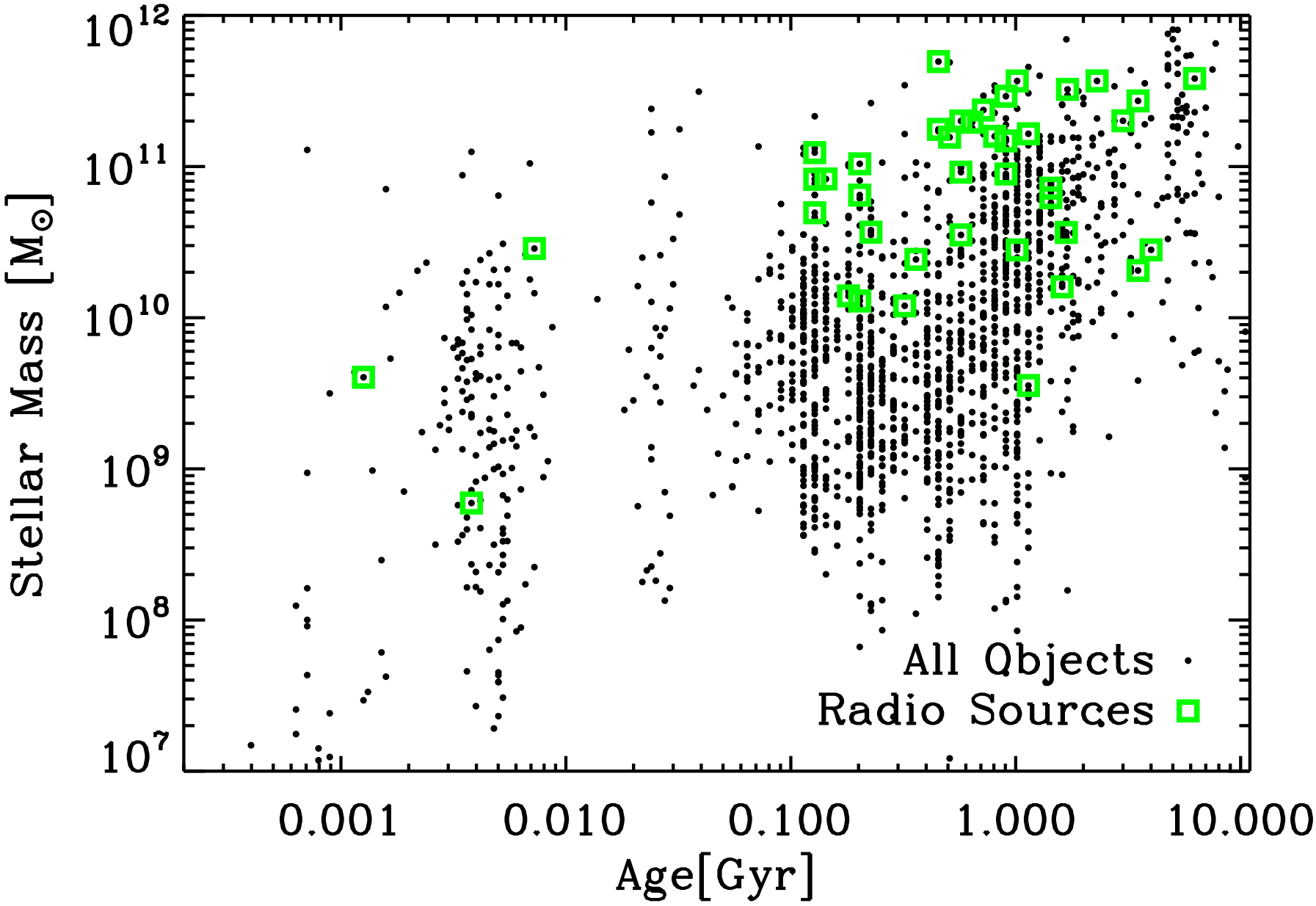

Cohen et al. (2008): Best fit Stellar Mass vs. Age: Radio and field galaxies.

- Radio galaxies are a bit older than the general field population, but by no more than $\lesssim$0.5–1 Gyr on average.

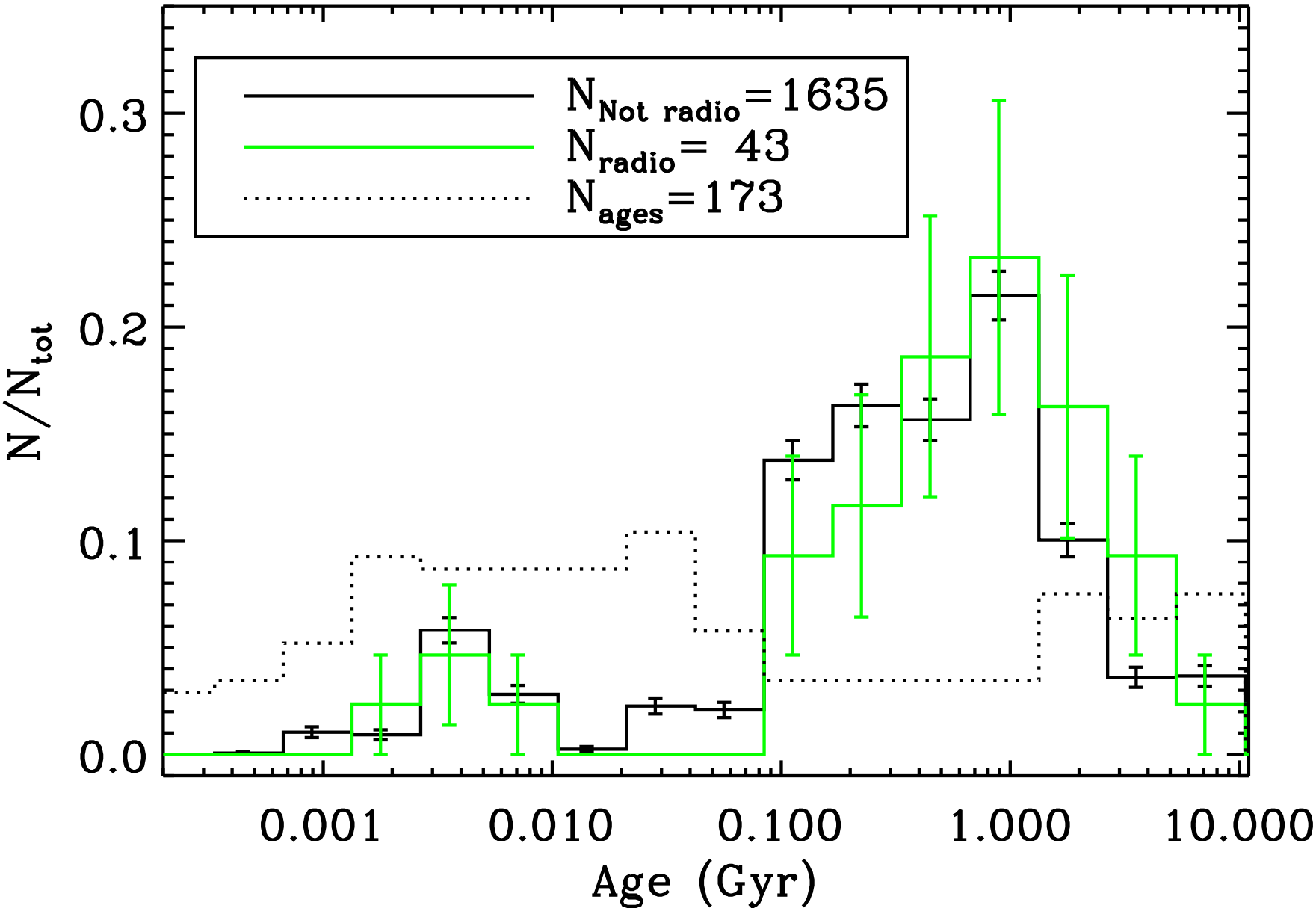

Cohen et al. (2008): Best fit Stellar Mass distribution: Radio and field.

For t$\gtrsim$0.1 Gyr: Best fit Δt(Radio X—field)$\simeq$0.5–1 Gyr. $\chi^2(\Delta t{=}0){>}1$.

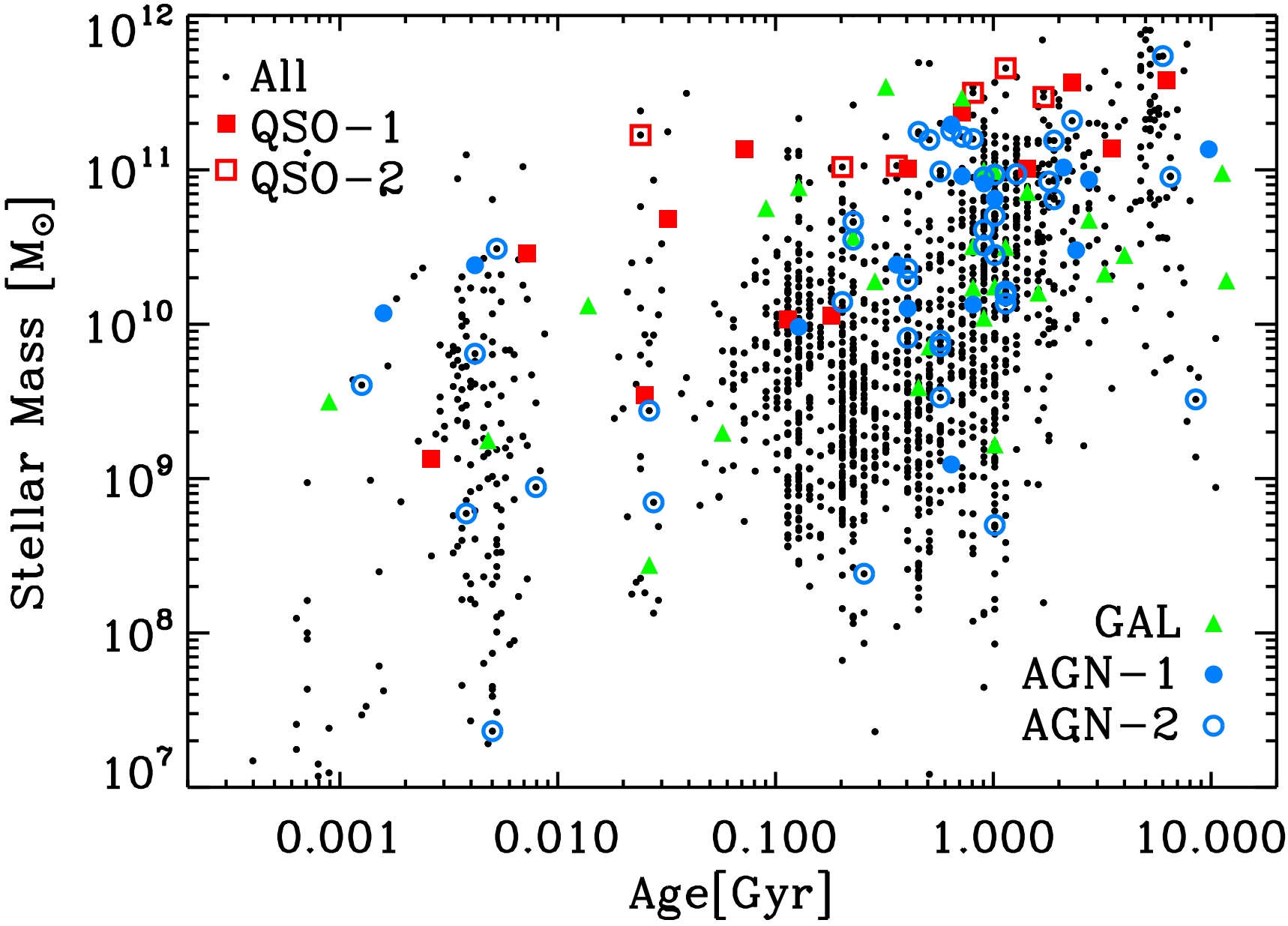

Cohen et al. (2008): At all ages, the most massive hosts are QSO-1/2's (based on *X-ray classes* from Szokoly et al. 2004).

- This is illustrates the well known L_X-L_{opt} correlation.

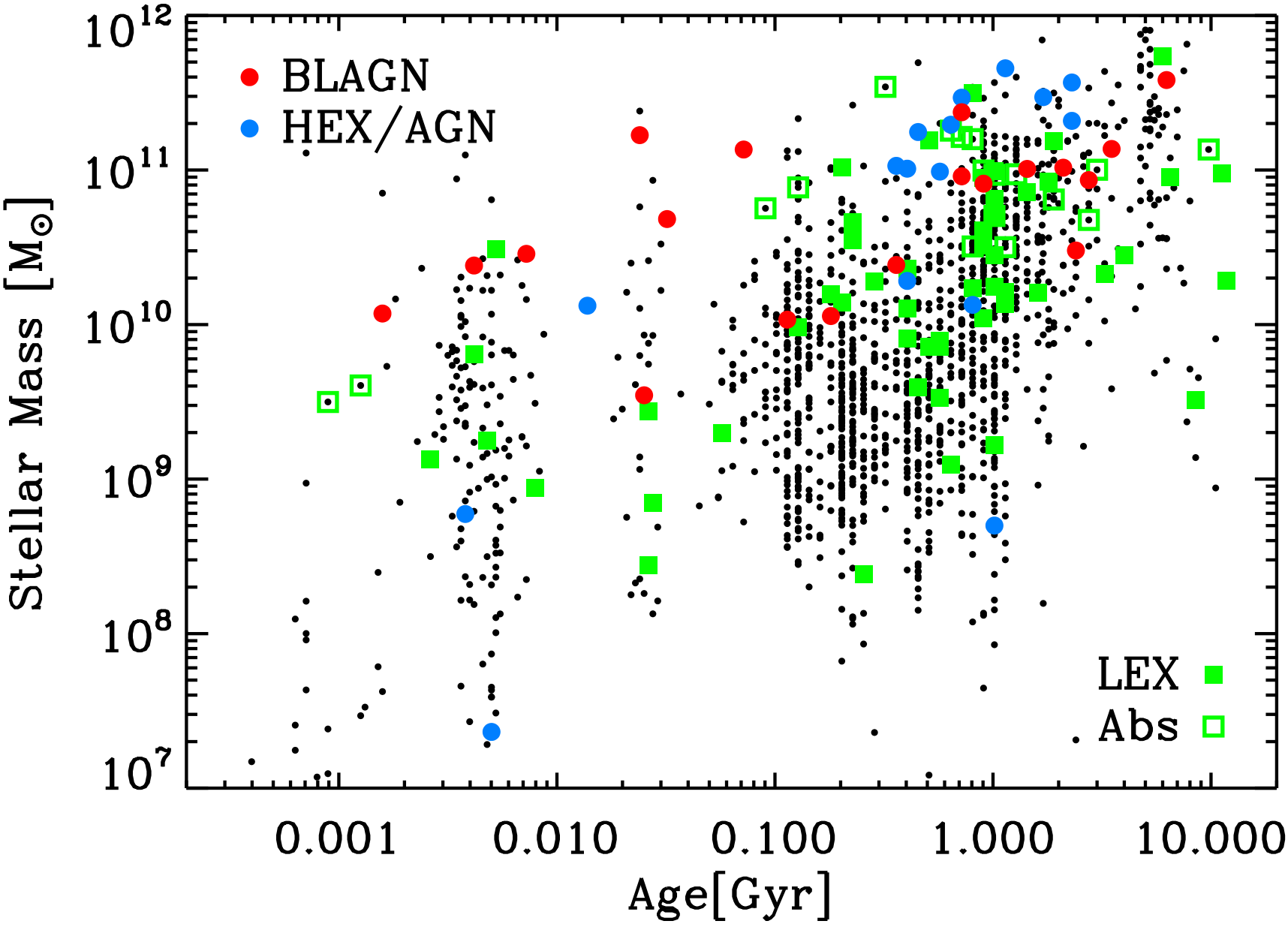

Cohen et al. (2008): At all ages, the most massive hosts are QSO-1/2's (based on AGN lines in *optical spectra* by Szokoly et al. 2004).

Most $\gtrsim$0.5–1 Gyr SEDs do not show AGN signatures in optical spectra.

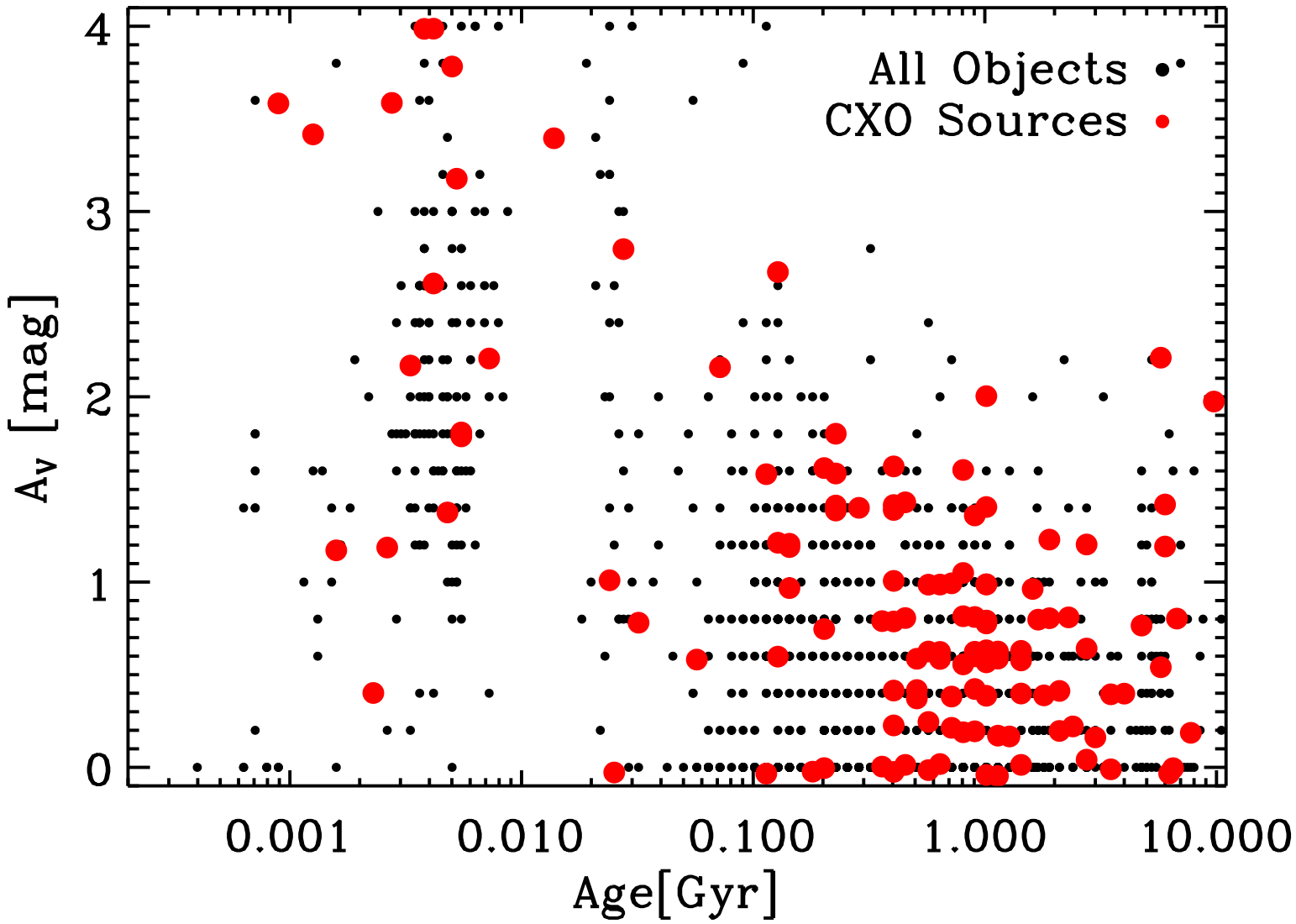

Cohen et al. (2008): Best fit extinction A_V distribution: X-ray and field.

- In Hopkins et al. (2006, ApJS, 163, 1) scenario, dust and gas are expelled *after* the starburst peaks and *before* before the AGN becomes visible.

Older galaxies have less dust after merger/starburst/outflow. But age-Fe/H.

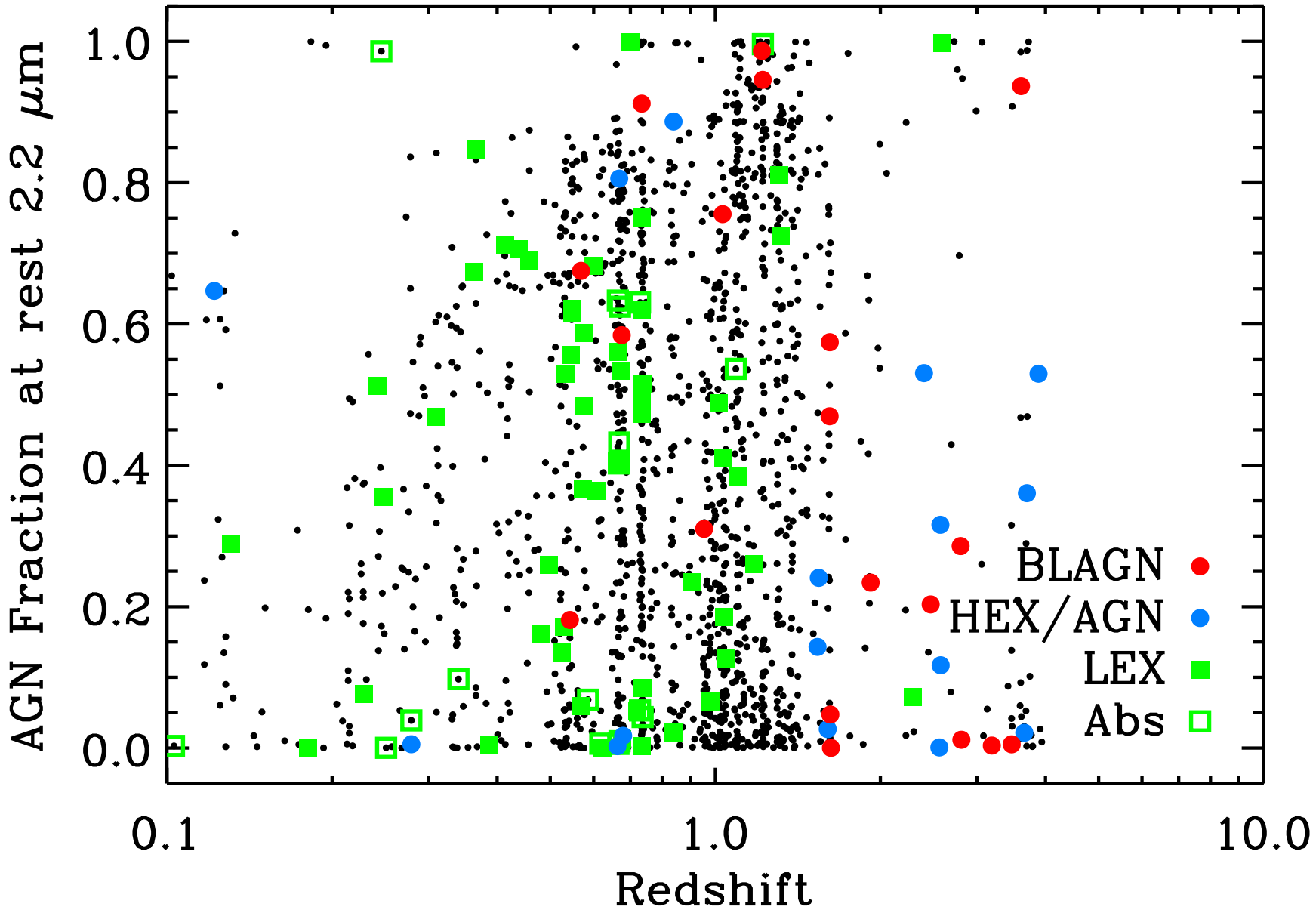

Cohen et al. (2008): Redshift distribution of best fit 2.2 μm AGN fraction:

All optical AGN types: emission lines and absorption features.

- For majority of AGN-1's: $\lesssim$50% of 2μm-flux comes from the AGN !?

(6) Summary and Conclusions

(1) Tadpoles have a redshift distribution very similar to that of field galaxies $\Longleftrightarrow$ Tadpole galaxies may be good tracers of the galaxy assembly process.

(2) Variable objects have a redshift distribution similar to that of HUDF field galaxies $\Leftrightarrow$ They likely trace brief(!) episodes of SMBH growth.

• There is very little overlap between (1) and (2): HUDF tadpoles likely preceed the variable objects.

(3) Epoch dependent density of major mergers precedes peak in X-ray selected AGN ρ(z), but by no more than 1.4 Gyr.

(4) Radio and X-ray selected galaxies are on average 0.5–1 Gyr older than the typical FBG or LBG age of 0.1–0.3 Gyr.

AGN GROWTH STAYS IN PACE WITH GALAXY ASSEMBLY, BUT RADIO / X-RAY SOURCE APPEAR $\lesssim$1 Gyr AFTER MERGER/STARBURST

(7) Future studies with the James Webb Space Telescope

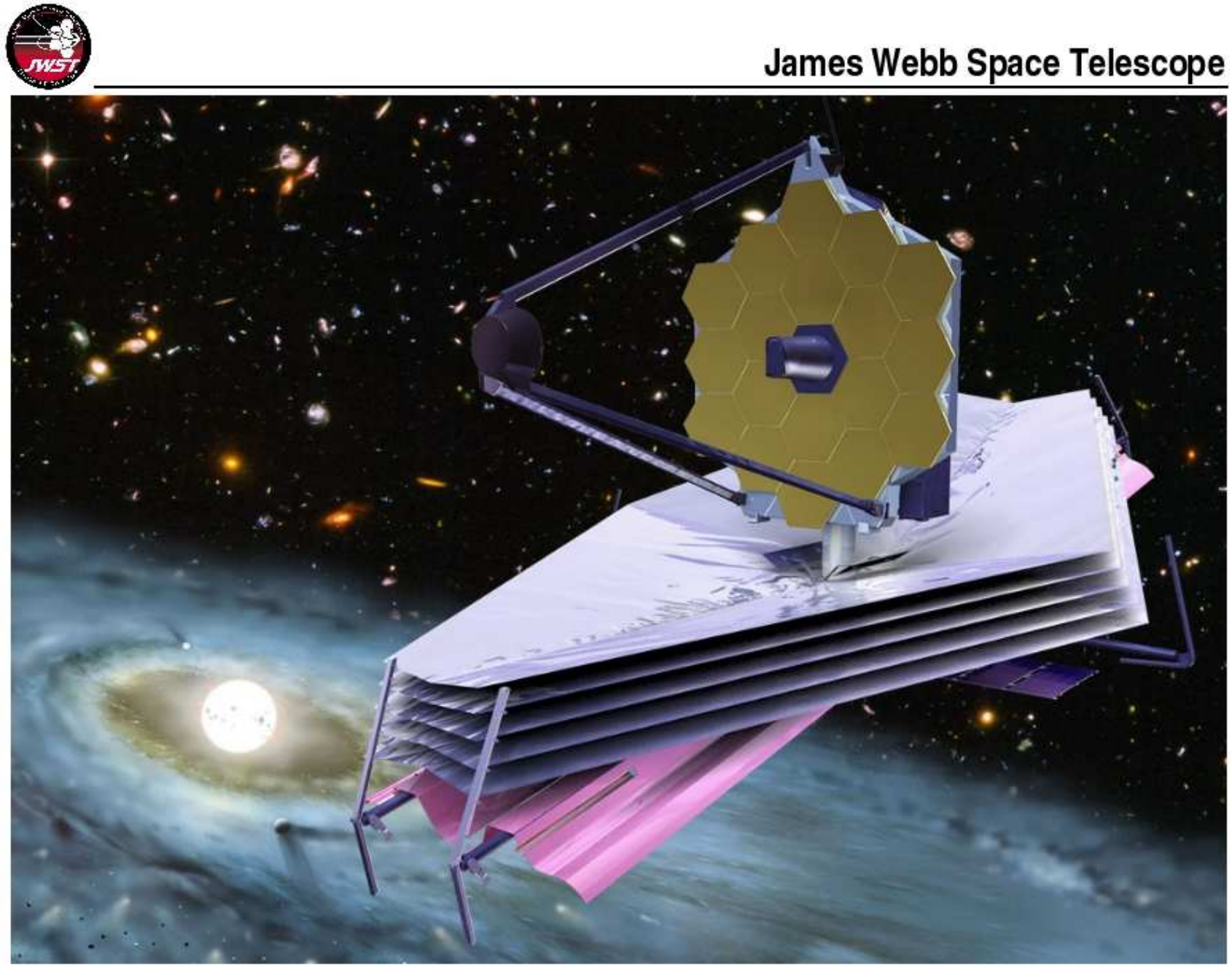

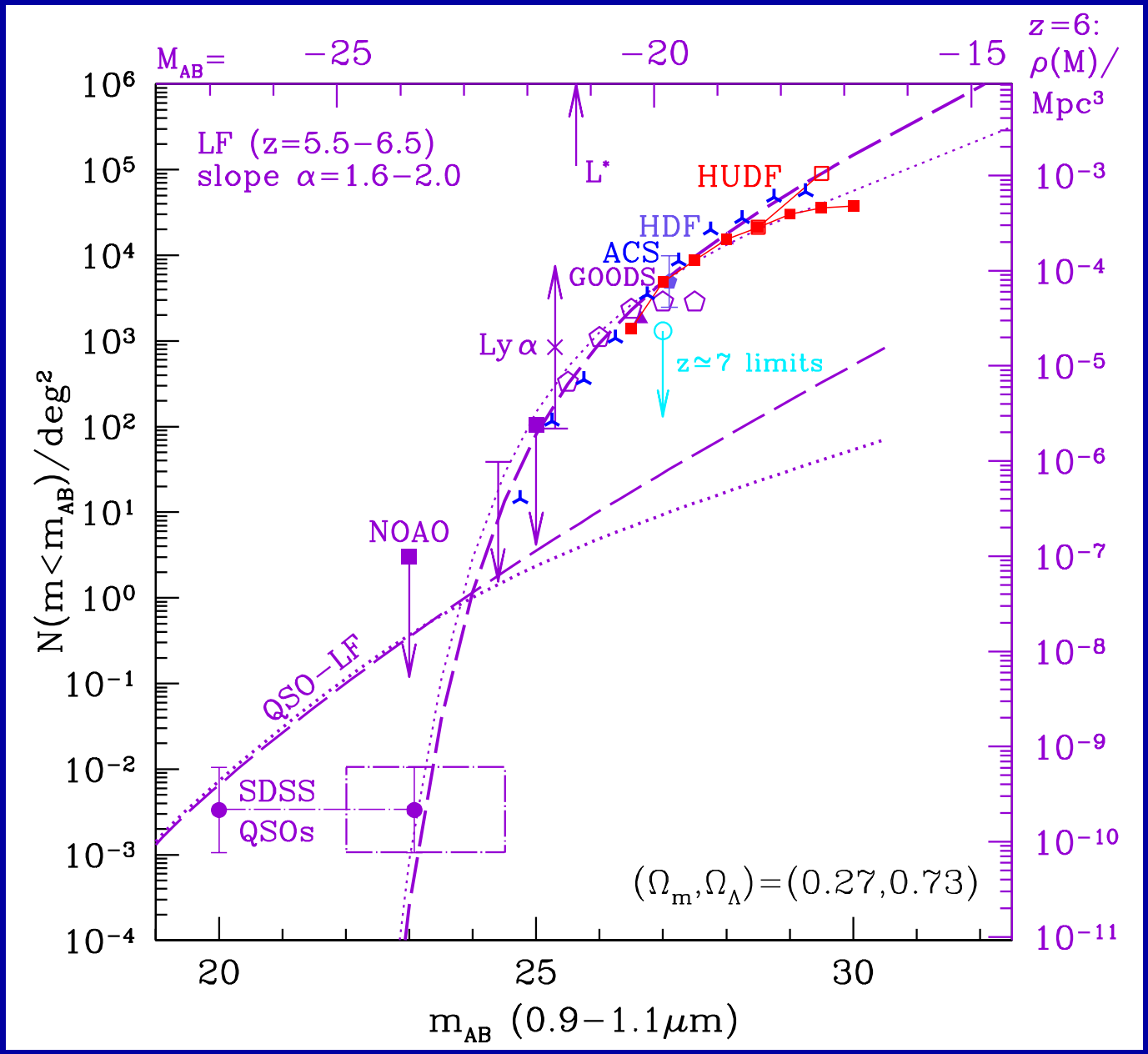

HUDF shows that luminosity function of $z\simeq 6$ objects (Yan & Windhorst 2004a, b) is very steep: faint-end Schechter slope $|\alpha|\simeq 1.8\pm 0.2$.

$\Rightarrow$ Dwarf galaxies and not quasars likely completed the reionization epoch at $z\simeq 6$. This is what JWST will observe for $z\simeq 7$–20, and SKA for $z\lesssim 6$.

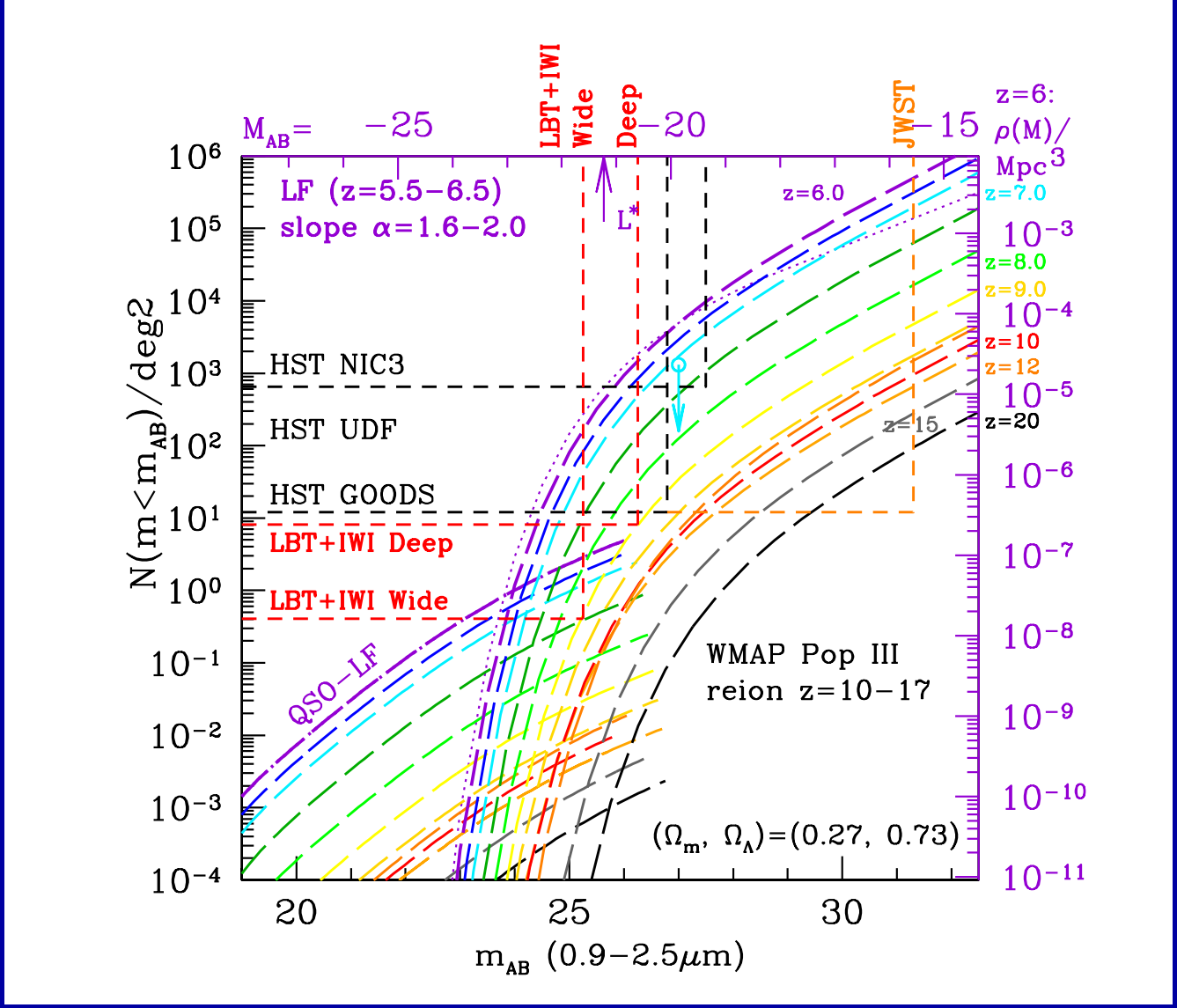

- With proper survey strategy (area AND depth), JWST can trace the entire reionization epoch and detect the first star-forming objects.
- Red boundaries indicate part of the galaxy and QSO LF that 4–10m class telescopes with wide-field IRCam can explore to z=9 and AB$\lesssim$25 mag.
- Co-evolution of supermassive black-holes and proto-bulges for z$\lesssim$10.

SPARE CHARTS

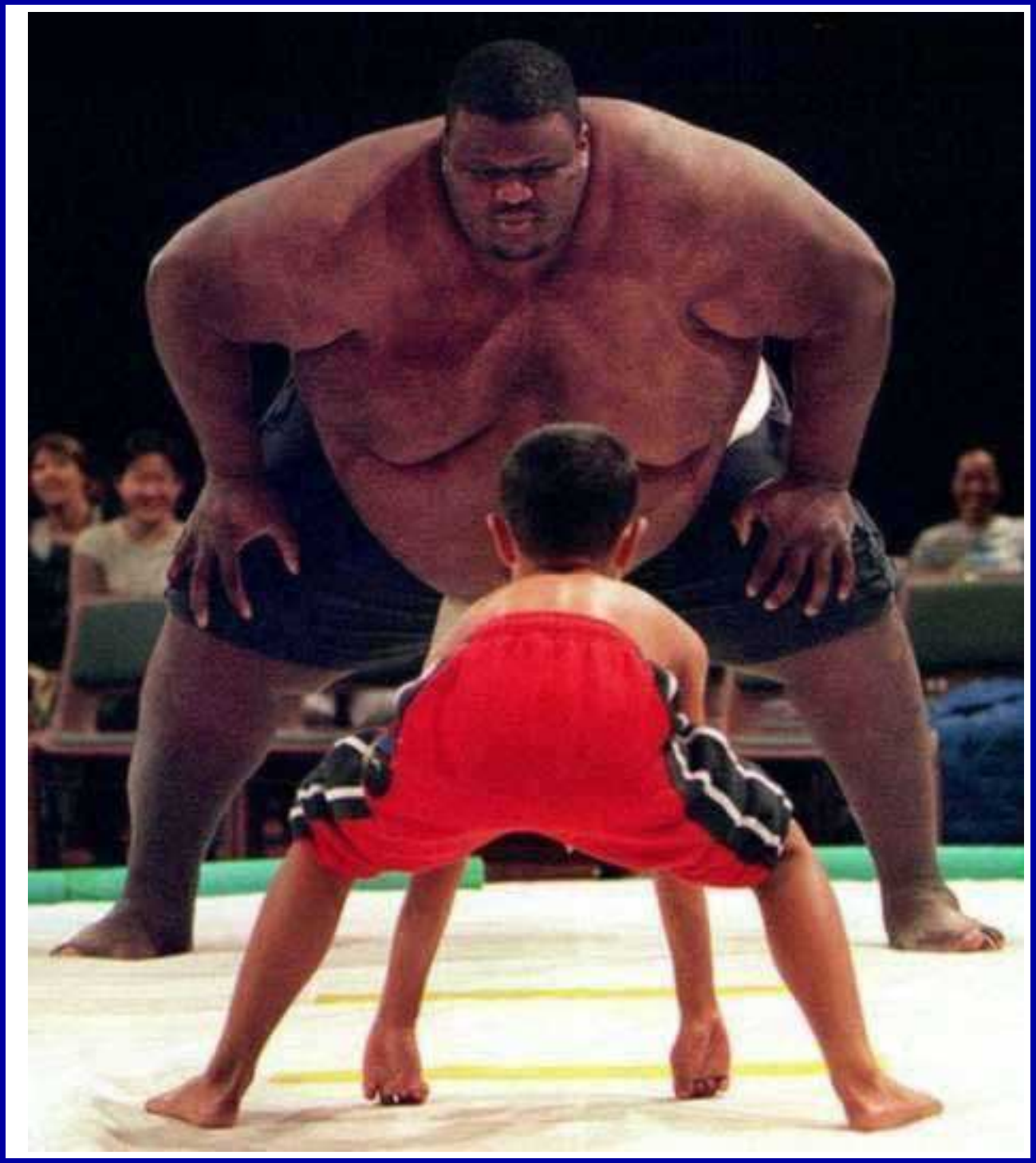

At the end of reionization, dwarfs had beaten the Giants, but ...

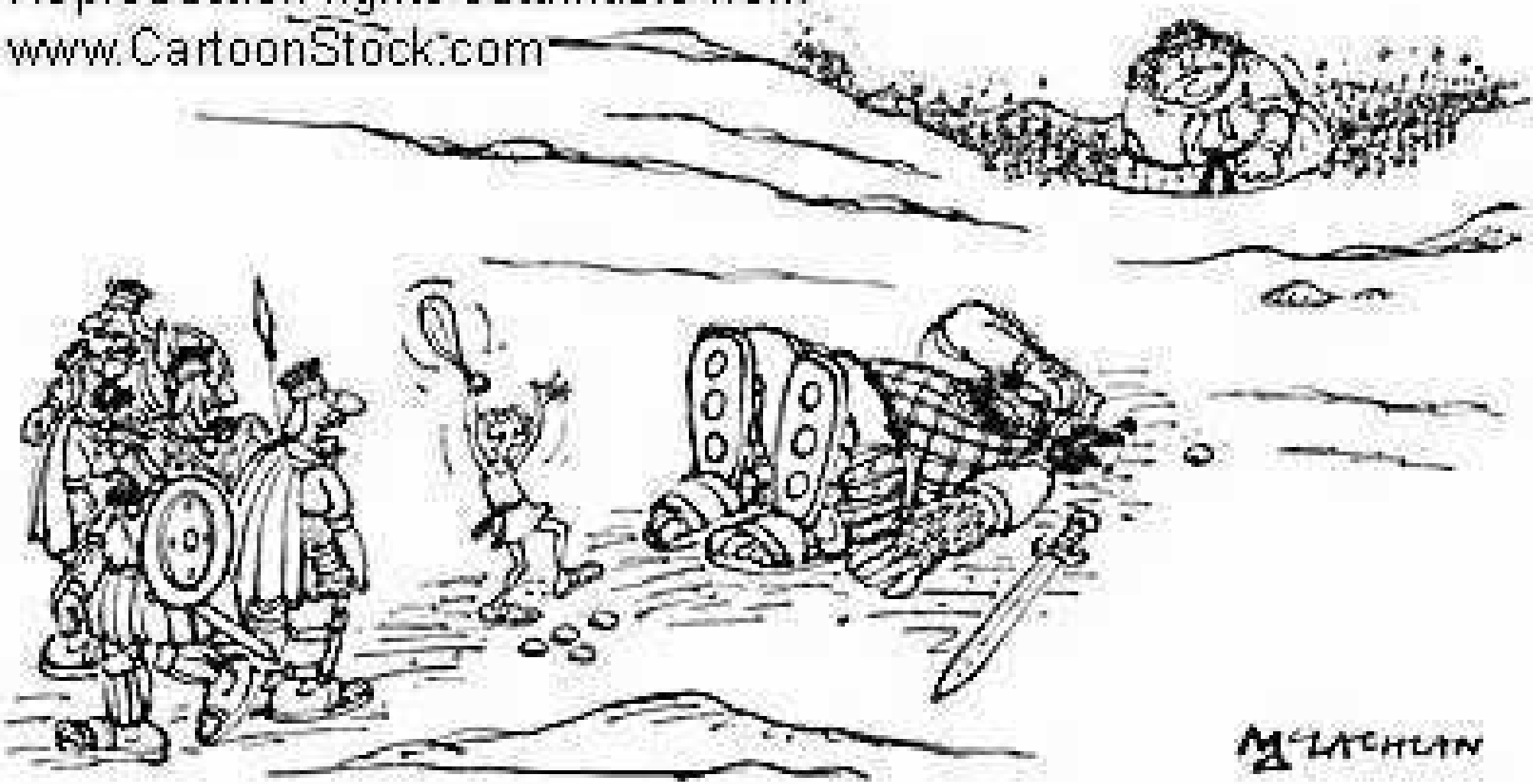

"You've done it now, David - Here comes his mother."

What comes around, goes around ...

Caveat: Can the Hard-UV of weak AGN outshine Dwarf Galaxies?

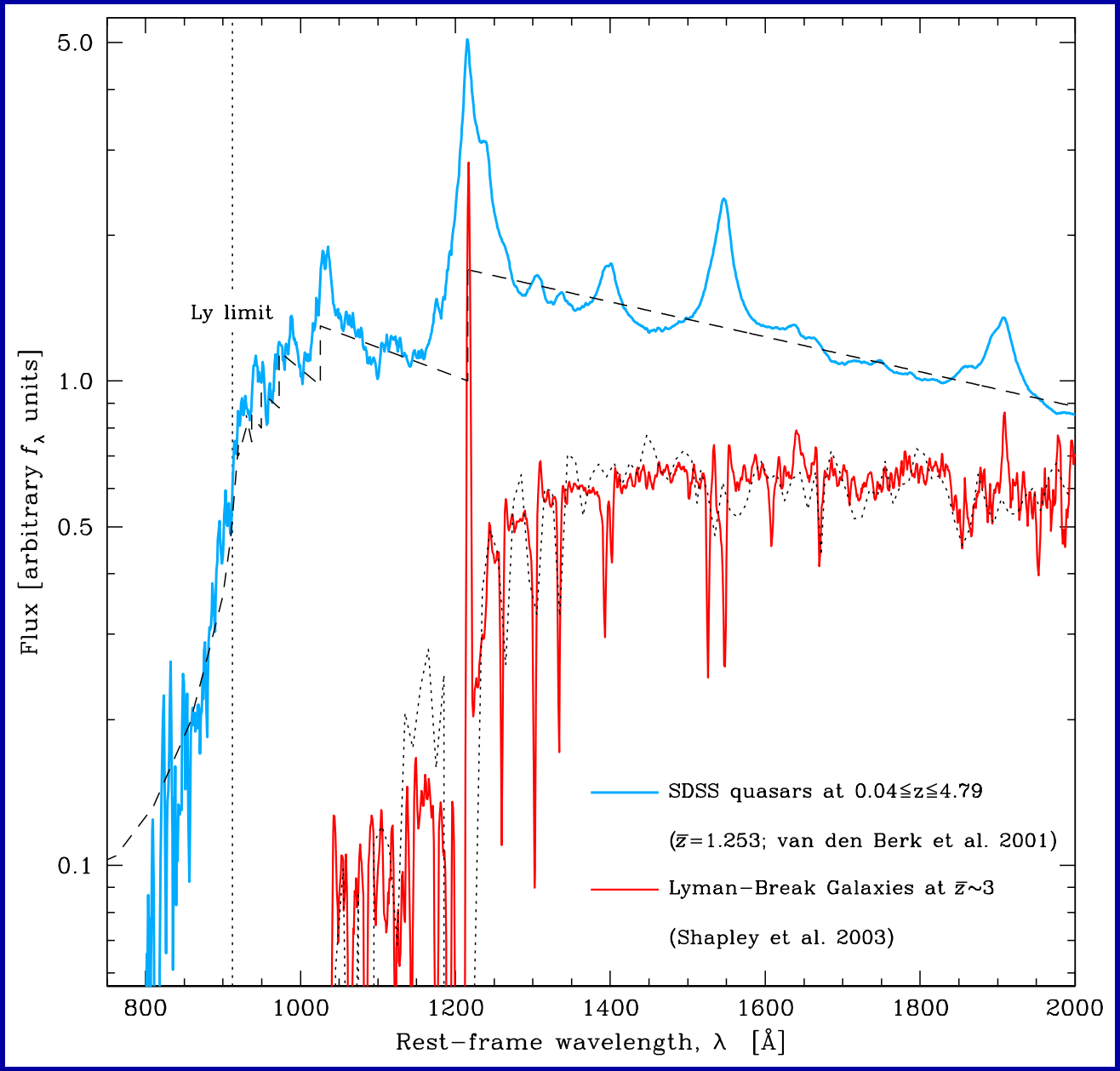

- In principle, the hard-UV of QSO's and weak AGN can outdo the young SED's of LBG's or dwarf galaxies, but likely by no more than $\gtrsim$1 dex.

Total EII/S0 Sabc Irr/Mergers

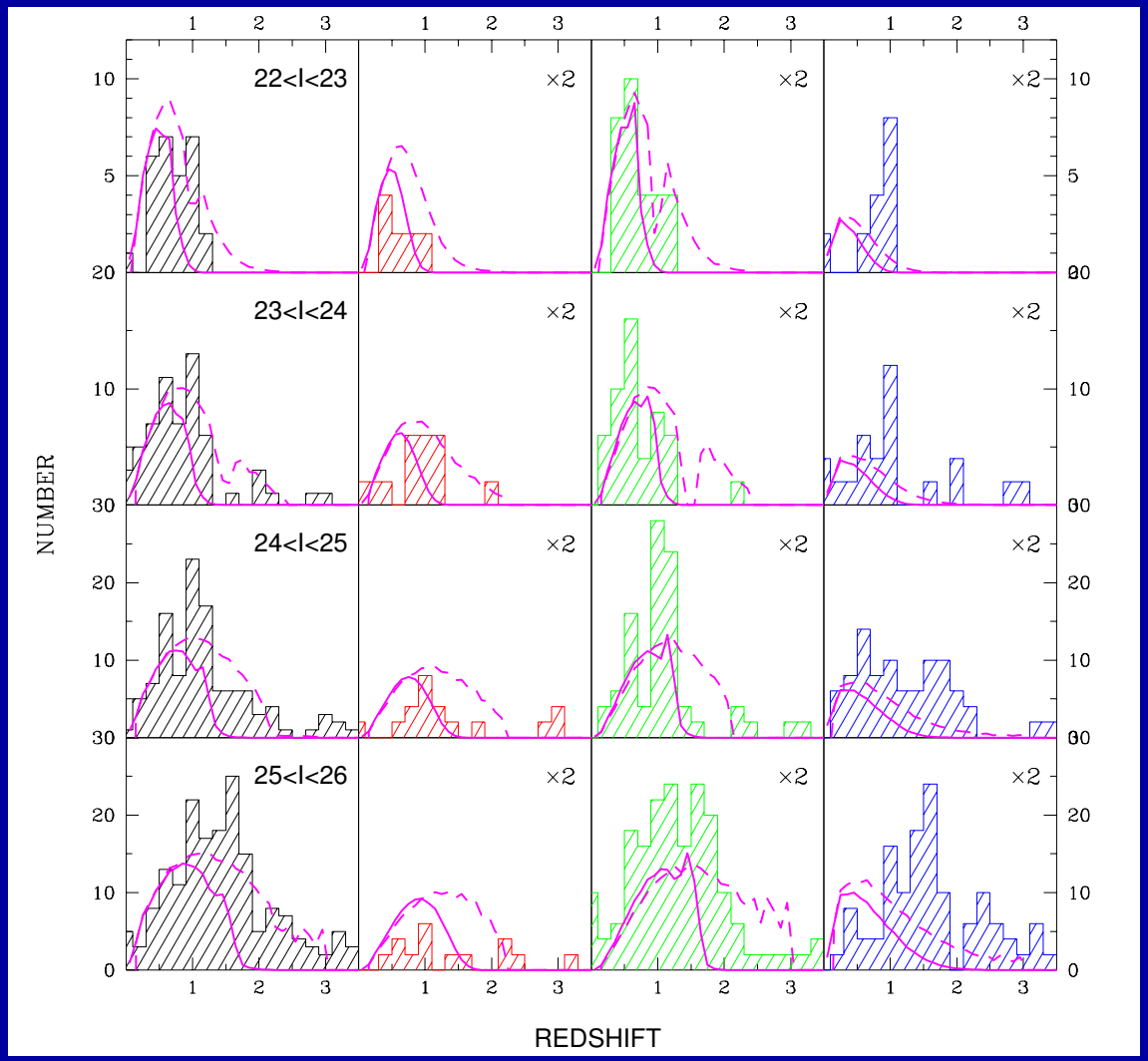

- JWST can measure how galaxies of all Hubble types formed over a wide range of cosmic time, by measuring their redshift distribution as a function of rest-frame type.
- For this, the types must be well imaged for large samples from deep, uniform and high quality multi-wavelength images, which JWST can do.

Driver et al. 1998, Astrophys. J. Letters, 496, L93

Dynamical ages of Dwarf Galaxies at z≃4–6?

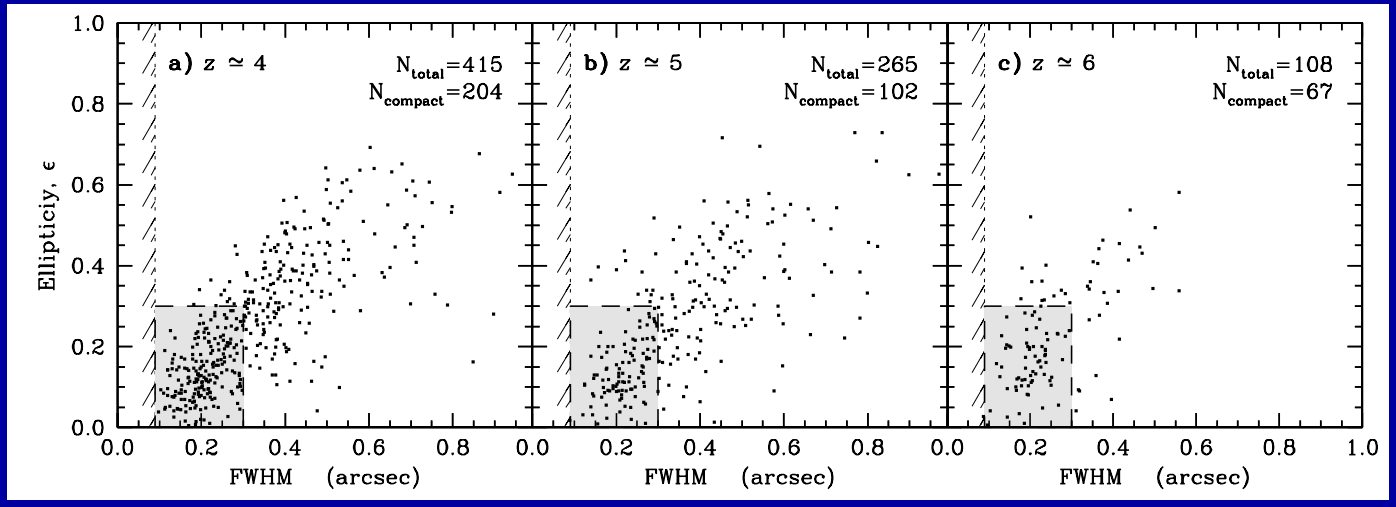

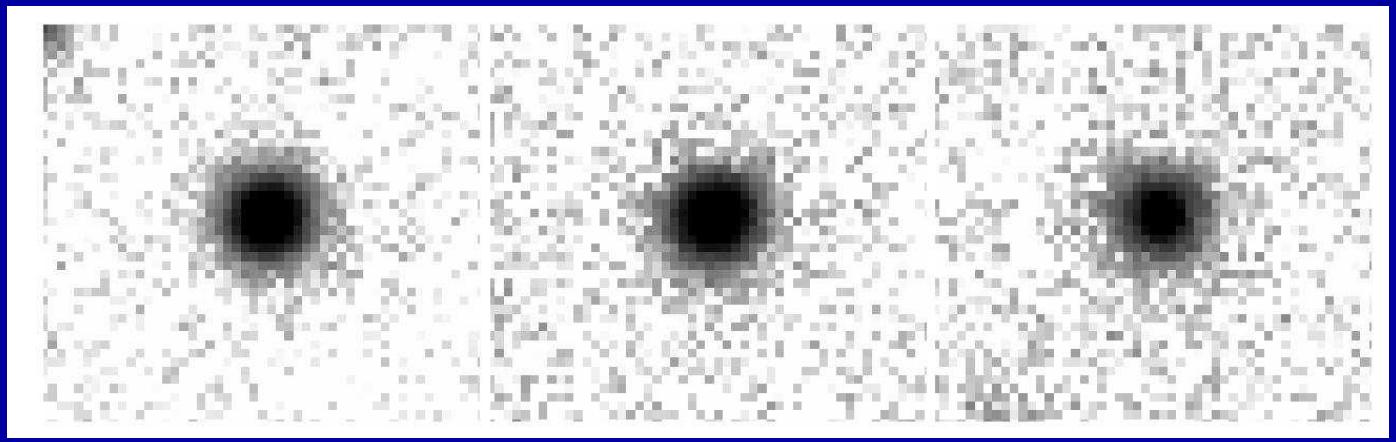

- Select all isolated, nearly unresolved ($2r_e \lesssim 0\farcs3$), round ($1\text{–}b/a \lesssim 0.3$) HUDF B-drops, V-drops, and i-drops. to AB=29.0 mag
- Construct average image stack and light-profiles of these dwarf galaxies at z≃4, z≃5, and z≃6.
- If these compact, round objects are intrinsically comparable, each stack has the S/N of ∼5000 HST orbits (≃300 JWST hrs; Hathi ea. 2008 AJ).

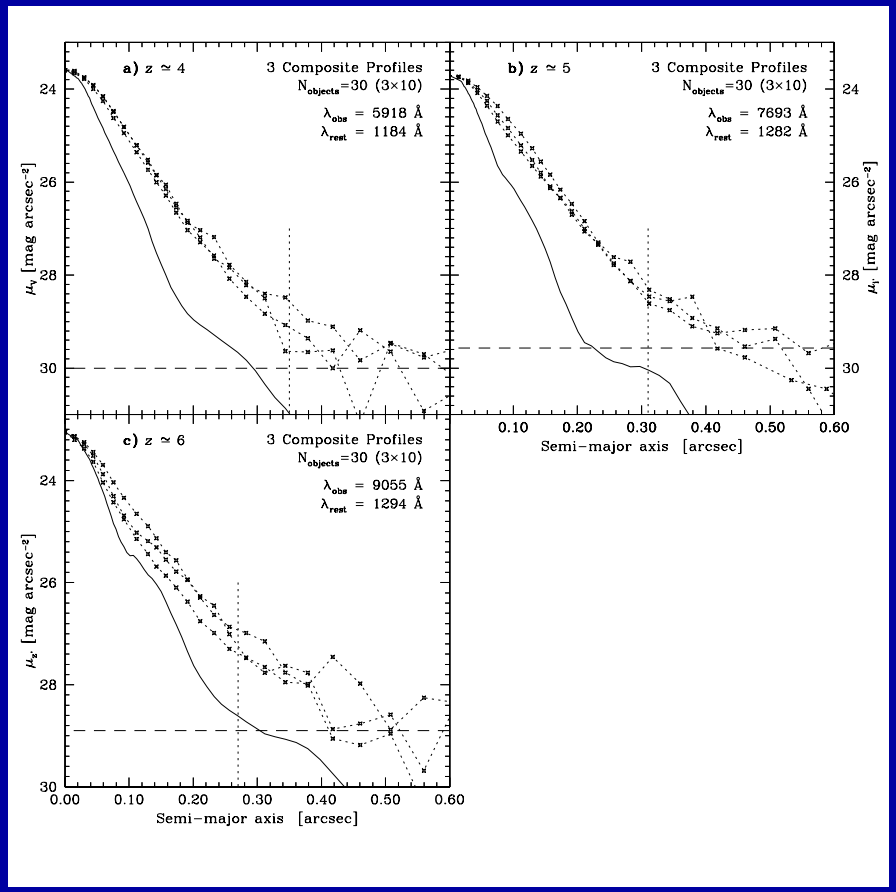

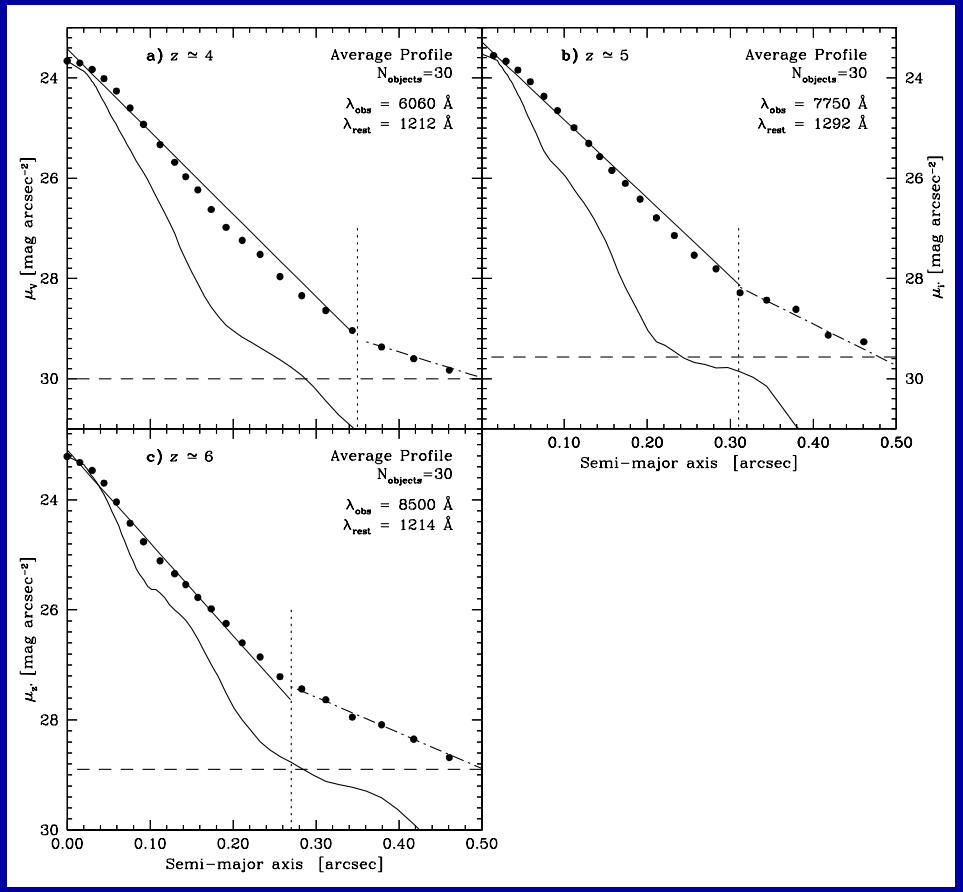

- HUDF sky-subtraction error is 2–3.10^{-3} or AB$\simeq$29.0–30.0 mag/arcsec^2
- Average 5000-orbit compact, round dwarf galaxy light-profile at z$\simeq$6–4 deviates from best fit Sersic n$\simeq$1.0 law (incl. PSF) at r$\gtrsim$0$''$.27–0$''$.35.
- If interpreted as virial radii in hierarchical growth, these imply dynamical ages of $\tau_{dyn}\simeq$0.1-0.2 Gyr at z$\simeq$6–4 for the enclosed masses.

$\Leftrightarrow$ Comparable to their SED ages (Hathi et al. 2008, AJ, 135, 156).

$\Rightarrow$ Global starburst that *finished* reionization at z$\simeq$6 started at z$\simeq$6.5–7?

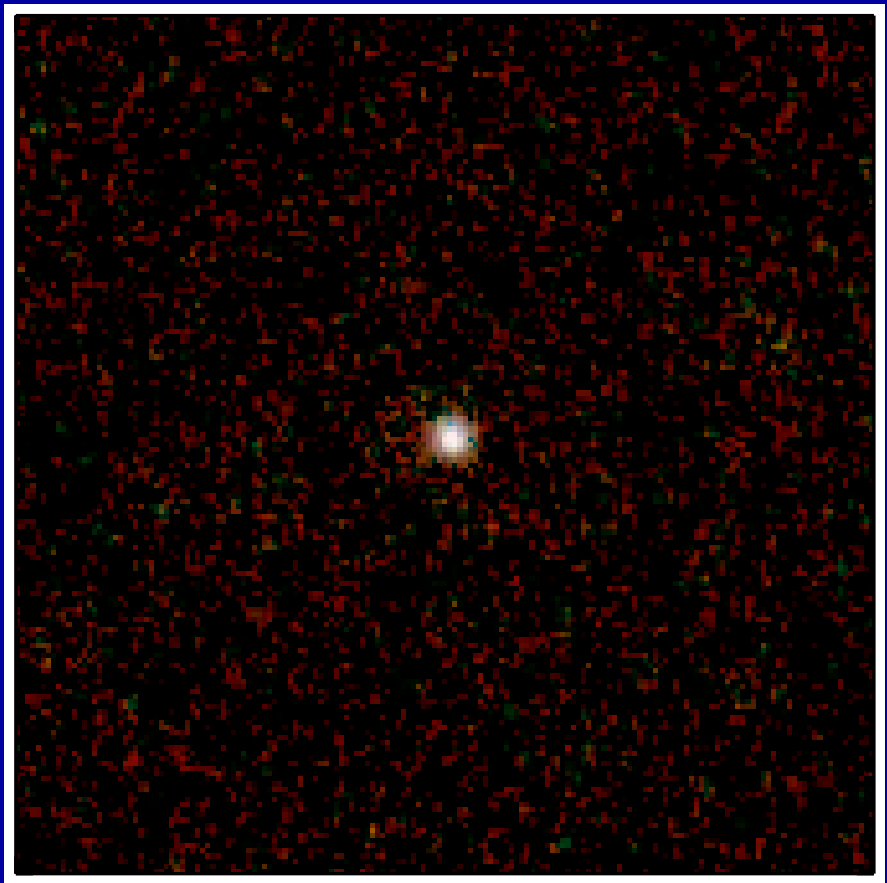

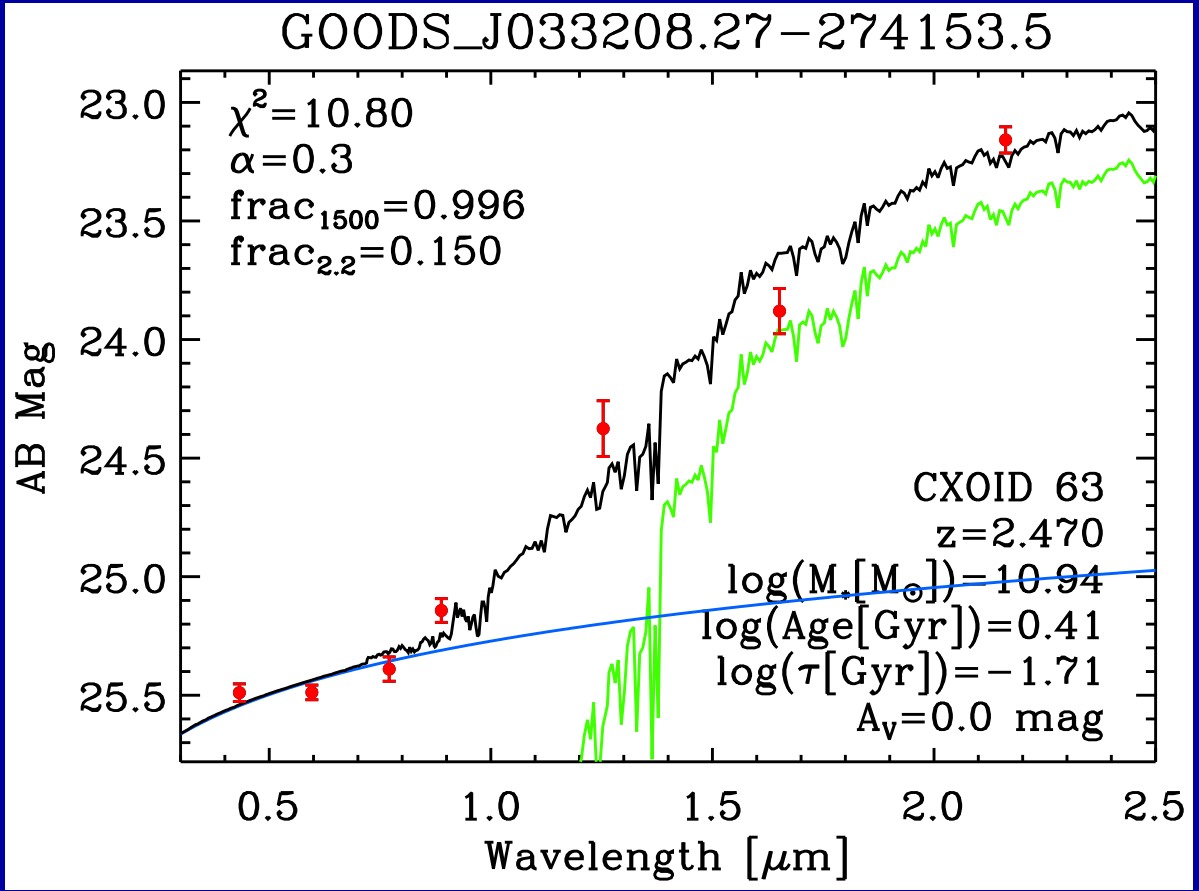

Cohen et al. (2008):

GOODS/VLT BVizJHK images

Best fit Bruzual-Charlot (2003) SED

+ power law AGN.

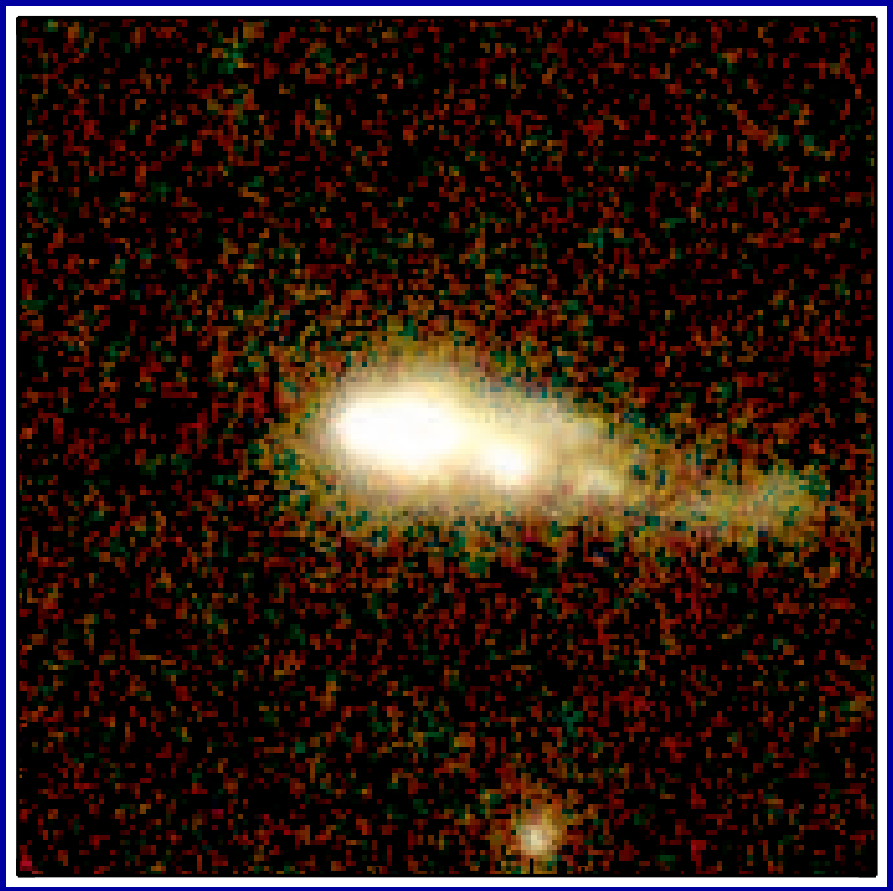

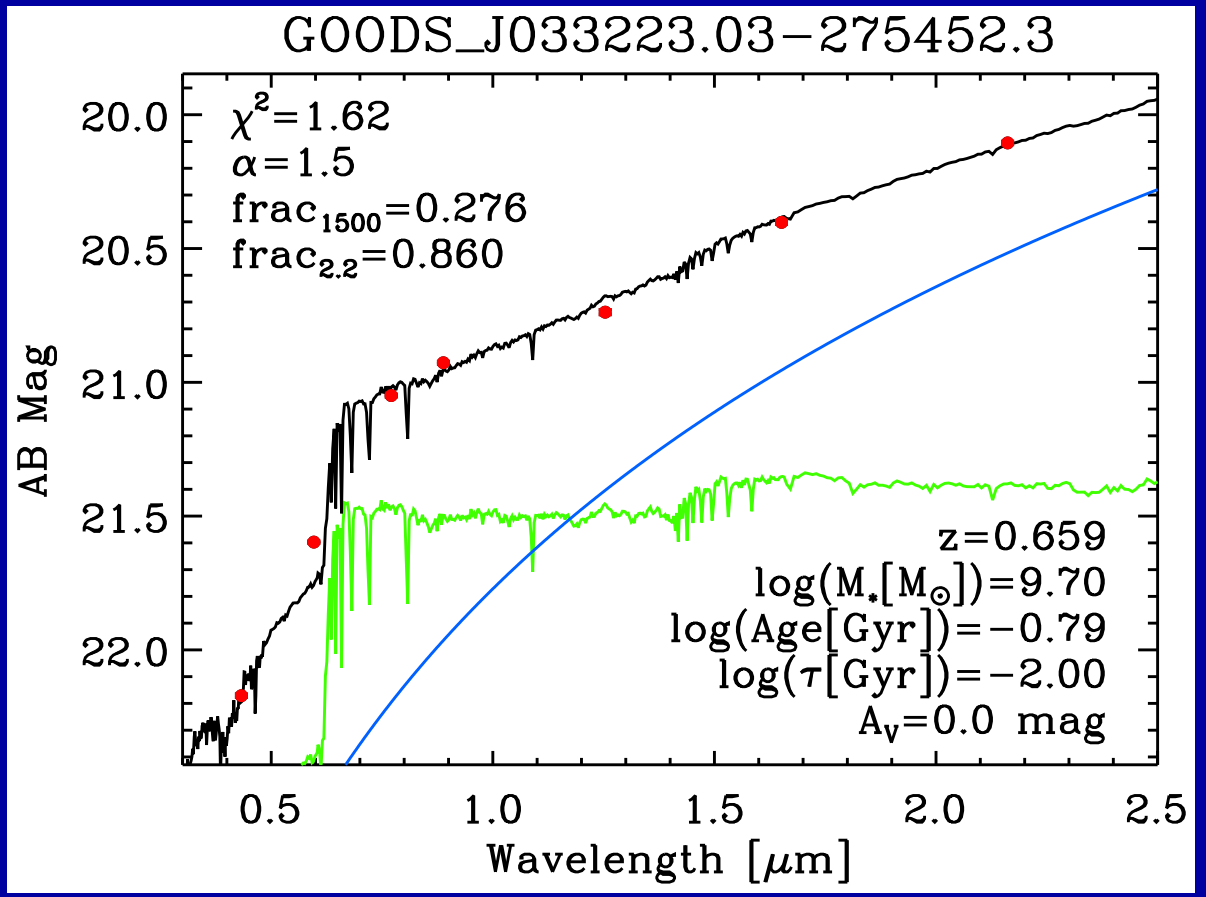

Cohen et al. (2008):

GOODS/VLT BVizJHK images

Best fit Bruzual-Charlot (2003) SED

+ power law AGN.

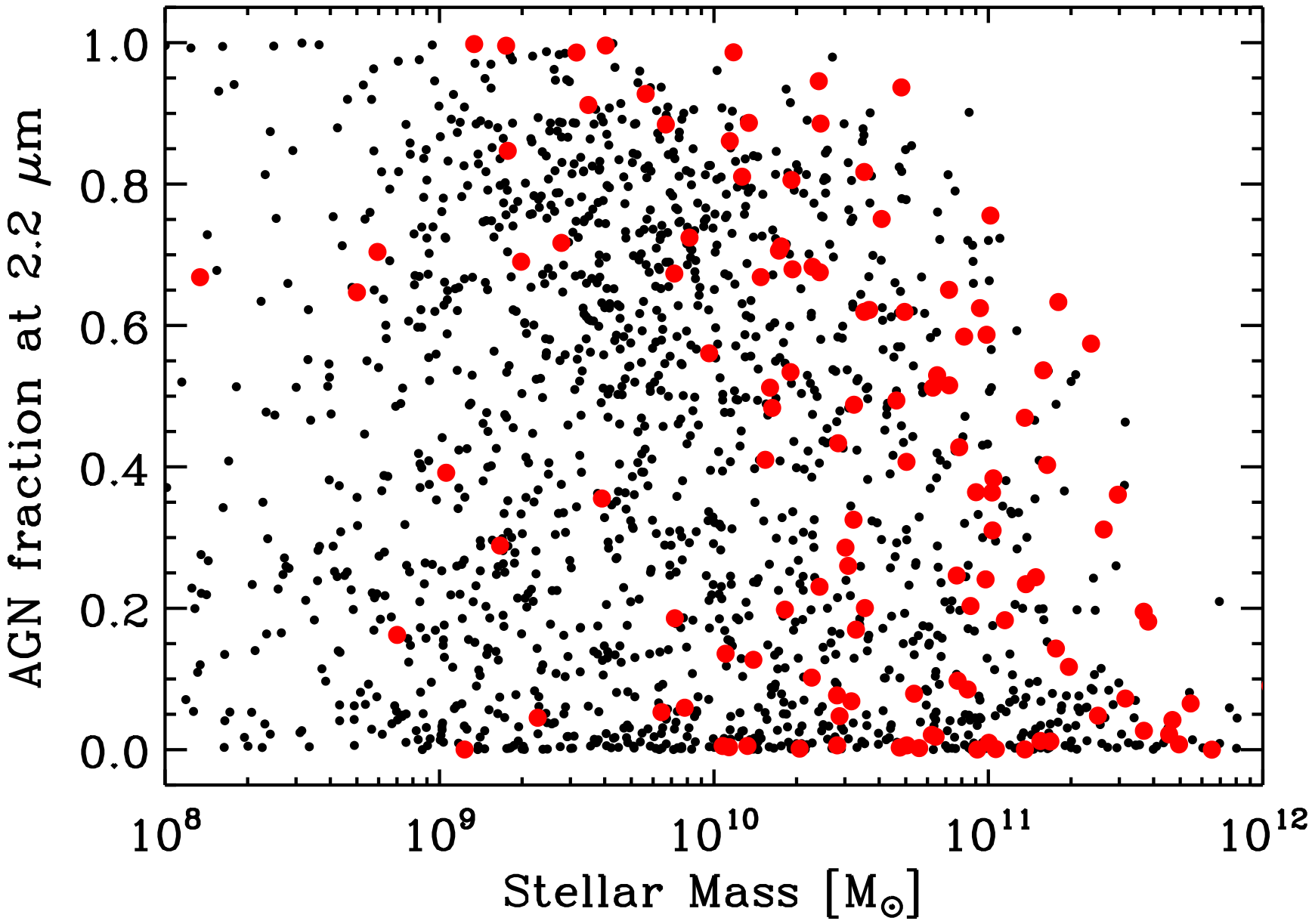

Cohen et al. (2008): AGN fraction vs. Stellar Mass: X-ray and field gxys.

$\Rightarrow$ Many more with best-fit f(AGN)$\gtrsim$50% to be detected by Con-X !?

(7) Future studies with the Hubble Wide Field Camera 3

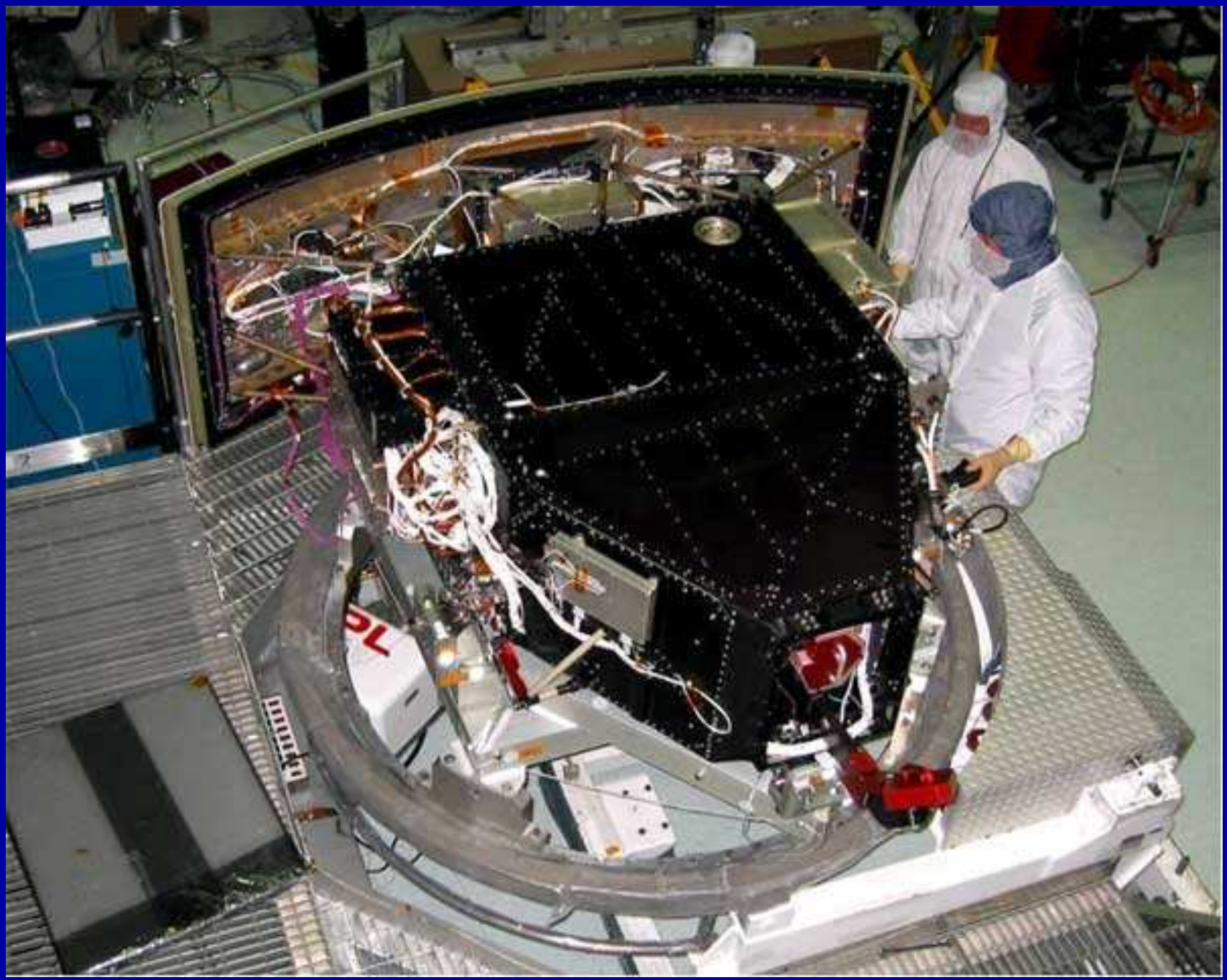

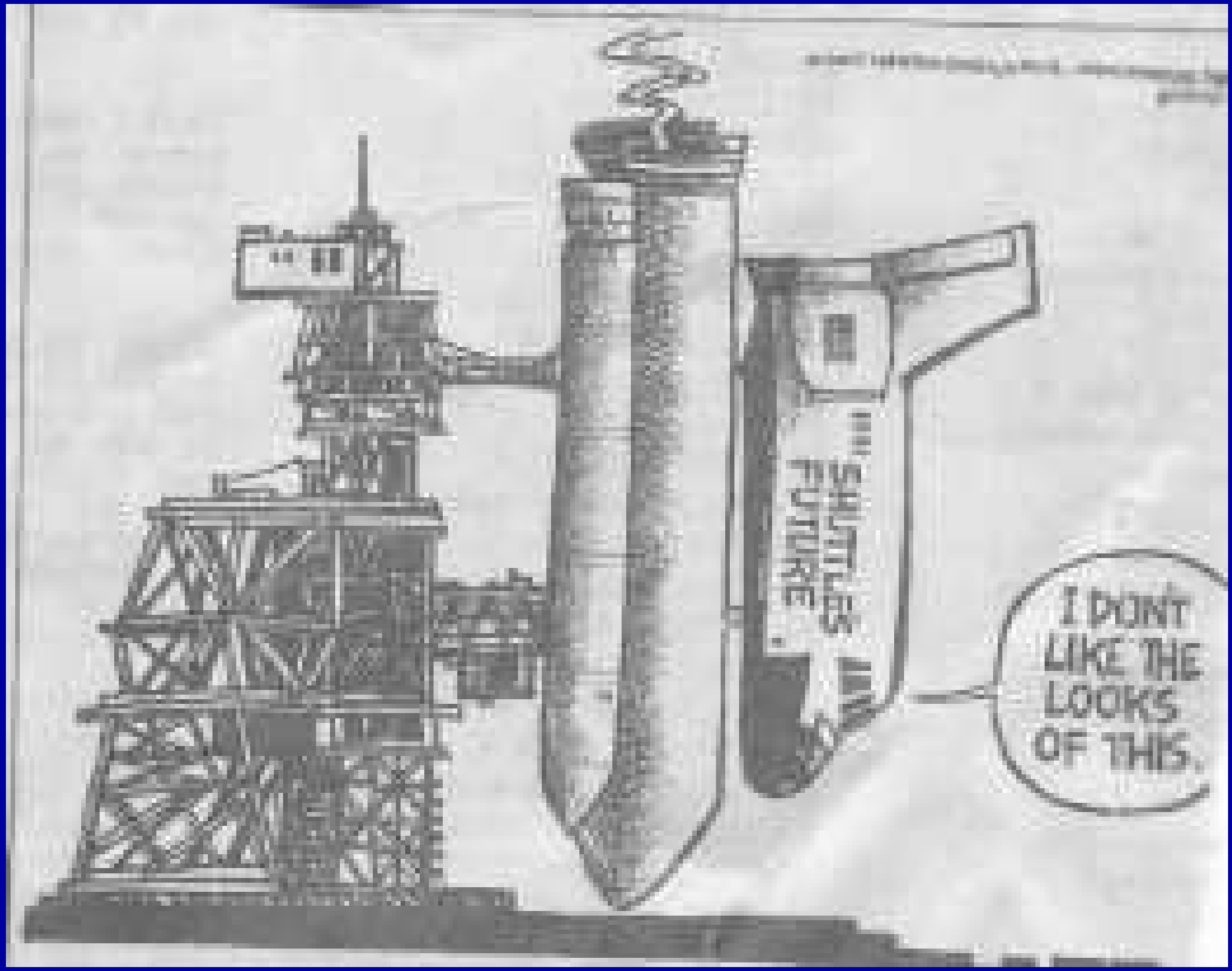

If no further Shuttle issues, WFC3 will get launched on We. Oct. 8, 2008 ...

(7) Power of combination of Grism and Broadband for WFC3

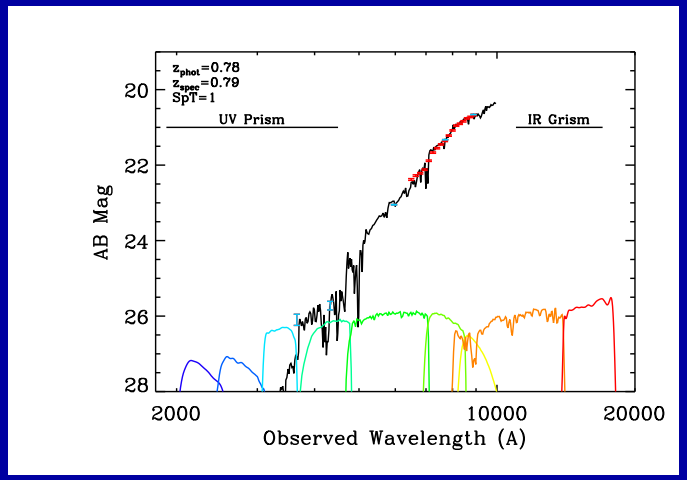

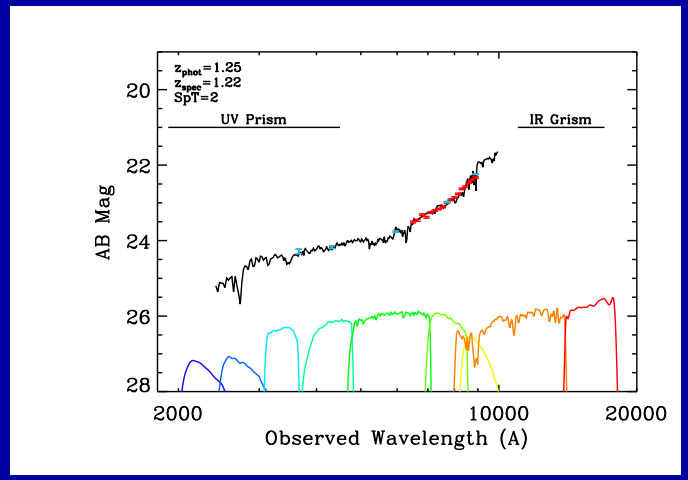

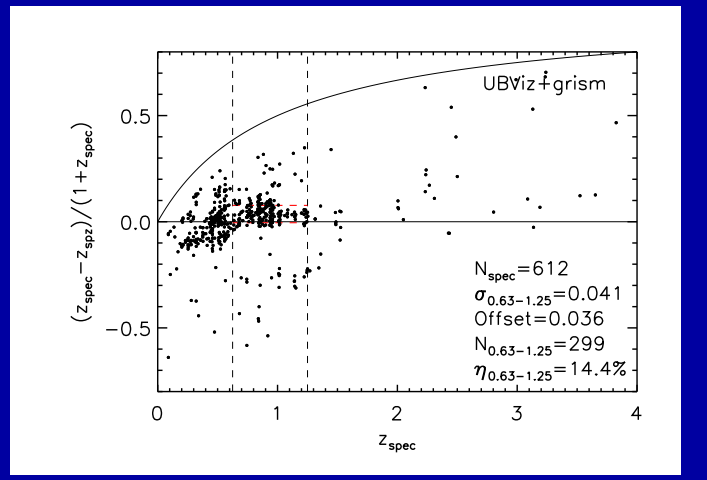

Lessons from the Hubble ACS grism surveys "GRAPES" and "PEARS" (Malhotra et al. 2005; Cohen et al. 2007; Ryan et al. 2007, ApJ, 668, 839):

- (a) Spectro-photo-z's from HST grism + BViz(JH) considerably more accurate than photo-z's alone, with much smaller catastrophic failure %.
- (b) Redshifts for $\gtrsim$13,000 objects to AB$\gtrsim$27.0–27.5 mag; $\sigma_z/(1+z)\lesssim 0.04$.
- (c) Expect $\lesssim$0.02–0.03 accuracy when including new capabilities of WFC3: UV and near-IR broad-band imaging and low-res grism spectroscopy.
- WFC3 will provide full panchromatic sampling of faint galaxy spectra from 0.2–1.7 μm, permitting high accuracy photo-z's for faint galaxies of all types to AB$\simeq$27.0–29.0 mag (10σ for $\sim$2–80 orbits/filter).

Faint-end LF-Slope Evolution (fundamental, like local IMF)

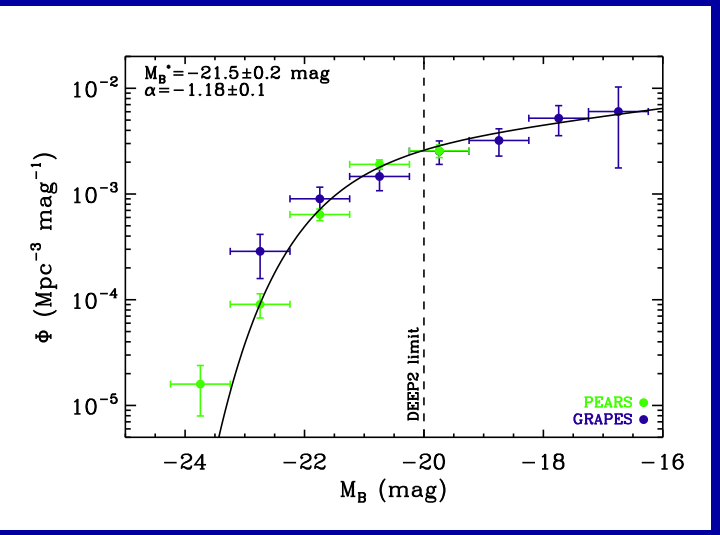

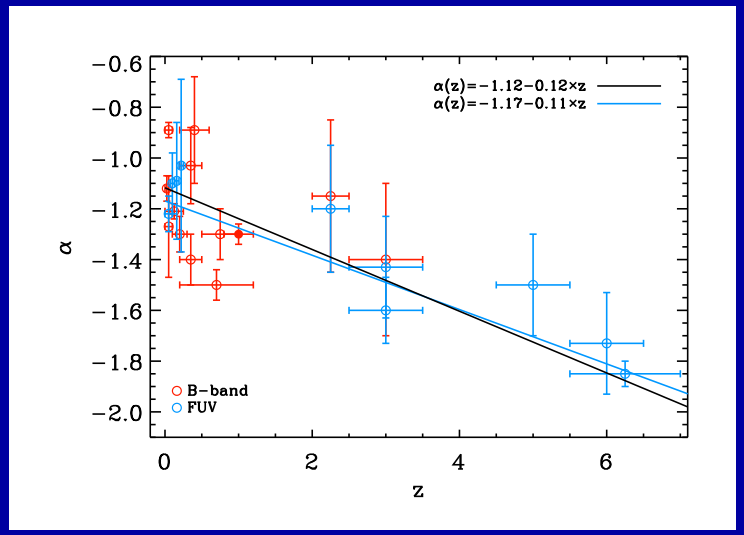

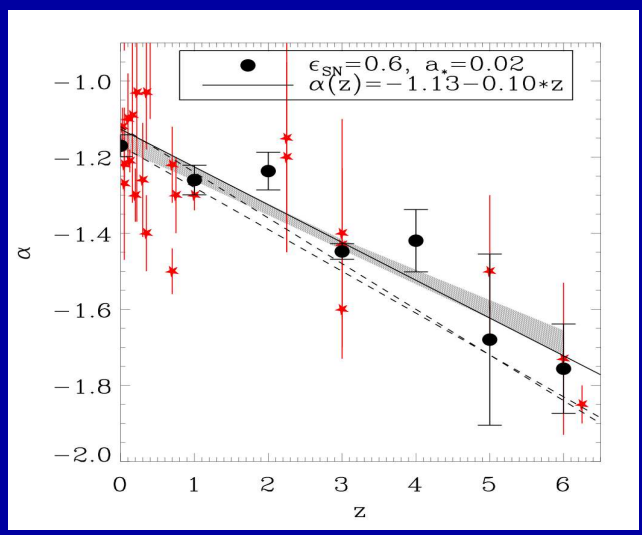

Faint-end LF-slope at $z \gtrsim 1$ with accurate ACS grism z's to AB$\lesssim$27 (Cohen et al.; Ryan et al. 2007, ApJ, 668, 839) constrains hierarchical formation:

- Star-formation and SN feedback produce different faint-end slope-evolution: new physical constraints (Khochfar ea. 2007, ApJL, 668, L115).
- JWST will provide fainter spectra (AB$\lesssim$29) and spectro-photometric redshifts to much higher z ($\lesssim$20). JWST will trace α-evolution for $z \lesssim 12$.
- Can measure environmental impact on faint-end LF-slope α directly.
- Expect convergence to slope $|\alpha| \equiv 2$ at $z > 6$ before feedback starts.
- Constrain onset of Pop III SNe epoch, Type II & Type Ia SN-epochs.

MORE SPARE CHARTS ON HUDF TADPOLES AND VARIABLE OBJECTS

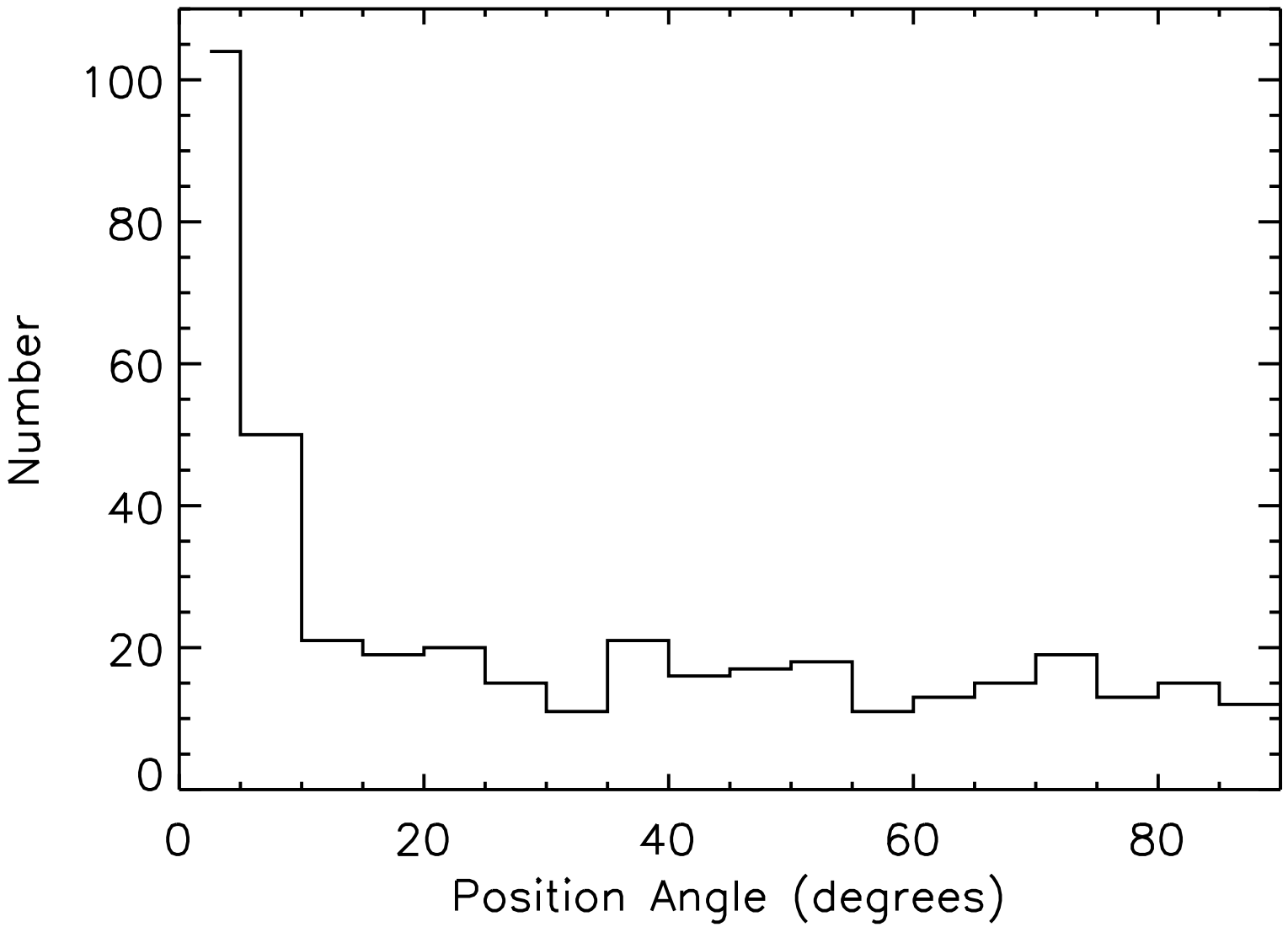

ΔPA(off-axis knot—tail) distribution of tadpole galaxies in the HUDF:

- Clear excess of knots at $|\Delta\mathrm{PA}| \lesssim 10$ deg.

$\Rightarrow$ Most tadpoles are likely real, rather than chance superpositions.

Input Parameters for IDL Tadpole Finder script:

Parameter	Value
(A) b/a limit: knots	>0.70
(B) b/a limit: tails	<0.43
(1) Distance to center (in a-axis units)	<4
(2) PA difference (tail-knot in degrees)	<30
Total number of tadpoles selected by script	140
Total number of tadpoles selected by eye	25
Total number of tadpoles selected	165

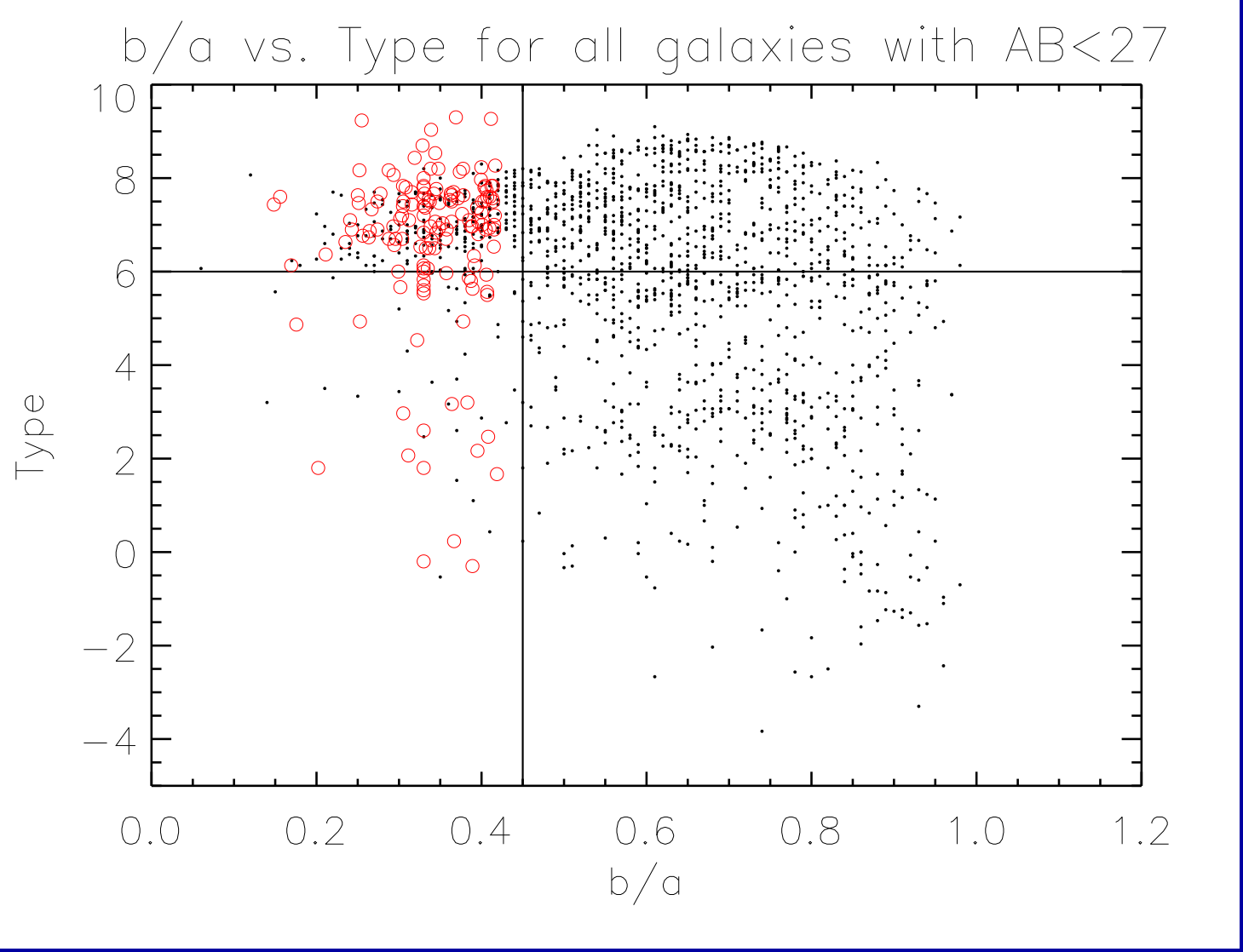

Ellipticity vs. rest-frame HUDF Type to i_{AB} =27 mag:

- Fraction of Flat Late-Types/All Late-Types = 26%
- Fraction of Flat Early-Types/All Early-Types = 7%

$\Rightarrow \exists$ likely an excess of truly linear structures among flat late-type objects.

$\Rightarrow$ Not all tadpoles are edge-on late-type disks.

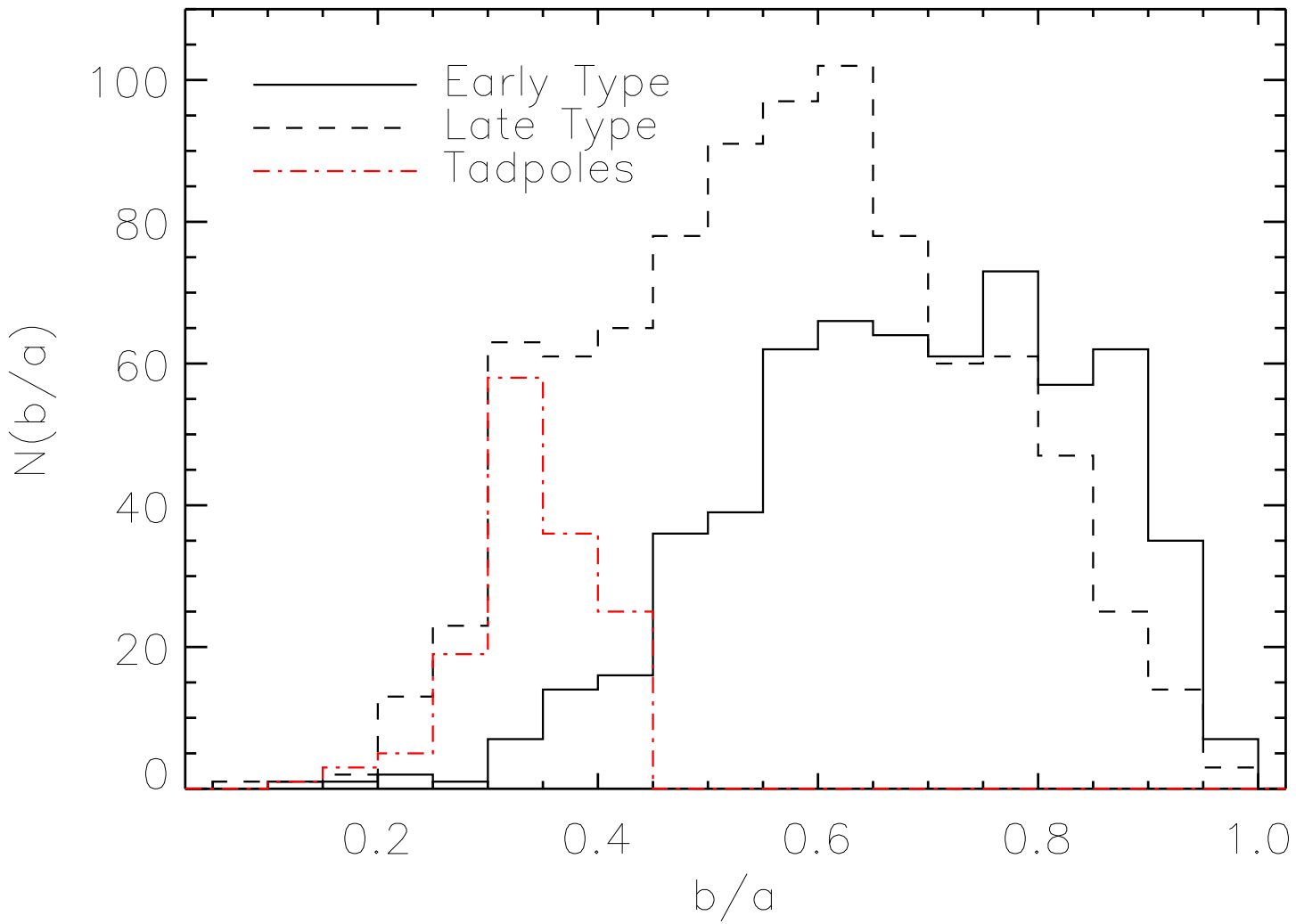

Ellipticity distribution to i_{AB} =27 mag:

$\Rightarrow$ $\exists$ likely an excess of truly linear structures among flat late-type objects.

$\Rightarrow$ Not all tadpoles are edge-on late-type disks.

Summary of HUDF Data and Epochs Used

Observation dates/Orbits:	B	V	i	z	Total
09/24/2003-10/02/2003	6	18	18	50	50
10/03/2003-10/28/2003	22	20	58	56	156
12/04/2003-12/22/2003	6	8	18	20	52
12/23/2003-01/15/2004	22	20	50	50	142
TOTAL ORBITS:	56	56	144	144	400
Total number of exposures	112	112	288	288	800
Total exposure time (s)	134880	135320	347110	346620	963930

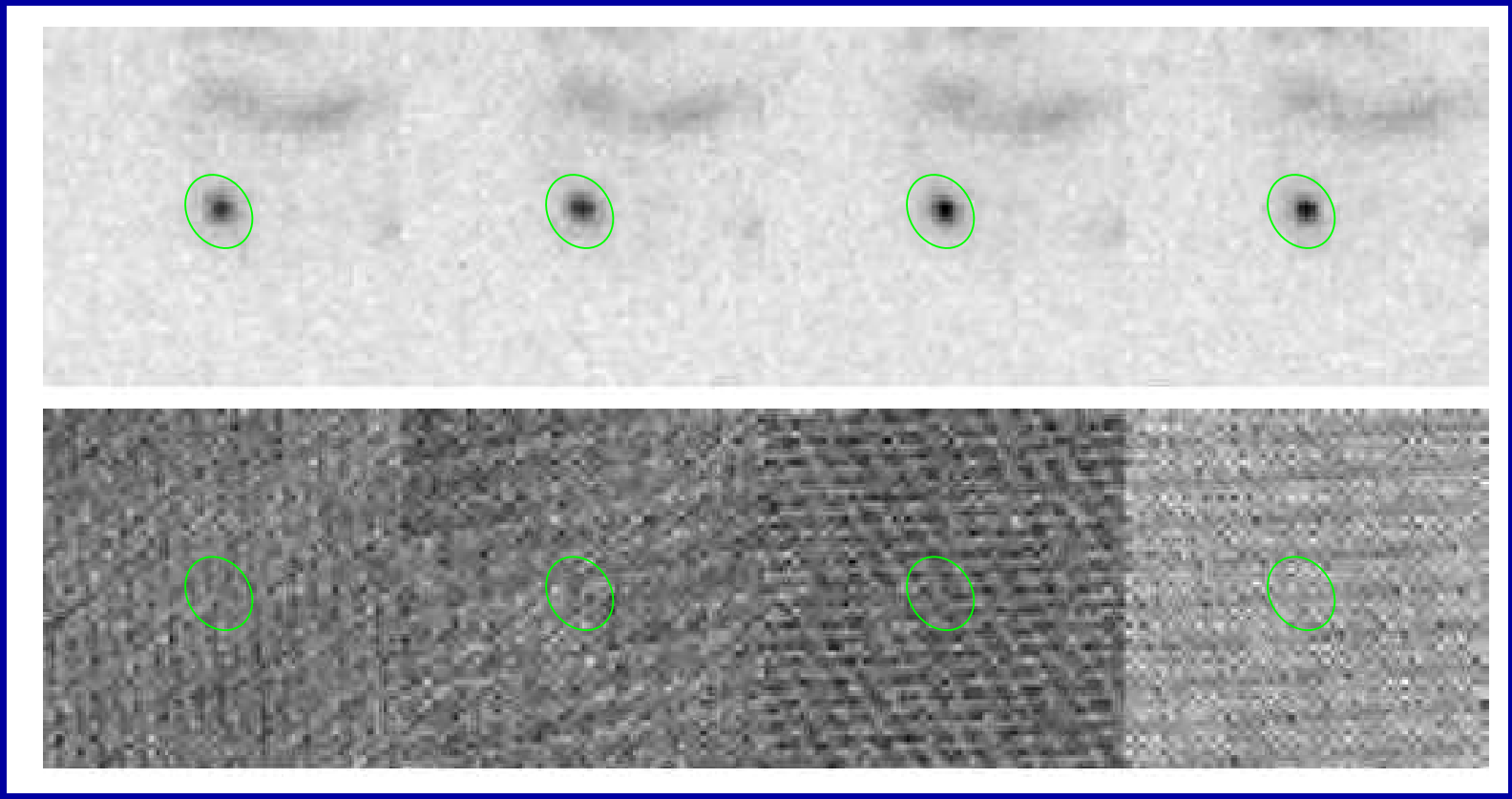

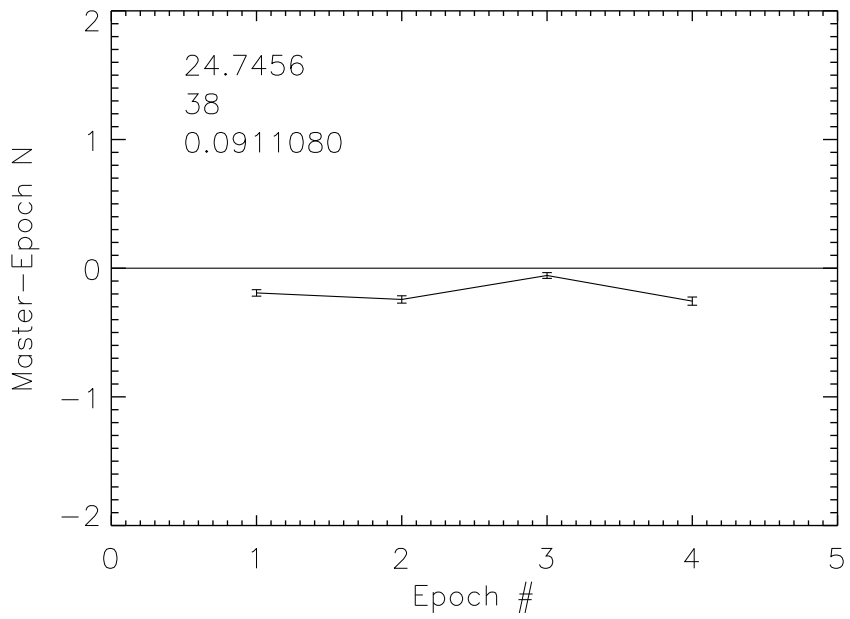

i'-Var Cand # 38 (z=1.122):

9% variability, AGN